AN ANALYSIS OF TRACHEID LENGTH VERSUS AGE IN A 4842-YEAR-OLD

BRISTLECONE PINE (*PINUS LONGAEVA* D.K. BAILEY)

CALLED PROMETHEUS

by

TERESA HALUPNIK

Presented to the Faculty of the Graduate School of

The University of Texas at Arlington in Partial Fulfillment

of the Requirements

for the Degree of

DOCTOR OF PHILOSOPHY

THE UNIVERSITY OF TEXAS AT ARLINGTON

December 2008

ACKNOWLEDGEMENTS

ABSTRACT

AN ANALYSIS OF TRACHEID LENGTH VERSUS AGE IN A 4842-YEAR-OLD

BRISTLECONE PINE (*PINUS LONGAEVA* D.K. BAILEY)

CALLED PROMETHEUS

Teresa Halupnik, PhD.

The University of Texas at Arlington, 2008

Supervising Professor: Howard J. Arnott

After Prometheus, an ancient bristlecone pine (*Pinus longaeva* D.K. Bailey) located in the Great Basin National Park, had been cut down, it was determined that the tree had been the oldest living organism at over 5000 years of age. Great Basin bristlecone pines are famous for their longevity, living thousands of years under extreme conditions of temperature and moisture at high altitudes. For the majority of conifer trees, a period of rapid growth in tracheid lengths has been observed from the pith up to ten to forty years of age. Since most pine trees live for an average of 100-300 years, it was hypothesized that, for a tree with the potential to live thousands of years, the juvenile growth phase might be of longer duration than trees that live much shorter lives. Tracheid lengths were measured from century sample points on Prometheus, as well as points near the pith and the year of felling. A juvenile growth phase was identified that lasted at least one hundred years. In addition, an unusually strong decrease in tracheid length at the year -800 was noted and commented upon. Crossdating was successful between Prometheus and

two local bristlecone tree ring chronologies. Additional observations revealed the presence of many partial rings which reinforces the importance of crossdating Prometheus to bristlecone tree ring chronologies in order to determine its true age. The mean tracheid length data were compared to Salzer and Kipfmueller (1998) reconstructed temperature and moisture episodes. Tracheid lengths decreased during warm periods and increased during cool periods. These results confirmed that warm periods increase the length of the growing season, resulting in the production of shorter tracheids. When the mean widths of one-hundred-year intervals of Prometheus were compared to long-term climatic events, the ring widths were wider during the cooler period, narrower during the warmer period, and the widths spiked during two of the Bond events. This is contrary to the belief that warm periods result in wider rings, therefore it was determined that water stress during the warm period and abundant water availability during the cool period were the likely causes of the variable ring widths.

TABLE OF CONTENTS

vii

viii

LIST OF ILLUSTRATIONS

xii

LIST OF TABLES

CHAPTER 1

SUMMARY

At the base of Wheeler Peak, there is a bristlecone pine tree which was named Prometheus. From this tree, a slab of wood was removed. It is the oldest known single piece of wood, containing at least 4842 years of growth. Contrasting it with cores removed from living (or dead) trees, the Prometheus slab allows the examination of growth rings from one side of the slab to the other. Only a few studies about tracheid length in bristlecones exist, and none concern such a distinctive tree as Prometheus.

The primary study investigated the relationship of tracheid length to age. Without seriously harming the wood, small samples, the size of toothpicks, were removed from the long edges of the slab. The samples were macerated to allow the inspection of individual tracheids, the cells that make up the majority of wood tissue. They were measured using a series of computer image analysis techniques.

It was hypothesized that, despite having lived for over 4800 years, Prometheus would exhibit a juvenile growth phase at the beginning of its life. In this study, while anomalies in tracheid length were noted, a juvenile growth phase lasting about 100 years was found. This project also utilized crossdating techniques to understand the relationship of the "pith piece" of Prometheus to the main slab. This, along with other data, supports the probability that the age of Prometheus is over 5000 years.

Complimentary studies were conducted in which the mean width of each 100-year interval was compared with associated tracheid lengths. The width of the century ring widths were compared with reconstructed temperature or moisture conditions taken from the literature.

Another study concerned the length of tracheids and the width of the tree rings at the sampling point, which were compared to each other in search of a correlation.

CHAPTER 2

PINUS LONGAEVA, THE GREAT BASIN BRISTLECONE PINE

2.1 Overview

This dissertation concerns the length of tracheids in one tree—a historically famous tree named Prometheus. It is a member of a unique species: the Great Basin bristlecone pine, *Pinus longaeva*. While later chapters will cover specific aspects of this notable tree, this chapter deals with the basic characteristics of *P. longaeva* and its history. This introductory material is necessary to uniquely place Prometheus in its rightful space and time. It is essential to understand the distinctive nature of this specimen in order to draw appropriate conclusions from this work. It is crucial to use this unique tree as carefully as possible in order to extend the current findings to both bristlecones and other tree species.

2.2 Physical Description of the Great Basin Bristlecone Pine

The Great Basin bristlecone pine can grow to a height of 15 meters with a trunk dbh (diameter at breast height) of two meters or more. The thick trunk and short branches taper upward, contorting and twisting along their length. In trees of advanced age, the cambial edges die back, receding to a narrow strip of vertical bark with a limited, dense amount of foliage (Figure 2.1A) (Kral 1993). Of 96 bristlecone pine trees examined in the White Mountains of California, four age classes of trees had increasing numbers of trees experiencing cambial dieback: 3 of 31 in the age group 0 – 500 years old, 11 of 35 in the age group 501-1000 years old, 6 of 9 in the age group 1001 – 1500 years old, and 21 of 21 in the age group that contained trees greater than 1500 years old (Lamarche, Jr. 1969).

3

Mature *Pinus longaeva* bark is red-brown with thick irregular and blocky ridges. Young branches resemble long bottlebrushes due to the persistent needle leaves and closely spaced needle whorls (Figure 2.1B). The needles, five in a deciduous fascicle, are 1.5 - 3.5 cm long and 0.8 - 1.2 mm wide. They lack extensive resin residue and will persist for 10 - 43 years before they fall. The two adaxial surfaces of the needles have white grooved stomatal lines, while the abaxial surfaces are smooth with a thick hypodermis of two cell layers. Marginal resin ducts, usually two, lie along the abaxial surface. Being a haploxylon pine, nearly all of the needle leaves contain one vascular bundle (Figure 2.1C). The mature pollen cones (7-10 mm) are purple-red in color. Immature seed cones are ovoid, 6 – 9.5 cm in length, and purple or green. Seed cones mature in two years, shifting color to brown before shedding their seeds. Cone scales terminate in a dorsal umbo. *P. longaeva* umbos terminate in a thin prickle, 1 - 6 mm long (Figure 2.1D). Seeds are pale brown and are mottled with dark red. The articulate wings are loosely attached, and 10 - 12 mm in length (Kral 1993). Bristlecone pine seed has no stratification requirements (a period of moisture and cold before germination can occur), and has high germination rates in laboratory trials (Hiebert and Hamrick 1983).
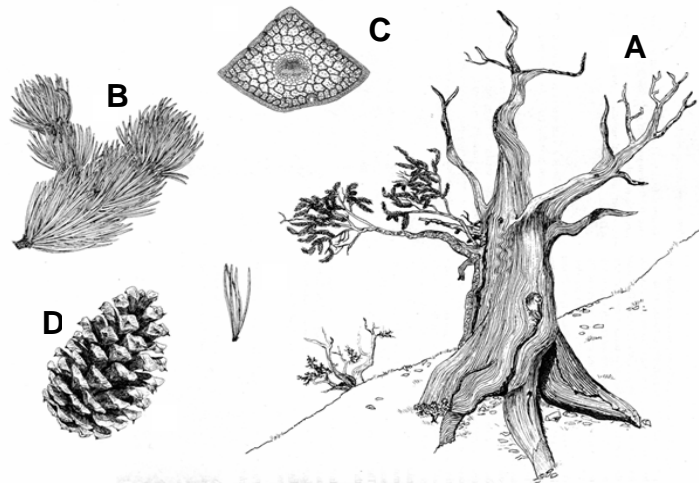
Figure 2.1 *Pinus longaeva* characteristics. A. Twisted and tapering tree form. A strip of bark is located on the left side of the tree, associated with the living branches and leaves. B. Bottlebrush appearance of a branch. C. Cross section of a needle leaf. Note the single vascular bundle of a haploxylon pine. D. Mature female cone with bristles on the tips of the dorsal umbos (Farjon 2005).

<u>2.3 Habitat of the Great Basin Bristlecone Pine</u>

P. longaeva is endemic in the states of California, Nevada, and Utah, primarily growing at subalpine elevations, 1700 to 3400 meters above sea level (5600 to 11000 feet).   At the upper treeline on isolated mountain summits and ridges, it grows in nutrient poor soils – limestone, dolomite, or marble. In the White Mountains of California, Great Basin bristlecone pines grow in dolomite, a sedimentary rock composed of calcium magnesium carbonate. In the four mountain ranges of Utah and eastern Nevada that contain bristlecone pines, limestone is the primary substrate for those that grow on Ward Mountain (Egan Range), and in the Twisted Forest (Markagunt Range). Between these two ranges, on Wheeler Peak, pines grow on quartzite glacial till (Hiebert and Hamrick 1984).

There exists limits to where vegetation can exist – abiotic and biotic conditions dictate the division between favorable and unfavorable growing conditions. Bristlecone pines have the ability to grow at treeline, the upper limit of mature trees greater than three meters in height. Two other lines or vegetation distributions have been defined: timberline, which is the edge of continuous forest, and the tree species line, the edge of trees less than three meters in height (Figure 2.2A). Extreme variations in temperature and wind can produce stunted or deformed trees or vegetation, generally called krummholz. Thus, the tree species line is also referred to as the krummholz line. Looking beyond such factors as human interference, fire, and wind and soil composition, numerous scientists (Daubenmire 1954; Wardle 1965; Grace 1977) have determined that treelines around the earth have a common temperature minimum during the growing season - a seasonal mean of 5.5 – 7.5 degrees C.   It was suggested that summer mean temperatures lower than those would inhibit the physiological processes required for the development of new tissue. Krummholz trees survive at slightly higher altitudes and lower air temperatures. The ground around these stunted plants receives abundant radiant soil warming, thus warming the air temperatures near ground level. To further illustrate the connection of temperature to the position of the treeline, the snowline (year-round snow) is used as a temperature proxy, showing how the treeline position shifts with temperature. In general, treelines worldwide form at a combination of

5

altitude and latitude and are a reflection of the growing season temperatures (Figure 2.2B) (Körner 1998). There is evidence that treelines have fluctuated with climate change. Kullman (1988) reviewed Scandinavian reports of treeline locations for three species over 900 years, and concluded that the treelines had moved down in altitude, due to a maximum drop in temperature of two degrees C (Figure 2.3). Observations of the higher attitude trees above places like Sheep Mountain and the Patriarch Grove in California show young seedlings hundreds of feet above the current mature trees (Arnott 2008). On Sheep Mountain, there is also evidence that mature trees once grew substantially above these current juveniles. This shows that the tree line of bristlecones has varied considerably in the near term past – moving down from colder average temperatures and upward for warming environments (such as now).
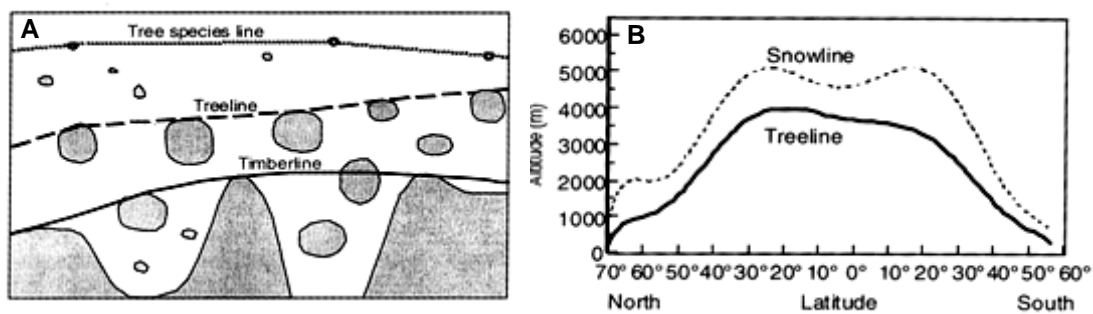
Figure 2.2 Treelines and their connection to altitude, latitude, and temperature of the growing season. A. Diagram illustrating the differences between timberline, treeline, and tree species line. B. Graph of altitude and latitude for treeline and snowline (Körner 1998).
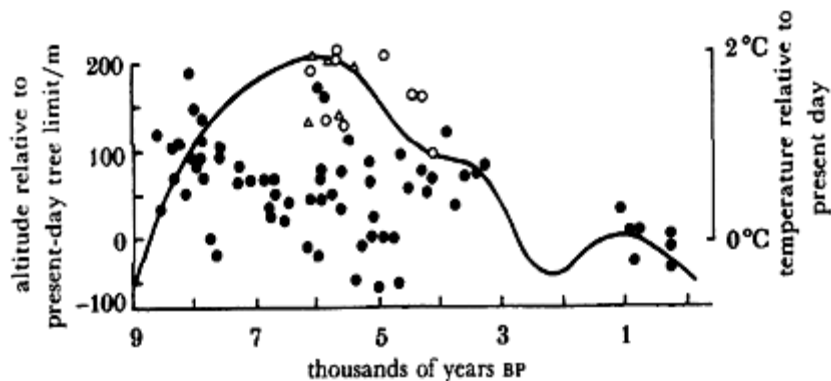
Figure 2.3 Relative altitude and temperature for treelines across 9000 years. The treelines moved downward in altitude for temperature changes up to 2 degrees C. Solid circles indicate *Pinus sylvestris*. Open circles indicate *Betula pubescens*, and triangles are *Alnus incana* (Kullman 1988)

6

2.4 History of the Great Basin Bristlecone Pine

To discuss the evolution of dendrochronology, one must start with Andrew E. Douglass (1867-1962). As a young man at the University of Arizona, he pioneered the art of examining annual tree rings of *Pinus ponderosa* Dougl. ex Laws. and relating them to patterns in precipitation. Since tree ring widths form a serial record of annual climates, Douglass was the first *scientific* dendrochronologist, creating master sequences of ring width data correlated by year, and perfecting the practice of cross-dating – matching the ring patterns of a single species in a specific area. In 1937, Douglass established the Laboratory of Tree-Ring Research at the University of Arizona in Tucson. His student, Edmund Schulman (1908-1958), wanted to expand tree ring sequences by studying timber used in ancient cities. To better understand centuries-old lumber, Schulman investigated the characteristics of what he called "overage" conifers—trees that live for over a millennia. In pursuit of an explanation for their longevity, Shulman catalogued similarities of growth form and habitat in the old trees. He defined these distinctive characteristics as "longevity under adversity." Schulman noted that the longest-lived trees, found at high altitude, were shorter and wider than their lowland counterparts. Their forms would spiral and twist, and the cambial edges of these trees would die back to a narrow, vertical living strip of bark with sparse foliage. These trees would typically grow in areas of limited moisture and/or temperature, in nutrient-poor soils (Cohen 1998).

In the summer of 1953, following rumors regarding the location of some "very old" trees, Schulman visited Inyo National Forest in the White Mountains of California. The bristlecone pines of the White Mountains, at that time known as *P. aristata* Engelmann, were the ancient trees he had been searching for. He dated one tree at over 4,000 years of age and named it "Pine Alpha." Another tree, dated at over 4,600 years of age, he named "Methuselah." In 1956, it was Schulman who first suggested that tree-ring chronologies could be used to correct timelines derived from radiocarbon dating techniques. When Schulman died in 1958, C. Wesley Ferguson continued Schulman's research in the White Mountains. During his lifetime, Ferguson extended

7

the bristlecone chronology of tree rings to 8,686 years. In the early 1960s, he passed along dated bristlecone samples to radiocarbon dating specialists.

Many other scientists have studied bristlecones, attempting to correlate climate variation with ring width. Hal Fritts, Valmore Lamarche, Donald Graybill, Harold Mooney, and Tom Harlan have all studied the tree-ring record of bristlecones towards this end (Cohen 1998).

Research of the bristlecone pine is not limited to dendrochronology. Scientists have studied their needle leaves (Ewers 1982), needle fascicles (Ewers and Schmid 1981), secondary xylem and phloem anatomy (Connor and Lanner 1990), and genetic variation (Hiebert and Hamrick 1983; Lee *et al* 2002). Related topics have also been explored, such as the dispersal of bristlecone seeds by the Clark's nutcracker (Lanner *et al* 1984).

2.5 Crossdating Techniques

Tree ring dating was pioneered by astronomer Andrew Douglass during his search for patterns of plant responses to solar cycles. Crossdating depends upon the sensitivity of trees to environmental conditions. The more that a tree responds to variations in temperature or water availability, the greater the variation in width from ring to ring. A tree that produces variation in ring widths is said to be sensitive. A tree with a lack of variation in ring widths is said to be complacent (Fritts 1976). The original method of Douglass was simple. Obtain a sample of wood, prepare the surface to see the rings, record ring anomalies on graph paper (thin, wide, partial, missing, or frost rings), and match your piece of graph paper to others until crossdating was achieved. These plots are called skeleton plots and are still being utilized today (Figure 2.4). Lines are placed on the graph paper for narrow rings—the longer the lines, the narrower the ring. Medium rings are not marked on the graph. Wide rings are marked with a "b." If any ring anomalies are observed—frost rings, for example—these are also noted on the skeleton plot.
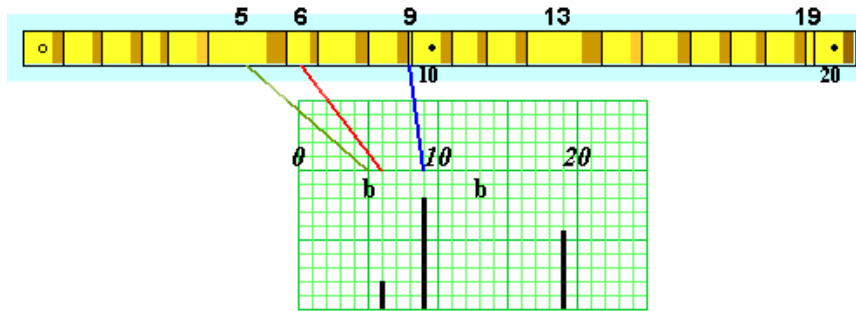
Figure 2.4 Example skeleton plot used for crossdating trees. Wide rings are indicated with the letter "b." Rings 5 and 13 are wide rings. Medium rings are not marked. Narrow rings are designated with a line; the shorter the line, the narrower the ring. Rings 6, 9, and 19 are narrow rings (LTRR 2008).

Full cross sections of trees provide the greatest amount of information. But, if obtaining such sections is impossible or undesirable, thin radial cores, 4 – 5 mm in diameter, can be removed from any kind of wood—living, dead, or artifacts fashioned by humans for some practical or artistic purpose. In fact, as early as 1918, Douglass was analyzing beams from southwestern ruins (Aztec Ruin and Pueblo Bonito, New Mexico) and determining dates of their felling (Kuniholm 2001). The tree ring patterns on Dutch wood panels covered with oil paintings were not found in the Netherlands tree chronologies, but instead were correlated to German trees growing along the Rhine (Eckstein *et al* 1986). Cedar boards from a Dynasty XII Egyptian sarcophagus, -663 to -525, were matched to the same tree (Figure 2.5). Immediately, the wide and narrow ring patterns are obvious (Kuniholm 2001).

Extremely sensitive trees with a short growing season, such as the bristlecone pine, can produce partial rings or even skip a growing season under adverse conditions (Figure 2.6). If sensitive trees are exposed to limited growth factors at the beginning of a season, missing rings (the cambium is not activated) or partial rings (the cambium is sporadically activated) can occur. If a tree contains partial (discontinuous) or missing rings, they can still be crossdated. Comparison of a tree with missing rings to one that is not missing rings can help to accurately date the tree with the missing rings. Two hypotheses have been suggested for the formation of partial rings:

9

nutrient or auxin limitation. Sugars produced in the crown will first be utilized by the growing tissues, including the cambium closest to the expanding buds and the crown. Nutrients diffuse downward, so if they are limited in supply, they may run out and the cambium near the base of the tree will remain dormant. The result is missing or partial rings (Fritts 1976). Larson (1956) proposed another theory for partial rings. Auxin from expanding buds activates the cambium out of dormancy and spreads downward. The downward spread is more rapid down exposed branches – those that are not shaded (suppressed). Slash pines (*Pinus elliotii* Engelmann) that were suppressed exhibited partial rings, sometimes multiple years missing in one place. Partial rings have been observed in suppressed Monterey pine (*Pinus radiata* D. Don) where the trees were growing in close stands and were bare of branches (Harris 1952). Bormann (1965) also noticed partial rings in suppressed white pines (*Pinus strobus* L.).
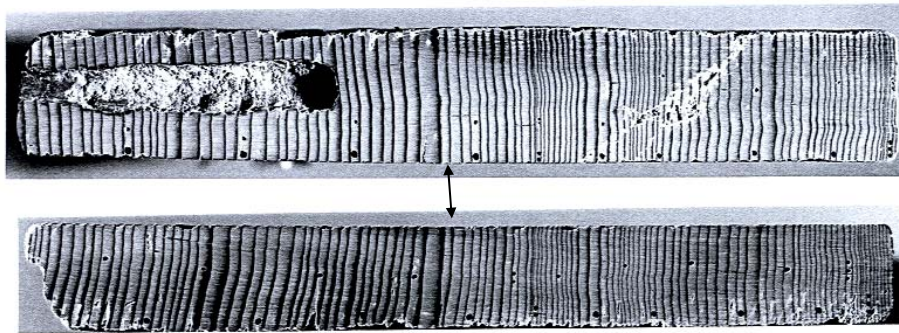
Figure 2.5 Two cedar boards from an Egyptian Twelfth Dynasty sarcophagus. The sarcophagus currently is located in the Boston Museum of Fine Arts. The two cedar pieces were determined to be from the same tree. The ring pattern of wide and narrow rings is visually apparent. The arrow points to a matching wide ring (From Kuniholm 2001).

As an alternative to drawing skeleton plots, computer software programs have been developed to accept ring measurements and to statistically match tree ring sequences to each other. CrossDate, by Greg Lazear and Thomas Harlan, is a program that statistically matches series of ring measurements for the best correlation value and also draws a skeleton plot for the two tree ring sequences being matched.

10
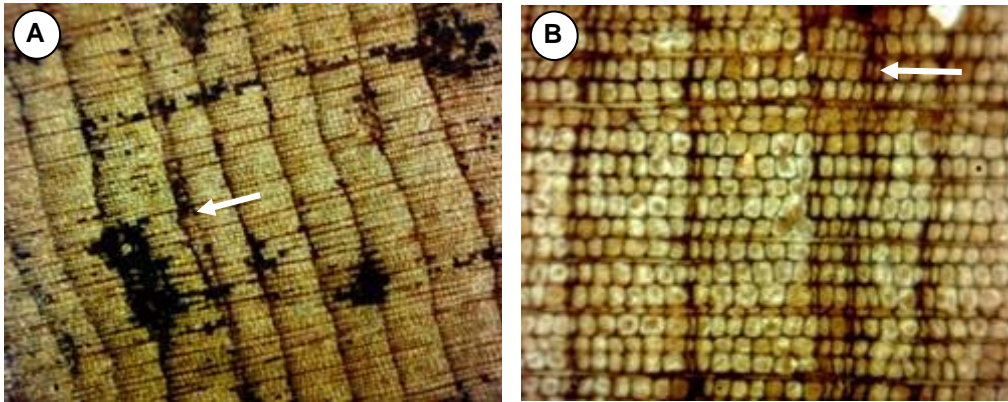
Figure 2.6 Partial rings from Prometheus. Arrows are pointing to the partial rings. A. Partial ring located at approximately -1603 (100X). B. Partial ring located at approximately 175 (400X). Note the slightly smaller cells with thick darkened cell walls. These are latewood cells and indicate the end of each growing season.

Using crossdating, the sequences of the annual rings in multiple trees in one location can be assembled into master chronologies. Master chronologies have the advantage of being a "complete record" of rings; rings are added to the chronology that may be present in one tree, but not another. To build a longer sequence of years, crossdated chronologies are then set in order, beginning with an absolutely-dated tree. The sequence is built in step-wise fashion into the past as far back as the overlapping ring sequences will allow (Fritts 1976). *Pinus longaeva* (bristlecone pine) chronology is now over 8,700 years with a tentative extension to near 10,000 years (Arnott 2008). While not specifically intended to benefit scientists working with carbon dating techniques, bristlecone chronologies became essential for calibrating curves depicting the ratio of carbon-14 to carbon-12 versus age.

2.6 Bristlecone Pines and Radiocarbon Dating

There are three isotopes of carbon – carbon-12, carbon-13 (both stable) and carbon-14, which is unstable or radioactive. Carbon-14 is formed by cosmic radiation from nitrogen-14. All three forms of carbon in the atmosphere become oxidized into CO_2 gas. CO_2 is taken up by plants through photosynthesis. Animals eating plants absorb the carbon in their tissues. In this way, plants and animals become a living reflection of the ratio of carbon isotopes in the

11

environment. Organisms die with the current level of carbon-14 fixed in their tissues. Carbon-14 is unstable. Libby (1952) was the first to measure and quantify the rate of decay for carbon-14. He realized that the year of death of an organism can be determined by comparison of the current ratio of carbon-14 to carbon-12 to the level contained within the sample. In 1949, Arnold and Libby published a paper favorably comparing the known ages of historically-dated pieces of wood as a check against their radiocarbon method.

However, deviations between radiocarbon age and the age determined by the counting of rings of bristlecone pine were noted. Starting at 5000 years before present, it was determined that the radiocarbon age curve deviated from the ring-counted age of the wood by 10% (Figure 2.7). The divergences were eventually determined to be due to carbon-14 fluctuations in the atmosphere. Two natural causes were identified: change in the intensity of the earth's geomagnetic field and fluctuating solar activity influencing the intensity of cosmic rays. The other changes of carbon were traced back to the actions of humans. Radiocarbon dates of dendrochronologically-aged trees, primarily bristlecone pine along with German and Irish oaks, have been utilized to produce an accurate calibration curve which now extends back over 10000 years (Currie 2004).
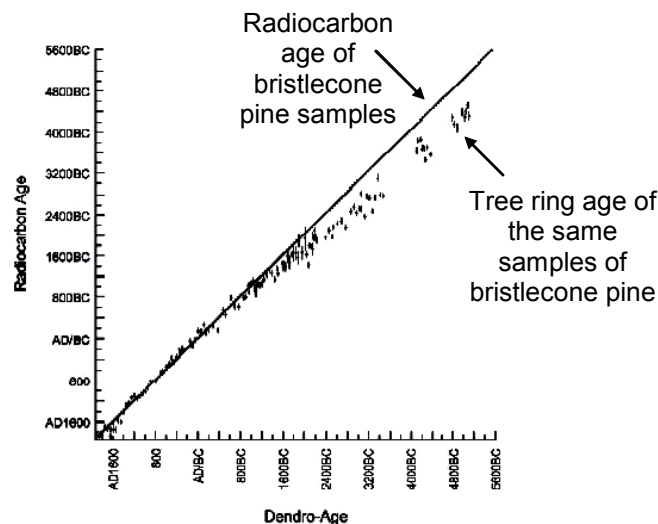
Figure 2.7 Radiocarbon age versus age of bristlecone pine trees verified by counting methods. The bristlecone pine age differs by 10% from the radiocarbon age (From Arnold and Libby 1949).

2.7 Taxonomy of the Great Basin Bristlecone Pine

In *Species Plantarum* (1753), Carolus Linnaeus described five species of *Pinus*. du Monceau (1755) designated three sections (subgenera) of *Pinus* based upon the number of needles per fascicle: *Bifoliis, Trifoliis*, and *Quinquefoliis.* Little & Critchfield (1969), using the International Code of Botanical Nomenclature, named subgenera as *Pinus* (containing *Bifoliis* and *Trifoliis*) and *Strobus* (*Quinquefoliis)* (Richardson 1998).

There are 111 species of *Pinus*. *Pinus* is a member of the Kingdom Plantae, Subkingdom Tracheobionta (vascular plants), Superdivision Spermatophyta (seed plants), Division Pinophyta or Coniferophyta (conifers), Class Pinopsida, Order Pinales, and Family Pinaceae (ITIS 2008). Within the Genus *Pinus*, pines are divided into two subgenera: *Strobus* and *Pinus*. The definitive character separating the two subgenera of *Pinus* is the number of vascular bundles per leaf. The Subgenus *Pinus*, the diploxylon pines, are named because their leaves contain two vascular bundles, while *Strobus* species, the haploxylon pines, have only a single vascular bundle (Figure 2.8) (Gernandt *et al* 2005).
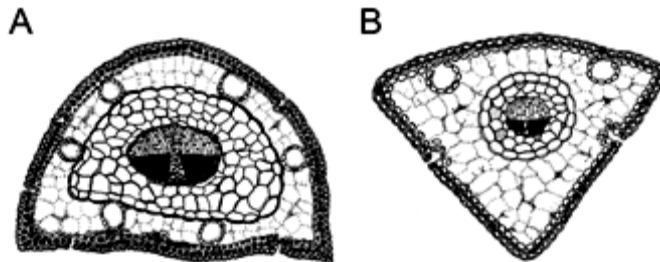
Figure 2.8 Diagrams of the cross sections of pine needle leaves. A. Two vascular bundles define the diploxylon pines. B. One vascular bundle differentiates the haploxylon pines (Gernandt *et al* 2005).

Pinus pines are also referred to as hard or yellow pines, because the wood of these pines contains significantly higher amounts of resin, and is harder than the *Strobus* species, or soft or white pines. Two additional traits are used when identifying pine species: first, the location of the cone scale tips, or umbos (dorsal or ventral), and second, whether the seedwings are firmly or loosely attached to the seeds (adnate or articulate, respectively) (Richardson 1964).

13

Figure 2.9, a cladogram, developed by Gernandt *et al* (2005) for the *Strobus* subgenus, lists the two sections of Strobus: *Quinquefolia* and *Parrya*. *Parrya* contains six subsections, one of which, *Balfourianae*, comprises the foxtail-bristlecone complex. *Balfourianae* contains three species: *Pinus aristata* Engelmann (Rocky Mountain bristlecone pine), *Pinus balfouriana* Greville & Balfour (foxtail pine), and *Pinus longaeva* D.K. Bailey (Great Basin bristlecone pine). The defining characteristics of *Balfourianae* are that the seeds are small with long articulate wings, and that the cones are cylindrical. In addition, the five leaves are short and have long retention periods – 10-35 years (Bailey 1970).

Figure 2.9 Cladogram of the Genus *Pinus,* Subgenus *Strobus*. The *Balfourianae* subsection is circled and enlarged for clarity (From Gernandt *et al* 2005).

Prior to 1970, only two species were recognized as being part of Subsection *Balfourianae*: *Pinus aristata* (bristlecone pines) and *Pinus balfouriana* (foxtail pines). The foxtail pine was the first of the subsection to be described. Greville & Balfour, traveling with the Oregon

14

Expedition in 1853, identified two allopatric populations of *P. balfouriana*, both in California: one group in the Klamath Mountains of northern California and the other in the southern Sierra Nevada (Bailey 1970). Engelmann, in 1863, described the "bristlecone pine," *P. aristata* Engelmann, using material collected in Colorado. Confusion followed the bristlecone pine when, in 1868, Watson collected bristlecone pine specimens from the East Humboldt Mountains in Nevada and named them *Pinus balfouriana* Murr. Another bristlecone specimen was collected by William Gabb in 1867 from the White Mountains of California, and was labeled *P. aristata* var. *decurva*, possibly referring to the curving pendulous habit of the bristlecone pines in that region (Bailey 1970). Engelmann (1880), in his revision of the genus *Pinus*, compressed the foxtail and bristlecone trees into a single species, which he called *P. balfouriana*. In this, he reduced his own bristlecone species, *P. aristata* Engelmann, into a foxtail pine. The concept of a single species with multiple variations for the foxtail complex persisted throughout the rest of the 19th and most of the 20th century (Bailey 1970).

In 1970, Dana K. Bailey, a former student of A.E. Douglas at the University of Arizona (Cohen 1998), published descriptions that separated the foxtails from the bristlecones by restoring *P. aristata* Engelmann to its original species level. Bailey further described another bristlecone species, *Pinus longaeva*. Figure 2.10 is a recreation of a map drawn by Bailey that indicated the approximate boundaries of the three Subsection *Balfourianae* species. The smaller groups in California are the foxtail pines, *P. balfouriana* Greville & Balfour: Klamath mountain groups in the north (in red) and the Sierra Nevada group to the south (yellow). The *P. aristata* Engelmann grouping (in green), found in Arizona, Colorado and New Mexico, is widely separated from the *P. longaeva* D.K. Bailey group (in blue). *P. longaeva* extends across three states – California, Nevada, and Utah.

In defense of his separation of the three species within *Balfourianae,* Bailey outlined several distinctions between them:

- The majority of *P. longaeva* and *balfouriana* needle leaves feature two large distal resin ducts just under the surface*. P. aristata* needles only contain one resin duct.

15

I	P. aristata
II	P. longaeva
III	P. balfouriana (Sierra Nevada)
IV	P. balfouriana (Klamath Mtns)
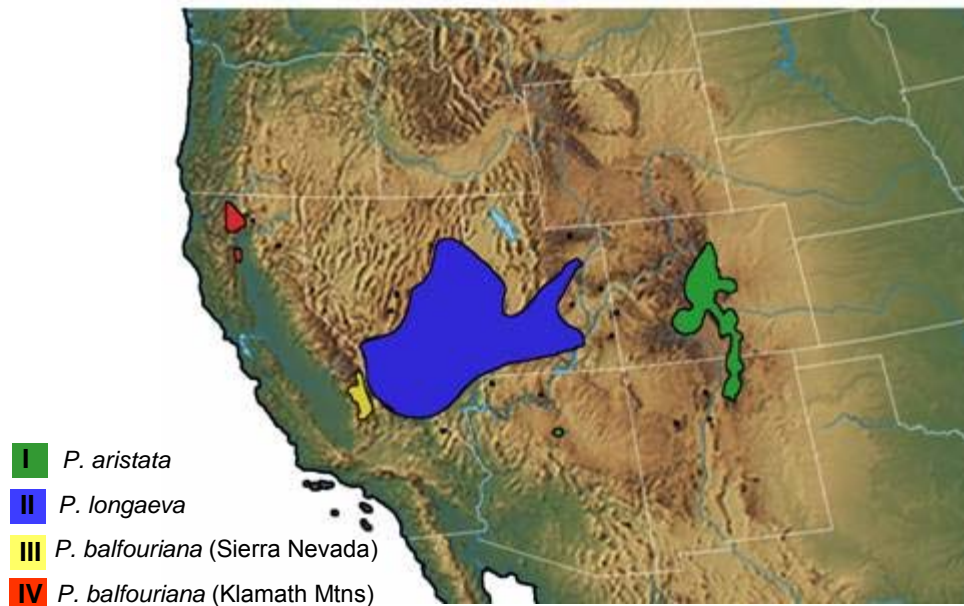
Figure 2.10. Recreation of a map drawn by D.K. Bailey in his 1970 division of the Subsection *Balfourianae*. He identified allopatric groups of foxtail and bristlecones which he designated as Population I (Colorado-Arizona trees), II (California-Nevada-Utah), III (Sierra Nevada foxtails), and IV (Klamath Mountain foxtails).

- *P. aristata* exhibits extensive white resin crusting on the surface of its needle leaves due to ruptures of its lone resin duct. *P. longaeva* and *balfouriana* resin ducts rupture far less often. This is likely due to the additional layers of cells between the ducts and the surfaces of the leaves.

- *P. aristata* trees splay their needles within the fascicle sheath and the effect was described as a soft brush. The needles of *P. longaeva* and *balfouriana* tend to remain closed and pressed closely to the branches. The appearance of the stems in these trees was described as a coarse brush, with the *P. balfouriana* needles showing even less tendency to spread apart than *P. longaeva*.

- *P. longaeva* retains needles for an average 25-30 years, compared to the 10-15 years of *P. aristata*. Needle retention in *P. balfouriana* was not examined in this study.

- *P. longaeva* cones are more rounded at the base. *P. aristata* cones generally have

  flattened bases. *P. balfouriana* cones have pointed conical bases.

- Cones of *P. aristata* are very resinous and therefore sticky when handled. *P. longaeva*

  and *balfouriana* cones are much less resinous.

- Cone bristles are different between the species. *P. aristata* bristles are stout and long

  and stick outward from the cones. Cones of *P. longaeva* have finer and shorter bristles

  than *P. aristata* and they tend to curve towards the cone. The bristles of *P. balfouriana*

  are the shortest and finest, and many bristles are lost by the time the cones reach

  maturity.

- *P. balfouriana* cones, compared to *P. aristata* and *P. longaeva*, have fewer cone scales

  and fleshier apophyses (the outer swollen portion of a closed cone scale).

- Mature *P. longaeva* trees exhibit twisting and pendulous growth forms, compared to the

  upright and erect forms of *P. aristata*.

Following Bailey's published description, *Pinus longaeva*, the Great Basin bristlecone pine,

has since been widely accepted as a separate species distinct from *Pinus aristata*, the Rocky

Mountain bristlecone pine, and *Pinus balfouriana*, the foxtail pine. It is interesting to note that

Bailey designated a tree living on the Wheeler Peak moraine as the type specimen for *Pinus

longaeva*. This tree is only ½ mile from Prometheus (Arnott 2008).

<u>2.8 Conservation Status</u>

The International Union for the Conservation of Nature and Natural Resources (IUCN),

founded in 1963, maintains an evolving and updated Red List of Threatened Species. This

functions as an inventory of the global conservation status of plant and animal species. In the

2006 update of the Red List, the Great Basin bristlecone pine was rated as VU (vulnerable). This

denotes a species likely to become endangered, unless the circumstances threatening its survival

and reproduction are improved. The IUCN justifies this rating by stating that the bristlecone

17

populations are "severely fragmented or known to exist at no more than ten locations", with a possible "continuing decline, inferred, observed or projected, in the number of mature individuals" (Conifer Specialist Group 1998).

CHAPTER 3

PROMETHEUS, A 4842-YEAR-OLD BRISTLECONE PINE

3.1 Overview

Specific trees are often recognized for their historical importance or size. For example, General Sherman is a well-known Giant Sequoia, famous for having the largest trunk diameter at its base (11.1 meters) and the greatest volume (1487 cubic meters). In the case of Prometheus, just after it was felled, it was identified as the oldest living tree. This chapter deals with the events surrounding the discovery of the tree along with a comprehensive look at the characteristics of the tree itself.

3.2 History of Prometheus

During the summers of 1963 and 1964, Donald Currey was conducting research in Nevada's White Pine county. Currey's dissertation material concerned correlating climate changes of the Little Ice Age with tree ring morphology. Bristlecone pines have the ability to grow very old, thus providing researchers with the rare opportunity to examine growth rings spanning thousands of years. A common method to retrieve samples of tree rings is to use a coring tool to extract a long cylinder of wood from a tree trunk. The procedure does not kill the tree, but, depending upon the skill of the user and the tree being sampled, the cores may be more or less usable. The sample may lack a complete clean series of rings, or the tool may lack the length to sample enough years for the given study. Coring tools can break, as did Donald Currey's in August of 1964. Given the lateness of the season and the difficulty of obtaining another tool, Currey asked for permission to cut down a tree to examine cross sections of the trunk. The Forest Service gave him permission to cut one tree and Currey selected WPN-114 (the 114th tree that he had sampled in the White Pine Mountains) (Figure 3.1) (Cohen 1998).

Years before, sometime between 1958 to 1961, a group of local naturalists named WPN-114 "Prometheus," after a Titan of Greek mythology, chained to a mountain by Zeus as punishment for stealing fire and giving it to man. On August 6, 1964, Forest Service personnel accompanied by Donald Currey used a chain saw to cut Prometheus down (Cohen 1998).

Figure 3.1 Donald Currey standing on a nonliving part of Prometheus, August 6, 1964. A forest service worker with a chainsaw is visible in the lower left of the photo (Keith Trexler).

Currey and the Forest Service employees were unaware of WPN-114's age and importance. They had no idea until afterwards, when the rings were counted, that this tree would turn out to be the oldest known non-clonal organism on Earth. After WPN-114 was felled, several slab-like sections were hauled down from the mountain (Figure 3.2). These sections, in pieces or in their entirety, have been displayed or stored in variety of locations. The Great Basin National Park visitor center, the Bristlecone Convention Center in Ely, Nevada (Figure 3.3), the University of Arizona Laboratory of Tree-Ring Research (Figure 3.4), and the US Forest Services' Institute of Forest Genetics have all held or still possess portions of WPN-114 (Cohen 1998). Donald Currey retained a main trunk slab, along with two v-shaped wedges—one contained the wood closest to the pith and the second was from a different tree nearby (Arnott 2008).

20

Figure 3.2 Sections of Prometheus wood after felling, August 6, 1964 (Keith Trexler, Forest Service).

Figure 3.3 Main slab section of Prometheus displayed at the Bristlecone Convention Center, Ely, Nevada. Note the similarity between this section and the one in Figure 3.4 (HJ Arnott).

Figure 3.4 Main slab section held by the University of Arizona, Tucson, Arizona. The oldest part of the slab is on the left. The bark covering the small strip of sapwood is visible on the right (HJ Arnott).

In August of 2002, Dr. Howard Arnott and his daughter Catherine Arnott-Thornton visited the site where Prometheus is located and photographed the tree's grove and the fallen stump and the area around it. The first photograph (3.5A) looks north towards the position of Prometheus. The ground surface is rough quartzite glacial till. The stump and fallen wood are visible left of the center. The trees in the foreground are at the treeline. In 3.5B, the photograph was taken standing at the stump and facing the south, towards Jeff Davis Peak. The mountain is rising rapidly in the background, approximately 100 feet from treeline. After viewing the Prometheus stump, Dr. Arnott and his daughter visited Donald Currey. At that time, Currey gave his slab and v-shaped pith wedge of WPN-114 to Dr. Arnott. In addition, Dr. Arnott was also given a piece of another tree nearby, henceforth referred to as "Buddy."

In the summer of 2003, Dr. Arnott brought scans of the Prometheus slab and pith sections to the Prometheus stump and aligned the scans to the fallen wood pieces. Figure 3.6A shows him lining up a scan with the location where the v-shaped pith wedge was removed. Large weathered pieces of Prometheus are still intact (Figure 3.6B).

The trunk slab is in five pieces, which fit together without gaps (Figure 3.7A). The bark in the foreground covers the sapwood—the last growing year is the first ring under the bark, 1964. The triangular v-shaped portion contains the rings closest to the pith, the first years of life for the tree (Figure 3.7B).

<u>3.3 Geographic Location of WPN-114</u>

Currey, in a 1965 issue of Ecology, described the location of WPN-114. The bristlecone pine stand where WPN-114 was located is in the eastern Great Basin (Figure 3.8A) within the boundaries of what is now the Great Basin National Park (Figure 3.8B), below the northeast face of Wheeler Peak. The Great Basin is a 200,000 square mile area that does not drain to either the Pacific Ocean or the Gulf of Mexico. All precipitation either evaporates, drains into inland lakes or ground water. Bounded by the Wasatch Mountains (east), the Sierra Nevadas (west) and the Snake River Plain (north), the Great Basin contains most of Nevada, half of Utah, and portions of Idaho, Wyoming, Oregon, and California (National Park Service 2008). The Great Basin National

22

Park was established in 1986, mainly in response to pressure from environmentalists to protect

the bristlecones and an extensive cave system, which includes the popular Lehman Cave.
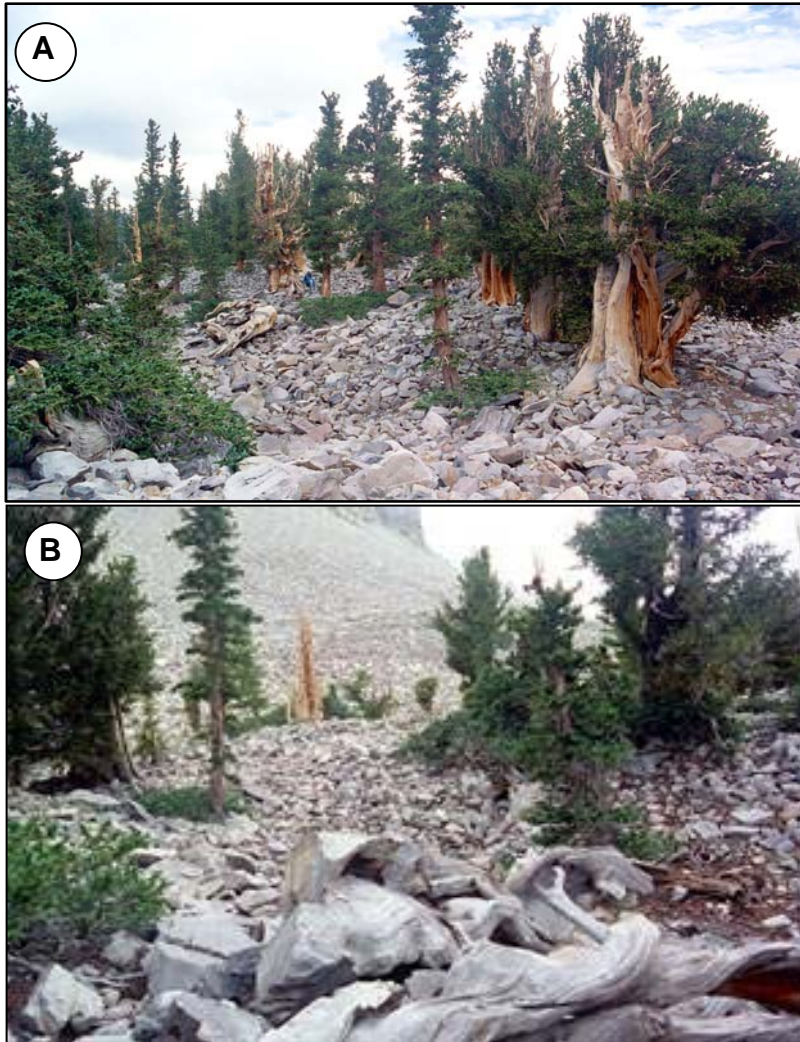
Figure 3.5 Site photographs of where Prometheus was felled, Great Basin National Park, August, 2002. A. Bristlecone pine grove. Facing north, the tree remains are located left of center in the photograph. B. Bristlecone pine grove. Facing south, with the tree pieces in the foreground, the mountains rise sharply in the background (HJ Arnott).

Figure 3.6 Dr. Arnott visits the Prometheus site in August, 2003. A. Dr. Arnott holds a scan of the pith section up to the cut limb where the wedge was removed. B. Dr. Arnott photographs the felled trunk and limb sections of Prometheus (Catharine Arnott-Thornton).
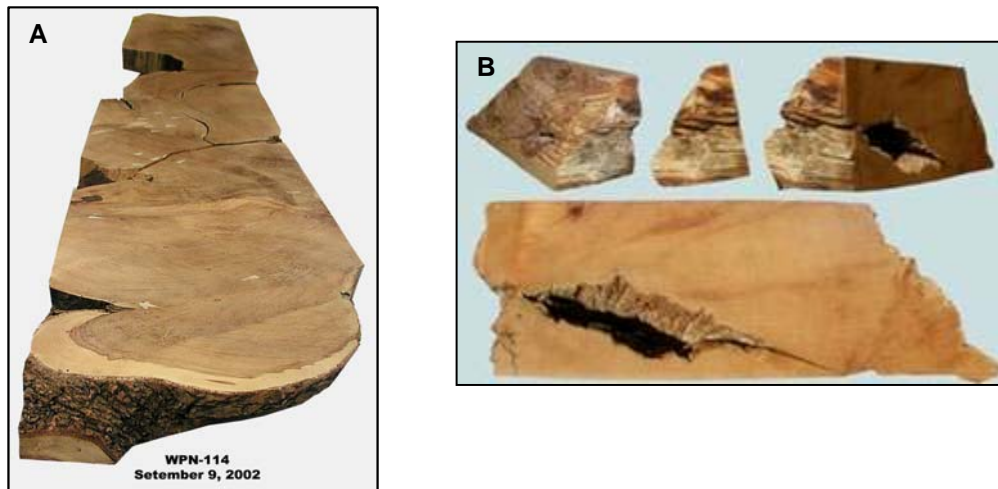
Figure 3.7 Photographs of the Prometheus wood given to Dr. Howard Arnott by Donald Currey. A. Main trunk slab made up of five separate pieces. The bark in the foreground covers the last year of life, 1964. B. Triangular v-shaped chunk of wood cut from higher in the tree in order to obtain the rings closest to the pith. The single piece is shown rotated to expose the different sides (HJ Arnott).
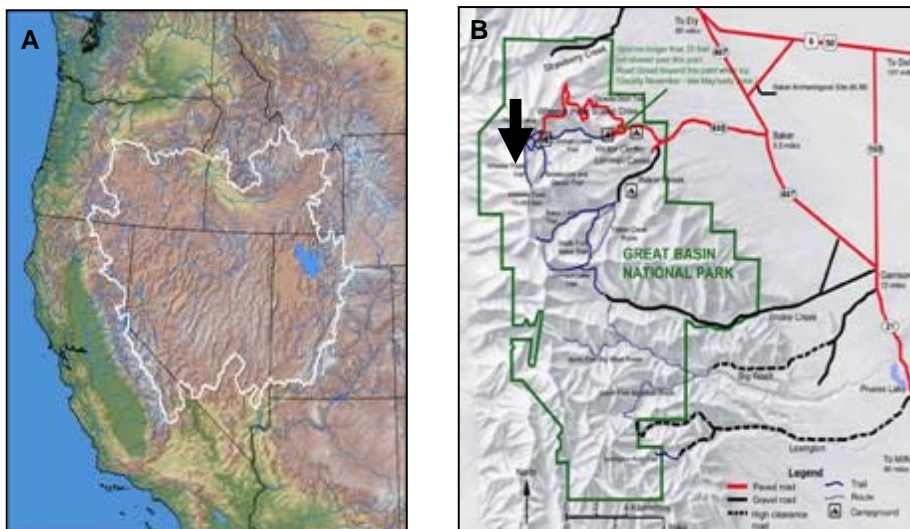
Figure 3.8 Outline of the Great Basin and map of the Great Basin National Park. A. The Great Basin is a large inland area that does not drain to either the ocean or the gulf (USDA). B. Map of the Great Basin National Park. An arrow marks the location of Wheeler Peak (National Park Service 2008).

In the Great Basin National Park, bristlecone pine stands are located between 2900 and 3200 meters in altitude (Beasley and Klemmedson 1980). The stand of trees where Prometheus was located extends over 300 acres, at altitudes ranging from of 9500 to 11000 feet . Prometheus is located at 10700 feet in altitude. Wheeler Peak is the twelfth highest mountain in the contiguous U.S. and the highest in the Great Basin, at a height of 13,063 feet (Figure 3.9). On the northeast side below the peak is a large glacial cirque (valley), with an extensive moraine (glacial debris field) below (Figure 3.10) (National Park Service 2008).
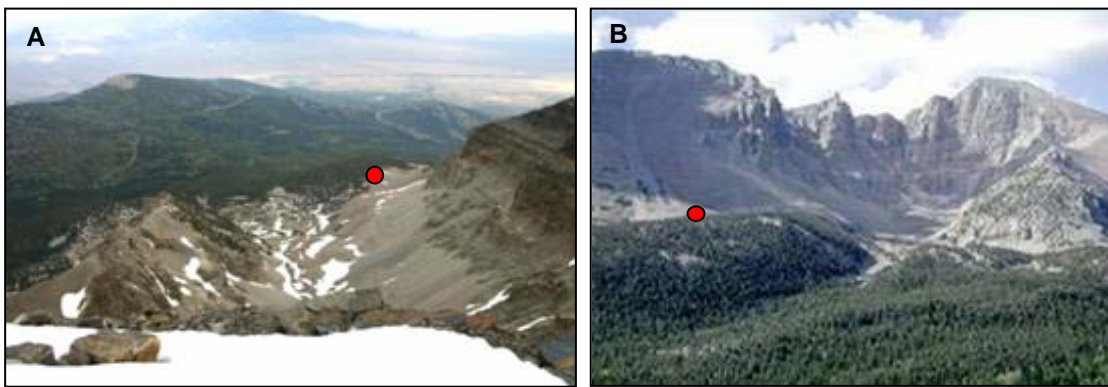
Figure 3.9 Wheeler Peak, Great Basin National Park. The approximate location of Prometheus is indicated by ●.   A. From the summit of Wheeler Peak, looking northeast (National Park Service).   B. From the base of Wheeler Peak, looking south (HJ Arnott).

3.4 Description of WPN-114

The trunk of WPN-114 demonstrated strip bark growth, a state in which the bark dies back from most of the tree's circumference. The remaining cambium, newly formed secondary xylem, and bark grow in one direction, normally towards the most protected side of the tree. According to Currey, WPN-114's strip of bark was 19 inches wide, and it faced north away from the mountains. In a photo of WPN-114 taken by Keith Trexler, a forest service ranger, the strip of living tree was located on the left side of the tree.   WPN-114 had a dead crown 17 feet high, while the living shoot was 11 feet high. The trunk had a 252-inch circumference, measured 18 inches above the current ground level. However, because of fallen quartzite debris, the ground surface that Currey encountered was approximately two feet above the original base of the tree.

The pith was missing until a point 76 inches above the ground. Currey and the forest service workers removed a slab 18-30 inches above the ground. Since the pith was missing from this slab, they removed a smaller piece of wood 76 inches above the ground that included the pith area (Figure 3.11) (Currey 1965).
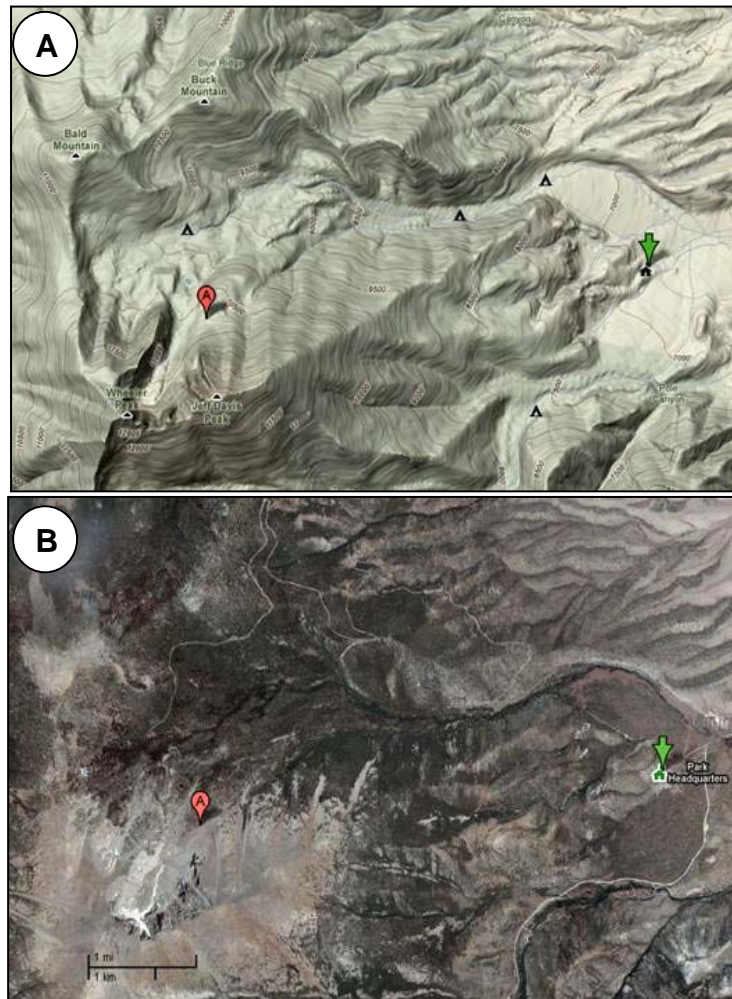
Figure 3.10 Topographic map and satellite image of the location of Prometheus. The location of Prometheus is marked with the letter A inside the red drop shape. Green arrows indicate the Great Basin National Park headquarters. A. Topographic map. Prometheus (10700 feet) is located to the northeast of Wheeler Peak (13063 feet) and to the north of Jeff Davis Peak (12771 feet). B. Satellite image. Prometheus is located at the treeline (Google maps 2008).

Figure 3.11 1964 photograph of Prometheus. Dimensions are shown with solid double pointed arrows. Approximate cutting lines are indicated with dotted lines. The red dotted lines indicates the cut lines for the trunk slab, removed 18-30 inches above the ground. The green dotted line indicates the location of the v-shaped pith wedge site, removed 76 inches above ground level and 46 inches above the trunk slab. (Keith Trexler, Forest Service).

Currey counted 4844 rings, using both the trunk slab and pith piece. He also measured ring width, documenting a mean width of 0.47 mm. Under low power magnification, he could discern both earlywood and latewood. Since the pith section was taken at a height 100 inches above the original base level, Currey concluded that WPN-114 must have started growing *about* 4900 years ago (Currey 1965). The exact age of Prometheus is difficult to establish. From counts in this study, there are 4842 rings; however there are partial and possibly absent rings that have not been counted. Therefore the statement by Currey that Prometheus is *about* 4900 years in age is an underestimate.

<u>3.5 The Great Basin National Park Habitat</u>

Temperatures are extremely variable in Great Basin National Park. The temperatures listed below in Table 3.1 are from a weather station located within the park, but the station is situated at 6850 feet in altitude. Prometheus was located at 10700 feet. Therefore, these temperatures are an underestimate at Prometheus' location (Renfro 2008). According to the temperature summary, only two months out of the year (July and August) lack a recorded temperature below freezing. If temperature is the determinant of the length of the growing season, as Körner (1998) suggests, the growing season in the grove where Prometheus stood must be brief. In fact, the growing season for bristlecone pines within the park is estimated to be six weeks (Great Basin National Park 2008).

Table 3.1 Temperature Summary (July 1948 to present) from the Great Basin National Park Weather Station (Great Basin National Park 2008)

	Month											
	Jan	Feb	Mar	Apr	May	June	July	Aug	Sep	Oct	Nov	Dec
Daily Max - C	5	7	9	13	19	24	30	28	24	17	9	6
Daily Min - C	-8	-6	-4	-1	4	4	14	13	8	3	-3	-7
Extreme High - C	19	18	21	25	31	36	38	35	33	27	21	18
Extreme Low - C	-29	-24	-18	-12	-11	-4	4	0	-6	-14	-21	-25
Days > 32 C	0	0	0	0	0	1	7	3	0	0	0	0
Days < 0 C	29	25	26	18	7	1	0	0	2	10	23	29

Rainfall in the Great Basin National Park averages 12.9 inches a year. A desert is defined as receiving ten inches or less of rainfall a year. The majority of the precipitation in the park falls as snow (Table 3.2). According to the Great Basin National Park website, snowfall is possible any time of the year at altitudes above 10000 feet. Prometheus is located at 10700 feet.

Table 3.2 Precipitation Summary (July 1948 to present) from the Great Basin National Park Weather Station. Located at 6850 feet above sea level, 39°00'N / 144°13'W in the county of White Pine, Nevada (Great Basin National Park 2008).

	Jan	Feb	Mar	Apr	May	Jun	Jul	Aug	Sep	Oct	Nov	Dec
Normal	0.9	1	1.4	1.3	1.1	0.9	0.9	1.1	0.9	1	1.2	1.2
Maximum	3.2	3.6	5	3	4.7	3.4	2.1	3.7	2.7	3	3.4	3.4
Max. 24 Hr. Precip.	2.2	1.6	1.5	1.6	1.6	1.4	1.1	0.8	2.4	1.1	1.5	1.6
Max. Snowfall	34	39	52	35	23	8	0	0	2	42	48	46
Days with Measured Precip.	7	7	8	8	7	5	6	5	4	5	5	6
Average No. Thunderstorms	0	0	0	1	5	7	12	12	4	1	0	0

3.6 Prometheus Main Slab and Pith Pieces

The main slab given to Dr. Howard Arnott by Donald Currey is composed of five pieces. The five pieces span the years between 1964 and -2568 with no gaps in the chronology. Due to the curvature of the rings and the irregular breaks between them (Figure 3.12), the five pieces overlap in years. In addition to these pieces, Dr. Arnott received a triangular piece of Prometheus, cut further up the trunk to obtain the rings closest to the pith. A flat section was trimmed from this pith piece, which broke into three pieces (Figure 3.13). Table 3.3 details the range of years on all eight pieces of the main slab and pith.
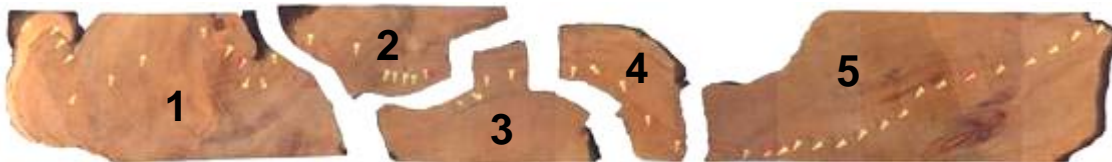
Figure 3.12 Scan of the surface of the Prometheus main slab piece, the five pieces separated from each other and numbered.

Figure 3.13 Scan of the surface of the Prometheus pith piece, the three pieces separated from each other and numbered.

Table 3.3 Start and End of the Years in the Main Slab and Pith Pieces of Prometheus. *the piece containing the rings closest to the missing pith.

	Piece number	Year start	Year end	Total years
Main slab pieces	1	1964	638	1325
	2	638	-362	1000
	3	638	-617	1255
	4	-360	-818	458
	5	-771	-2568	1797
Pith pieces	1	-1572	-2849	1277
	2	-1942	-2422	480
	3	-2422	-2878*	456

A strip of bark still covers the last year of growth for Prometheus, 1964, and the boundary between the sapwood and heartwood is clearly visible. The annual rings of the main slab pieces do not follow a concentric path or even arcs. The width of one hundred rings is variable, between and within the one-hundred-year intervals. The total footprint of the assembled slab pieces is 37.1 centimeters (14.6 inches) by 238.4 centimeters (93.9 inches) (Figure 3.14).

The overall footprint of the pith sections is 47.5 centimeters (18.5 inches) by 18.1 centimeters (7 inches) (Figure 3.15). The ring closest to the pith is marked -2878 and is thought to be the third or fourth ring from the missing pith (Figure 3.15). Pith piece #3 contains the rings closest to the original pith (Figure 3.16). Since the pith is missing, the age of the remaining rings

cannot be positively ascertained, but a reasonable guess is possible. For comparison purposes,

six cores of bristlecone pines from Sheep Mountain, California, were inspected (Figure 3.17).

Each core contained the pith and measurements were made of the approximate diameters of the

pith and first ring. From these, percentages of first ring widths to pith diameters were calculated

for all six cores (Table 3.4). Concentric circles were drawn on the photograph of the Prometheus

rings closest to the pith (Figure 3.18). The circles created rings with the same diameter as the

last known full ring nearest the pith, labeled "4." Each ring towards the center was sequentially

numbered 1-3. Assuming that each ring was the last ring before the pith, the percentages of ring

widths to pith diameters were calculated (Table 3.4). The Sheep Mountain percentages of first

rings to pith diameters range from 13.0 to 26.5 %. Prometheus percentages of possible first rings

to pith diameters range from 16.4 to 84.4 %.   Based upon the variability in Sheep Mountain trees,

the first ring after the pith could be 4, 3, or 2. Number 4 being the first ring after the pith is

unlikely as the percentage of that third ring to pith diameter is 84.4 %. Of course, the ring widths

could be greater or less than the ones created here. These percentages are conjectures based

upon a consistent ring width that matches the last known full ring.
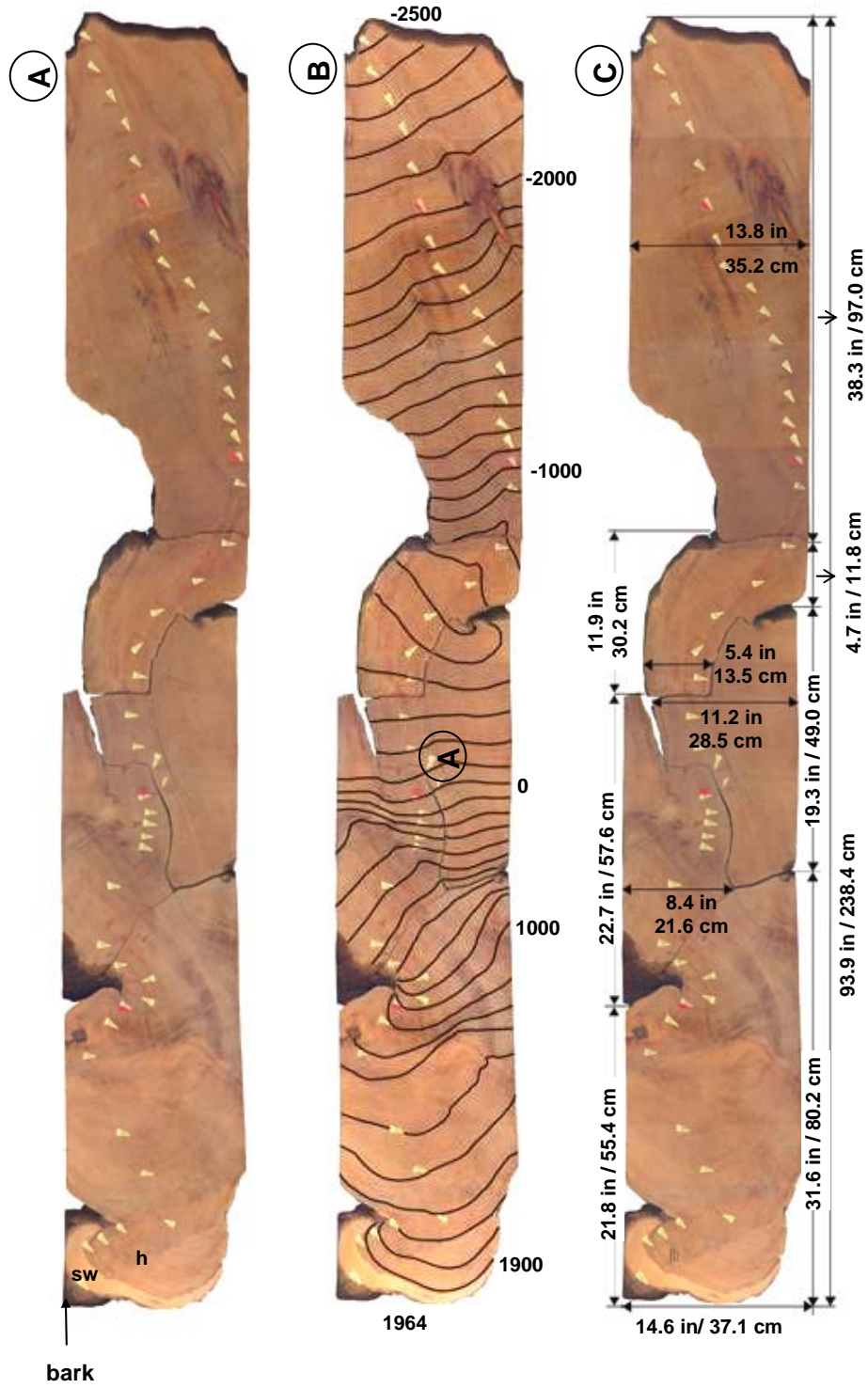
Figure 3.14 Three scans of the surface of the Prometheus main slab pieces. Yellow triangles are tape points that mark the centuries. Red triangles mark the millennia. A. Bark, sapwood (sw), and heartwood (hw) are noted. B. Century rings traced, with notations for 1964, 1900, 1000, 0, -1000, -2000, and -2500. C. Dimensions (Scans made by Martha Gracey 2008).

33
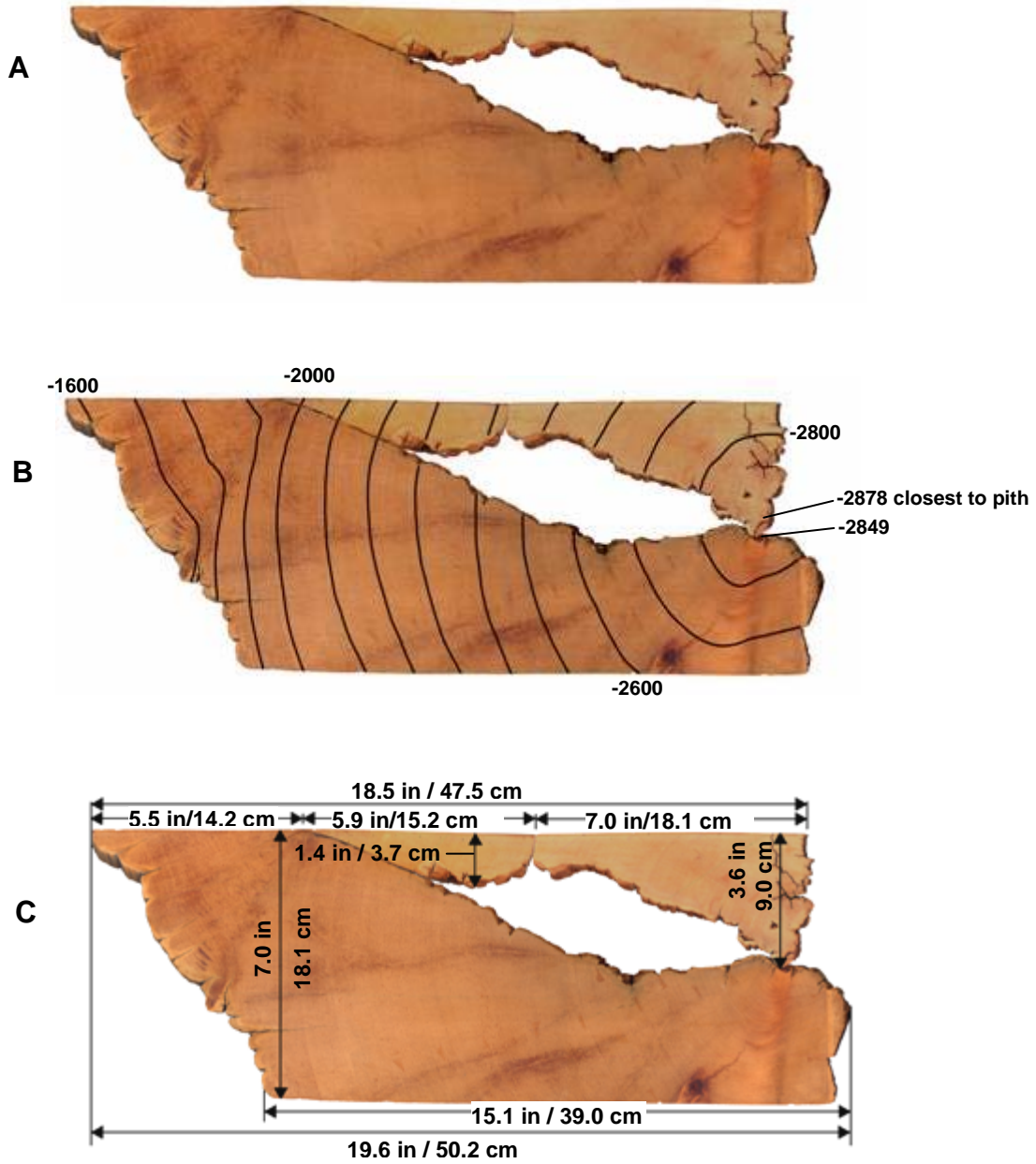
Figure 3.15 Three scans of the surface of the Prometheus pith pieces. A. Unaltered. B. Century rings traced, with notations for -1600, -2000, -2600, -2800, -2878 (ring closest to missing pith), and -2849. C. Dimensions.
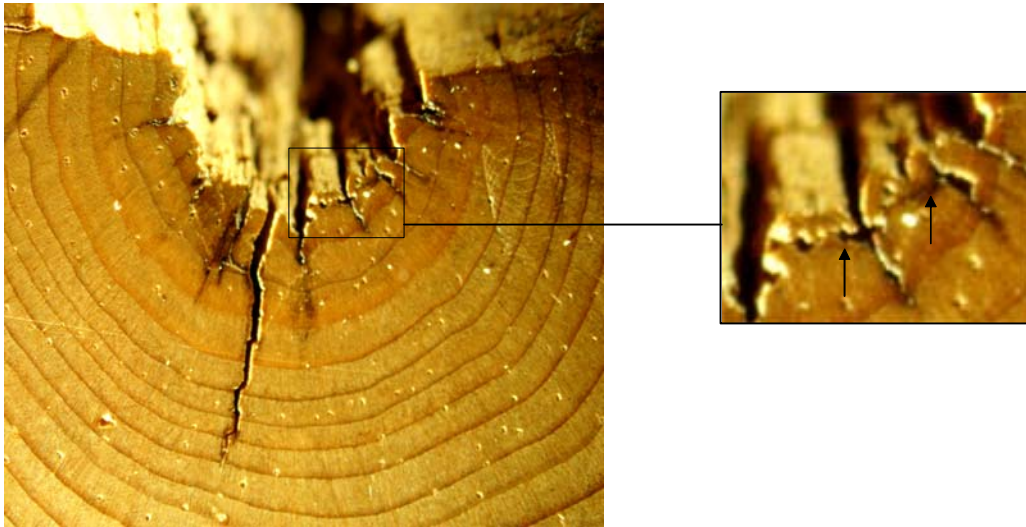
Figure 3.16 Micrograph of the Prometheus rings closest to the missing pith (25X). The small box is a closeup of the last latewood ring. Arrows point to the end of the previous ring (Modified from a micrograph by HJ Arnott).
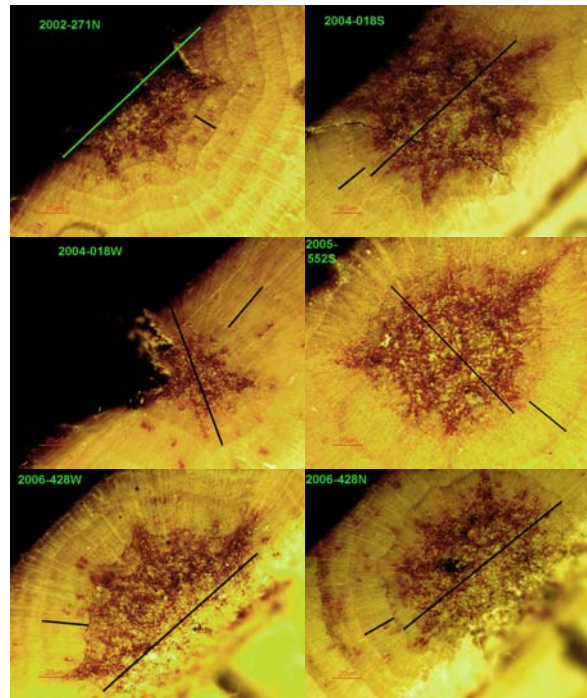
Figure 3.17 Close-up of the pith from cores removed from Sheep Mountain bristlecone pines (White Mountains, California). Lines indicate where the measurements of the pith diameters and first rings were obtained for the information in Table 3.4 (Modified micrographs from HJ Arnott).
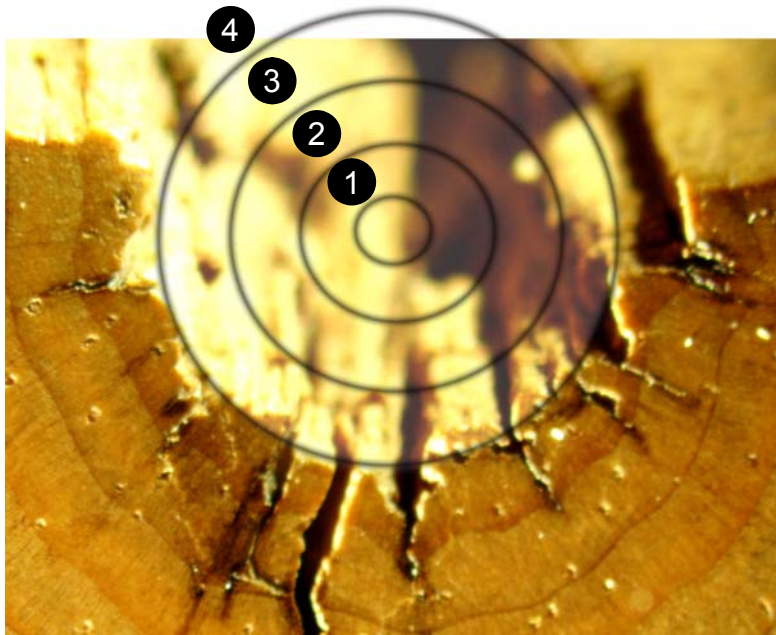
Figure 3.18 Close-up of the Prometheus rings closest to the missing pith. Circle 4 represents the last full ring present. Circles 1-3 approximate missing rings that have the same width as each other. Ring numbers correspond to the data in Table 3.4 (Modified from a micrograph by HJ Arnott).

Table 3.4 Comparison of the Percentage of First Ring Widths to Pith Diameters for Six Sheep Mountain Trees and Prometheus. Data corresponds to Figures 3.17 and Figures 3.18. Prometheus first ring 4 is the last full ring present nearest the pith. Rings 1-3 are possible rings that maintain the same width as Ring 4. Percentages vary in Sheep Mountain trees from 13.0 to 26.5 %. Percentages vary in Prometheus potential first rings from 16.4 to 84.4 %.

Sheep Mountain tree	Percentage of first ring width to pith diameter
2002-271N	13.0
2004-0185S	18.5
2004-18W	36.5
2005-552S	26.2
2006-428N	16.5
2006-428W	22.6
Prometheus first ring	Percentage of first ring width to pith diameter
4	16.4
3	18.5
2	33.3
1	84.4

CHAPTER 4

WOOD ANATOMY

<u>4.1 Overview</u>

This chapter primarily deals with the structure of wood, secondary xylem in pines. One type of xylem cell, tracheids, are the focus of this dissertation. Background information is provided for the organization of xylem, its replication process, and the variability in tracheid lengths that can be traced to (1) genetic controls, (2) changes in the tree as it ages, and lastly, (3) environmental conditions.

<u>4.2 Organization of Wood Tissues</u>

Except for the bark, the trunk of a tree is composed entirely of vascular tissue. The vascular cells, from an interconnected network from roots to leaves, conduct substances throughout the tree. Secondary xylem, the most abundant vascular tissue in a tree, provides the structure that allows water and dissolved minerals to move upward and sometimes downward. Water moves upward in the xylem due to transpiration at the leaf stomatas; as this water evaporates, it creates negative tension on the water in the xylem. Cohesion, the attraction of water molecules for each other, and adhesion, the attraction of water molecules to the walls of the xylem, help to maintain the column of water. Phloem, the second type of vascular tissue, moves dissolved sugars - the product of photosynthesis. Located towards the center of a mature tree, older xylem towards the center is rendered inactive as more xylem is created. In many trees, the sapwood (active xylem) and heartwood (deactivated xylem) can easily be told apart. Heart is usually a darker color than sapwood and is the result of the breakdown of normal cellular products, along with the presence of toxic or inhibitory substances.   In longitudinal and

transverse sections, the layering of the bark, phloem, and xylem can be clearly seen (Figure 4.1) (Esau 1977).

Xylem is organized in a tree in both a horizontal and vertical manner. Xylem rays move products laterally, between the outside and inside of the stem. Elongated xylem cells called tracheids move water vertically, upward from the roots. Xylem ray cells can be parenchyma (storage cells) or ray tracheids that move water horizontally. Longitudinal xylem tracheids can be further classified as earlywood or latewood tracheids. Earlywood tracheids have wider lumens and thinner walls than latewood tracheids.
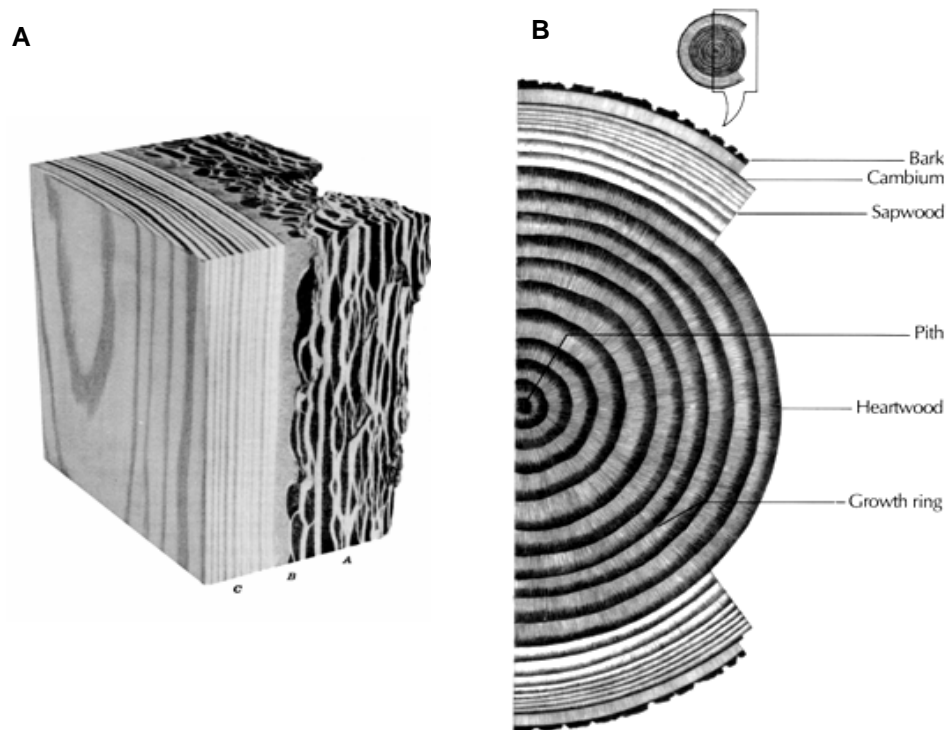
Figure 4.1 Longitudinal and transverse representations of a typical conifer trunk. A. Longitudinal section. From the left to right – the xylem (C), phloem (B), and the bark (A) (Panshin and de Zeeuw 1980). B. Transverse section. The pith (year one) is located at the center of the average tree, followed by heartwood (if present) and sapwood. The vascular cambium lies at the interface between the active xylem (sapwood) and the living phloem. Bark, a combination of inactive phloem and cork, covers the outside of the trunk (Hoadley 1980).

The difference in appearance between early and latewood tracheids is the reason that annual rings can be observed in most tree species. In addition, in pine, the pits (openings between adjacent cells) are round with borders in earlywood tracheids. Latewood tracheids have oval pits with reduced borders (Figure 4.2) (Esau 1965).
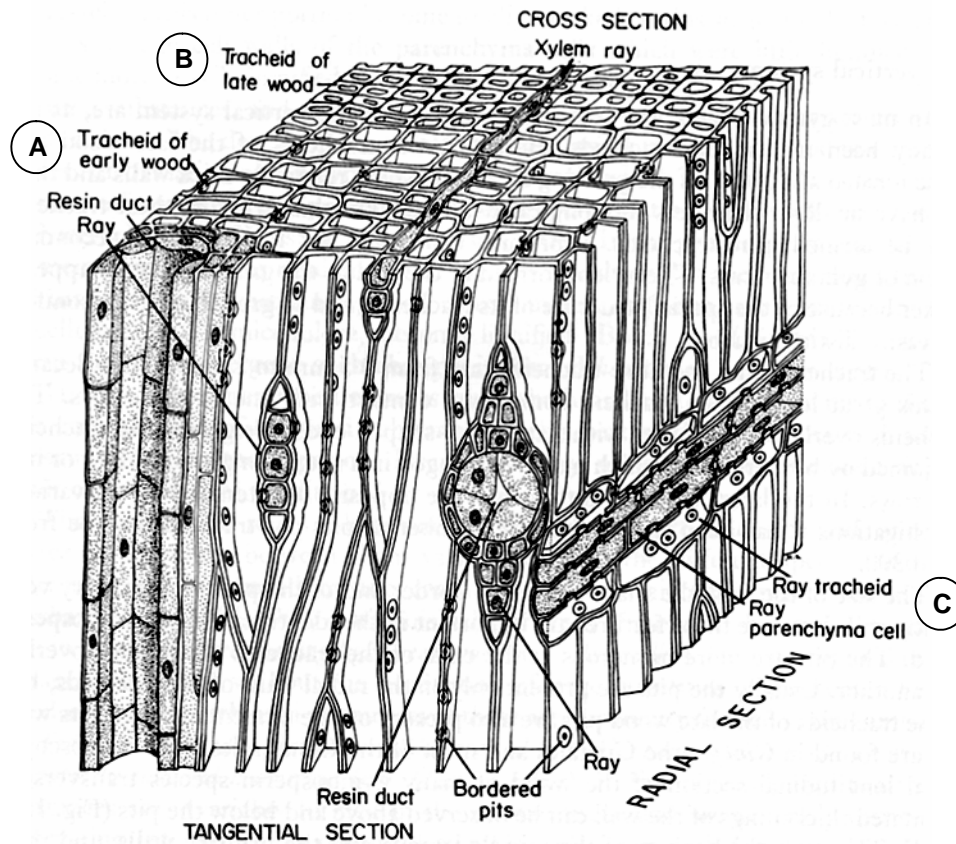
Figure 4.2 *Pinus* secondary xylem cells. A. Earlywood tracheids, in cross section, are characterized by having thinner walls and wider diameters. B. Latewood tracheids are have smaller lumens and cell thicker walls. C. Ray tracheid and parenchyma cells on a radial face (From Fahn 1969).

4.3 Xylem Replication

Two meristematic cylinders of cells lie longitudinally within the trunk and branches of a tree. The cork cambium is located on the outside of the living phloem. When mixed with the deactivated phloem, this cork comprises the bark of the tree, a protective covering that is continuously formed and sloughed off (Esau 1977).

39

Living phloem is separated from active xylem by the vascular cambium – a zone of undifferentiated cells that divide during growth, producing new xylem and phloem. Every growing season, meristematic cells in the vascular cambial zone, called initials, divide to produce two cells. One of the newly divided cells will remain an initial, a cell destined to divide again. The fate of the other cell depends on its location – specifically on which side of the initial that it falls. Cells to the inside of the initial are destined to become xylem cells and those on the outside will become new phloem cells. Initials destined to produce elongated tracheids or phloem cells are called fusiform initials while those that produce ray cells are called ray initials. The first vascular cell that arises from an initial is called a mother cell. Xylem mother cells are often capable of dividing two more times, producing, potentially, four cells total. Phloem mother cells can divide only once more (Panshin and de Zeeuw 1980).

As files of xylem and phloem are formed, and the girth of a tree expands, the need for new initials follows. To fill this need, initials will divide to produce new initials when the expanding circumference requires it. When initials divide to produce new xylem or phloem cells, the division is periclinal, parallel to the outside of the tree. When initials divide to form new initials, the division is anticlinal, perpendicular to the outside of the tree. Two anticlinal forms have been identified in conifers: pseudotransverse and lateral (Figure 4.3) (Panshin and de Zeeuw 1980). Bailey (1923) stated that expansion of the cambium is primarily achieved through pseudotransverse divisions. Lateral divisions have been observed to occur in conifers, but Bannan (1957) determined that lateral divisions comprise 1% or less of all anticlinal divisions. New initials are usually produced in excess of what is eventually required. Those with less contact with ray cells are typically eliminated, as are those that are the shortest (Bannan and Bayly 1956).
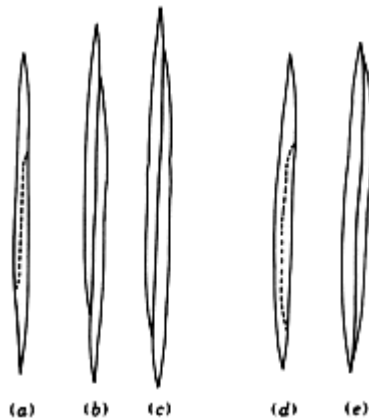
Figure 4.3 Anticlinal divisions of initials in gymnosperms. A – C. Pseudotransverse division. The two daughter cells elongate and slide along each other. D – E. Lateral division. The newly created cell elongates alongside the original (Panshin and de Zeeuw 1980).

The length of tracheary cells is determined by the size of the initials from which they arose and the amount of growth that occurs after division. Tracheids are no more than 10 – 15% longer than the initials from which they arose. In the beginning of the life of a tree, initials are shorter than those to come later and the tracheids are shorter as a result (Bailey 1920). There has been a history of interest in tracheids and why they are shorter during the juvenile phase of a tree's life. Philipson and Butterfield (1967) noticed that a greater frequency of pseudotransverse division leads to shorter initials. When a tree experiences a period of rapid growth, during its early life or during a favorable growing season, the rate of pseudotransverse divisions is the greatest. Then, during the early period of a tree's life, most new initials are retained (shorter ones are not eliminated). The rate of the formation of new cambial initials is rapid and short tracheids are the result. Later on, when the rate of new initial division slows down, the initials and the tracheids become longer (Bannan 1967). Cambial activity at the beginning of the growing season is thought to be initiated by two factors: a mean temperature of 40 degrees F for a week (Wilcox 1962) and the stimulus of diffusing auxins produced by the expanding buds (Wareing 1958).

41

4.4 Variability in Tracheid Length

Tracheids have been shown to vary in length within a growing season – a single annual ring. Bisset and Dadswell (1950) determined that, within growth rings of *Pinus radiata* D. Don*,* earlywood tracheids are shorter than latewood tracheids (Figure 4.4). Within a growth ring of White fir (*Abies concolor* Lindl. ex Hildebr.), earlywood tracheids were also shown to be shorter than latewood tracheids (Anderson 1951). Gerry (1916) found this same trend in Longleaf pine (*Pinus palustris* Mill.) and Douglas fir (*Pseudotsuga menziesii* (Mirb.) Franco*).* Red pine (*Pinus resinosa* Aiton*)* earlywood tracheids were also shorter than those from latewood in studies by Panshin and de Zeeuw (1980) (Figure 4.5).
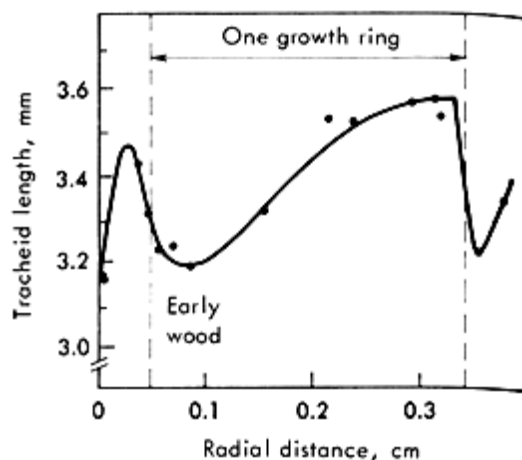
Figure 4.4 Tracheid length variation within *Pinus radiata* growth rings. Earlywood tracheids
are shorter in length than latewood tracheids (Bisset and Dadswell 1950).

Tracheid lengths also vary with height in a tree (Sanio 1872). As tree height increases from the ground upward, tracheid length is longest at one-third of stem height, decreasing above that point (Richardson 1964). For red pines (*Pinus resinosa)*, Panshin and de Zeeuw (1980) determined that the shortest tracheids were found at ground level. Tracheid lengths increased to a maximum length at twelve feet and then decreased as the height approached the crown at 28 feet.

Tracheid lengths vary between stems and branches, with branches having shorter tracheids than the stems from which they arose from (Sanio 1872). Tracheids in *Pinus resinosa* stems were longer than the ones in the branches (Panshin and de Zeeuw 1980).
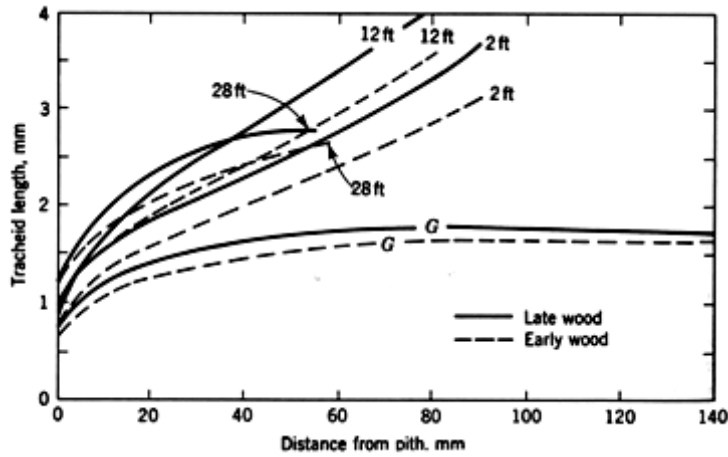
Figure 4.5 Tracheid length variation in height, earlywood vs. latewood, and distance from pith for *Pinus resinosa*. Earlywood tracheids were shorter than latewood tracheids and tracheid lengths increased with distance from the pith. Tracheids increased in length from ground level (G) to twelve feet from the ground, then decreased to the crown at 28 feet (Panshin and de Zeeuw 1980).
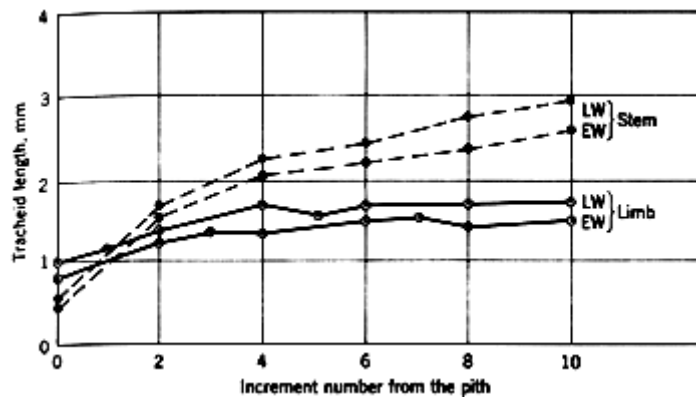
Figure 4.6 Tracheid length variation between stems and limbs of *Pinus resinosa*. Stem tracheids are shorter than limb tracheids (Panshin and de Zeeuw 1980)

Tracheid lengths of Frasier fir (*Abies fraseri* (Pursh) Poir.) were shorter on the windward side of a mountain versus those on the leeward side (Telewski and Jaffe 1986). For white spruce

(*Picea glauca* (Moench) Voss), lodgepole pine (*Pinus contorta* Douglas ex Louden), and Eastern

white pine (*Pinus strobus* L.), tracheids were shorter and ring widths were greater on the side of

the tree away from the wind (Bannan and Bindra 1970). Liese and Dadwell (1959) determined

that tracheids were shorter on the sunny side of various species of *Pinus* compared to the shaded

side. They conjectured that additional warmth on the sunny side of the tree stimulated cell

divisions, thus resulting in shorter tracheids.

The trend of conifer tracheid lengths increasing in age from pith towards the outside of

the tree has been well-documented. Many researchers have observed a consistent rapid

increase in tracheid lengths during the early part of a tree's life – the "juvenile" phase that takes

place between ten to forty years of age (Table 4.1). The rapid juvenile growth from pith outward

is thought to be the result of a close association of the apical meristem with the lateral meristems.

As the crown moves upward, the influence of the auxin from the apical meristem diminishes,

tracheid growth rates decline, and mature wood is formed (Figure 4.7) (Panshin and de Zeeuw

1980).

Bailey and Shepard (1915) recorded tracheid lengths for four trees. The longleaf pine

(*Pinus palustris* Mill.) was studied over the greatest time period (225 years). Tracheid lengths

increased rapidly in the juvenile phase, but afterwards, the tracheids fluctuated in size. For the

longleaf pine, the lengths increased and decreased five times (Figure 4.8).
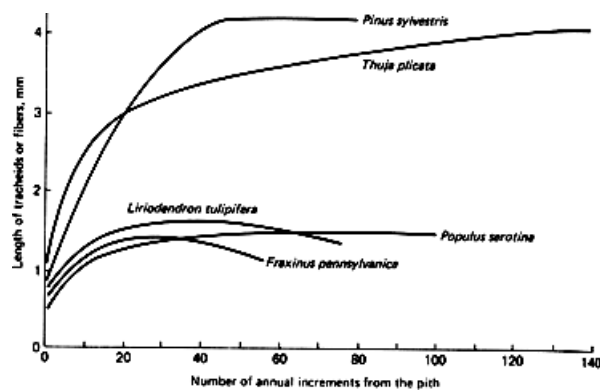
Figure 4.7 Tracheid length vs. age for four trees. The top two curves are conifers – *Pinus sylvestris* and *Thuja plica* Donn ex D. Don. Both trees experienced sharp tracheid length increases during the juvenile part of their lives (Panshin and de Zeeuw 1980).
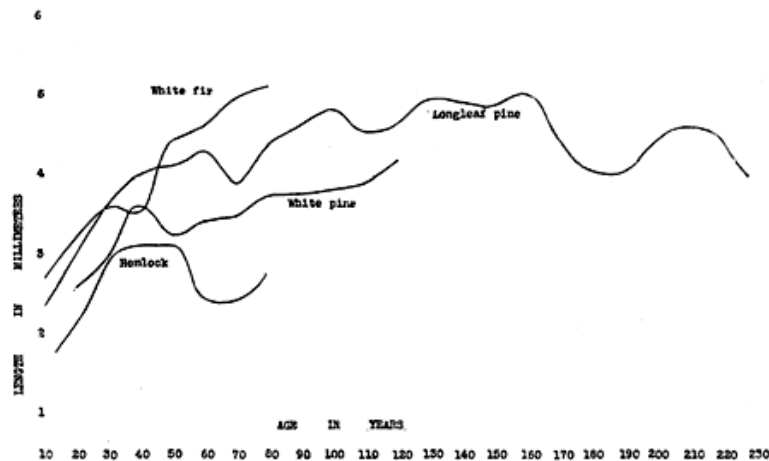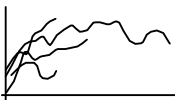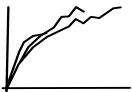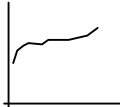
Figure 4.8 Tracheid length vs. tree age for four different conifers – white fir, longleaf pine, white pine, and hemlock. The juvenile growth phase is evident, but the tracheid lengths did not stay constant, instead increasing and decreasing (Bailey and Shepard 1915).

Attempts have been made to correlate tracheid lengths to genetics. Dadswell *et al* (1961) studied the extent to which certain wood characteristics are affected by heredity. Cell lengths were compared between a clonal set of *Pinus radiata* trees and a set of trees that were, presumably, not related to each other. Variations in tracheid length were correlated to the genetic relationships that the trees shared with each other. Echols (1955) demonstrated that the initial tracheid length of the F1 generation of slash pine (*Pinus elliottii*) trees corresponded to the lengths of their parents. In other words, trees with long or short tracheids produced progeny with tracheids that were an average of those of the parents.

Kienholz (1931) investigated the effect of site quality on the growth of lodgepole pines. He compared tracheid lengths of eighteen lodgepole pine trees (*Pinus contorta*) from three different habitats in the Cascade Mountains of southwestern Washington: sphagnum bog, virgin timber, and lava bed. There were appreciable differences in nutrient and moisture availability, soil and air temperature, and relative humidity between the sites. Competition for resources was deemed the greatest in the lava bed site. Pines in the lava beds had the slowest growth rate (smallest widths in annual rings), as well as the least amount of latewood, the smallest radial diameters of tracheids, the thinnest tracheid walls, and the shortest tracheids.

45

Table 4.1 Studies of Conifers Where the Authors Observed Tracheid Length Increases From Pith Outward During the Juvenile Phase. The number of trees in each study are noted. Thumbnail graphs were created by tracing over study graphs. The y-axis is tracheid length and the x-axis is age.

Author(s), year	Species (number of specimens)	Thumbnail graph
Anderson, 1951	White fir (1), Noble fir (1), Douglas fir (2)	
Baas *et al*, 1986	Great Basin bristlecone pine (2)	
Bailey and Shepard, 1915	White pine (1), Longleaf pine (1), Red spruce (1), Eastern hemlock (1), White fir (1)	
Bisset *et al*, 1951	Monterey pine (4)	
Chalk, 1930	Sitka spruce (1)	No graph available
Erickson and Harrison, 1974	Douglas fir (7)	
Kienholz, 1931	Lodgepole pine (18)	
Kramer, 1957	Loblolly pines (12)	
Lindstrom, 1997	Norway spruce (57)	
MacMillan, 1925	Red spruce (10)	No graph available
Taylor *et al,* 1982	White spruce (40)	

An inverse connection between tracheid length and ring width has been established. Bannan (1960) examined the relationship between tracheid length and ring width in white spruce (*Thuja occidentalis* L.) and postulated that a high rate of pseudo-transverse divisions, such as those that increase the circumference of the cambium, produce short cells, and that a slow rate of pseudo-transverse division produce longer cells. When trees are growing rapidly, usually due to favorable growing conditions, pseudotransverse divisions occur at an increased rate, to keep up with rapid circumferential growth. White spruce tracheid lengths were shown to shorten during rapid growth. Bisset *et al* (1951) studied Monterey pine (*Pinus radiata)* wood and determined that wider growth rings had the lowest average tracheid lengths and narrow growth rings had the highest average tracheids lengths. In 271 slash pine trees (*Pinus elliottii*) in 15 geographic areas across South Carolina and Mississippi, tracheid lengths, ring widths (radial growth), and specific gravity were measured. Mean tracheid length decreased when ring width increased, specific gravity increased, and when site quality decreased (Strickland and Goddard 1966). Tracheid length decreased with wider ring width in Sitka spruce (*Picea sitchensis* (Bong.) Carrière) (Dinwoodie 1963). In 2000, Fujiwara and Yang studied four Canadian conifers, examining one tree of each. Tracheid length decreased as ring width increased for jack pine (*Pinus banksiana* Lamb.) (r^2 = 0.508), balsam fir (*Abies balsamea* (L.) Mill) (r^2 = 0.496), and black spruce (*Picea mariana* (Mill.) Britton, Sterns & Poggenb.) (r^2 = 0.826).

CHAPTER 5

METHODS

5.1 Overview

Three separate studies can be identified in this chapter: crossdating, comparing the length of tracheids to age, climatic events, and ring width, and the direct comparison to ring width to climate. Crossdating the main slab to the pieces containing the rings closest to the pith was necessary in order to identify additional sampling sites for the tracheid length study.   The crossdating study was then expanded to cross date Prometheus to other trees: Buddy and two nearby tree ring chronologies.   The original, and by far the most intensive study, was to measure tracheid lengths.

The tracheid length study had several time-consuming phases:

- Determining the sampling points on the main slab by tracing pre-marked points to the outside of the slabs and, when those weren't available, counting rings to determine the sampling sites.

- Cross dating the main slab to the pith pieces to increase the amount of sampling points on the pith pieces.

- Preparing glass vials, removing the toothpick-sized wood slivers, and placing them in the correct vials.

- Chemically separating the tracheids.

- Mechanically separating the tracheids onto glass slides.

- Assembling composite micrographs of the slides.

- Measuring and compiling the tracheid lengths.

- Analyzing the tracheid length data.

5.2 Crossdating

5.2.1 Overlapping Main Slab and Pith Pieces of Prometheus

Crossdating is used to assign calendar years to individual rings by comparing tree ring sequences to each other. Before taking any samples from Prometheus, it was necessary to crossdate the main slab to the pith piece to extend the availability of samples closer to the rings near the pith. The main slab ends at the ring dated -2564 and the ring closest to the pith was originally estimated to be around -2850. Therefore, we could remove the years -2600, -2700, and -2800 from the pith piece, if we identified the sampling points. The pith pieces had not been conclusively dated to our knowledge, so crossdating techniques were used to overlap the largest pith piece (#1) with the main slab. Using a handheld microscope, the Proscope HR (Bodelin Technologies) (Figure 5.1), successive micrographs of the main slab surface were captured at 100X magnification. The images were merged together into a continuous montage with Photoshop 8.0 (Adobe). 270 rings were captured in a straight line from the oldest section of the main slab, encompassing the years between -2564 and -2295 (Figure 5.2). Since the pith "piece" is actually three pieces, 1056 rings were captured from the larger section (#1) (Figure 5.3). With Image-Pro Plus (Media Cybernetics), the widths of the rings in the montages were measured and the data compiled in Excel (Microsoft). Dr. Tom Harlan of the University of Arizona generously allowed the use of his crossdating program, Crossdate, to compare the ring width series of the main slab and pith pieces to each other. All raw ring width measurements had to be converted to a format recognized by the crossdating program; a text file of the measurements in a continuous four digit string was built and saved as a .dig file. The largest pith piece was then crossdated with the main slab piece.

49
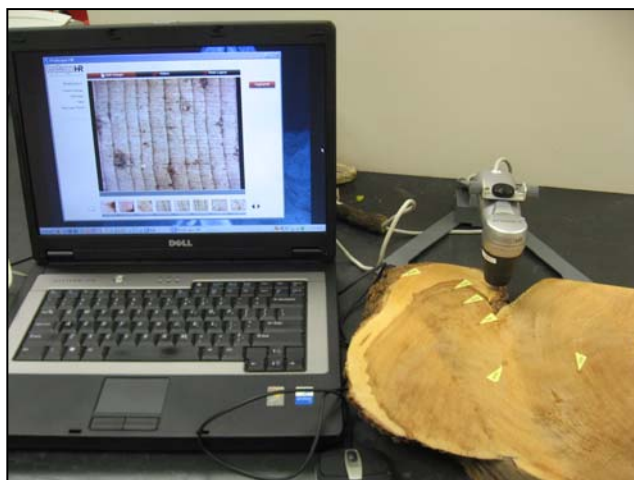
Figure 5.1 Example of the Proscope HR capturing images of Prometheus. In this photograph, the microscope is attached to a stand included in the kit. The microscope could be handheld, but with greater magnification (100X or 400X), the stand was necessary to stabilize the image and reduce motion blurring.
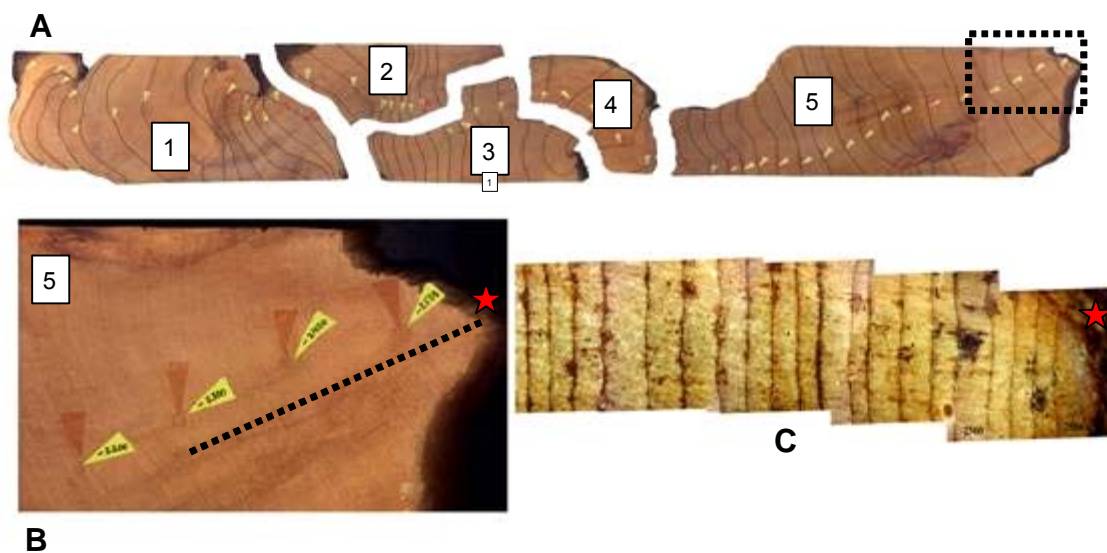
Figure 5.2 Location of the Proscope camera path on the #5 piece of the main slab. A. All five main slab sections. The dotted box on piece #5 encloses the location of the camera captures. B. Magnification of the dotted box in A. The dotted line indicates the path of the camera as it was moved progressively from the left to the right. C. Five Proscope digital micrographs (100X) knit together and ready for measuring. The red stars in B and C are placed at the last ring of the main slab, -2568.
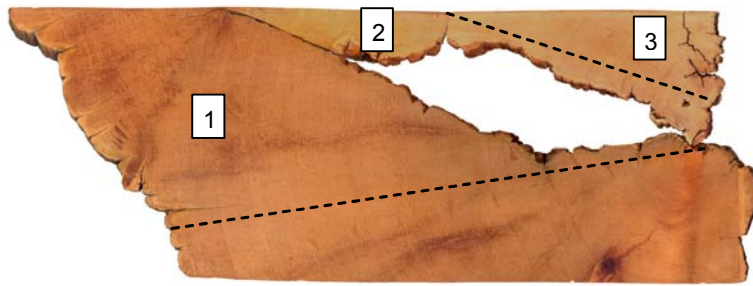
Figure 5.3 Location of the Proscope camera path on the pith pieces #1 and #3. Dotted lines on pieces # 1 and #3 indicate the location of the camera captures The right end of the line on piece #1 ends on ring #44 (relative to the last ring on piece #3) and the right end of the line on piece #3 ends on the ring closest to the missing pith, -2878.

5.2.2 Crossdating Prometheus to Additional Trees

Three additional attempts at crossdating Prometheus were made. Two bristlecone pine chronologies were available of tree stands nearby to Prometheus: Indian Garden and Hill 10842. The data for these two chronologies were already in a form recognized by the Crossdate program. The third crossdating attempt was to correlate Prometheus to a single bristlecone pine tree located approximately one hundred yards away from Prometheus. At the same time in 1964 that the sections of Prometheus were removed, a v-shaped section was cut from this additional tree, designated as Buddy. 300 rings were captured from both Buddy and Prometheus, dating backwards from 1900 to the year 1600. The same procedure outlined in the preceding section for taking digital micrographs, merging the images, and measuring the ring widths was employed for Prometheus and Buddy rings. The data was converted to the CrossDate required format and inputted for analysis into the CrossDate program.

<u>5.3 Tracheid Length Measurements</u>

5.3.1 Determination of Primary Sampling Sites

Before the crossdating attempts, the main slab pieces were meticulously examined for determining the approximate location of the even century years. Donald Currey had already marked the surface of the slabs with the accepted practice of piercing the wood surface with a sharp point to produce a "dot." One dot would indicate decade point other than a century or fifty-

51

year point. Two dots would be made for the fifty-year point. Three dots would indicate a century

mark. All centuries were marked, but fifty-year and decade points were sporadic. Since sampling

would only occur at the edges of the slabs, the century marks were traced to the outside edge

and marked with small flags of colored tape. In the cases where the century marks were not

available (when an overlapping slab piece did not contain the mark), one hundred rings were

counted from a known century point. When the main slab piece centuries were identified,

crossdating was performed to date the pith pieces. After the pith pieces were dated, tape points

were added to mark the points for sampling.

5.3.2 Removal of Wood Samples from Prometheus

The combined main slab of Prometheus has two long edges, roughly parallel to each

other. They were designated the W and E sides. The "W" and "E" were originally meant to

indicate the west and east sides of the tree, but it wasn't until after the preparation of the glass

vials and spreadsheets that it was discovered that the face of the slab that was sanded and

facing up was actually the underside of the slab. This meant that the W and E letters could not

represent west and east. Due to the fact that the samples had already been removed and placed

in marked vials, it was decided to keep the W and E designations but make it understood that

these were simply letters indicating a side of the slab and not cardinal directions (Figure 5.4).

Figure 5.4 Main slab of Prometheus with the W and E sides indicated. Dark lines trace the
century rings from edge to edge. The red arrows indicate years where the sampling sites
were unavailable.

With a dremel tool fitted with a diamond-coated burr tip, glass vials were prepared for the

wood samples by etching the year and side (W or E) onto the glass surface of the vials and onto

the lids (Figure 5.5). Using razor blades and forceps, Dr. Howard Arnott removed 85 toothpick-

52

size samples from both edges of the main slabs between and including the years of 1964 and -2500, with the following exceptions: 1900E, 1800E, 1700E, 1200E, 1100E, 1000E, 900E, 700W, 600W, -200E, and -300E. These sample sites were not available from the edges and further destruction of the wood was not deemed necessary at this point. Figure 5.6 illustrates how the years 1900E, 1800E, and 1700E end within the slab and were therefore omitted from the sampling.

Figure 5.5 Glass vial etched with sample year and side of Prometheus. In this vial, the year was 1900 and the side was W.
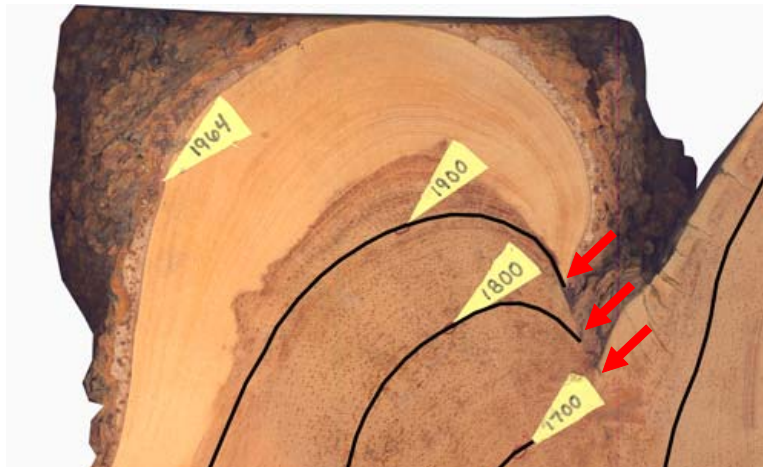
Figure 5.6 Scan of inaccessible sampling sites for Prometheus years 1700E, 1800E, and 1900E. Red arrows point to the E-sites that could not be reached with drilling or damaging the slab.

With razor blades and forceps, eight toothpick-size samples were removed from the century points on both edges of pith piece #1 between and including the years of -2600 and -2800. In addition, two samples of -2834 were removed.

5.3.3 Chemical and Mechanical Separation of Tracheids

The order of the samples chosen for maceration was random, with vials chosen without knowing their year. Prior to their processing, the plastic caps from the vials were removed and a small hole was drilled through the caps to allow for the expansion of the maceration solution. Once a week, approximately twenty milliliters of 1:1 30% hydrogen peroxide and glacial acetic acid was added to each of five vials and the caps were screwed on tightly. The vials were placed in a 70 degree C oven. After one week, the peroxide/acetic acid solution was replaced. After two weeks, the separation solution was drained off and replaced with deionized water. Two standard glass microscope slides per sample were etched with the dremel tool, identifying the year and the number 1 or 2. In turn, each sample in the group was prepared for mechanical separation with three three-minute rinses in deionized water. After the water rinses, the samples were placed into 5% safranin stain and remained there for five minutes. Five three-minute rinses in fresh deionized water finished the process. The samples were gently stirred with a needle probe for the first three water rinses and the safranin stain, with progressively more vigorous handling in the last five water rinses. By the end of the rinsing and staining processing, the tracheids were completely separated or in small clumps. With the aid of a dissecting scope and needle probes, tracheids were spread out upon the etched slides, each slide generously coated with deionized water. The slides were moved carefully to a laboratory slide warmer to dry off the remaining water. Glass coverslips were not applied at any point. Since the tracheids stuck well to the glass slides, no further preparation was necessary. All samples were processed and stored in marked slide boxes before the measurement phase.

5.3.4 Digital Capture and Measurement of Tracheids

An Eclipse 80i research microscope (Nikon Instruments) was used to capture digital images of all the slides. The "big picture" feature in the NIS Elements program (Nikon) acquired

54

successive live captures at 40X magnification, row by row, and assembled them into a micrograph of the entire slide (Figure 5.7). An average slide required approximately 8 images high X 15 images wide (120 total) for each montage. Upon completion of the merging of the images, a measuring tool of NIS Elements was used to trace and record the measurements of fifty tracheids per sample (Figure 5.8). Depending upon the quality of the tracheids, this necessitated the use of one or both slides. Care was taken to examine each tracheid for intact ends. All tracheid lengths were recorded on a Microsoft Excel spreadsheet.
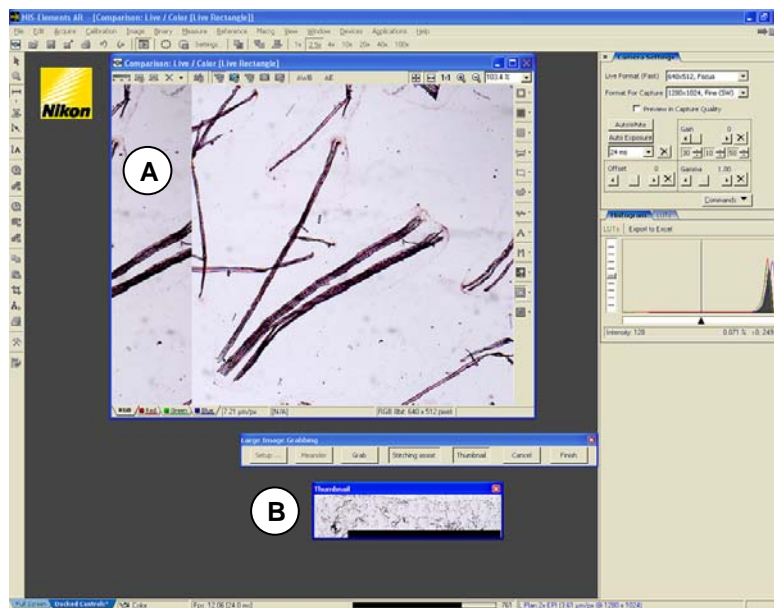
Figure 5.7 Screenshot of NIS-Elements "big picture" feature. This feature captured and knit together live images to create a montage. The left part of the large image (A) was provided by the program and the slide was moved on the stage to match up an approximate overlap. The incomplete montage (B) was supplied to watch the progress of the process.

5.3.5 Preliminary Study for Determining Sample Size

Before examining the 170 samples from Prometheus, tracheids were examined from a random sample of Prometheus. This test sample had been removed prior to the beginning of this study. The age of the test wood was unknown. Two slides were prepared from the single sample using the separation and measurement techniques detailed in section 5.3.3 and 5.3.4. Utilizing
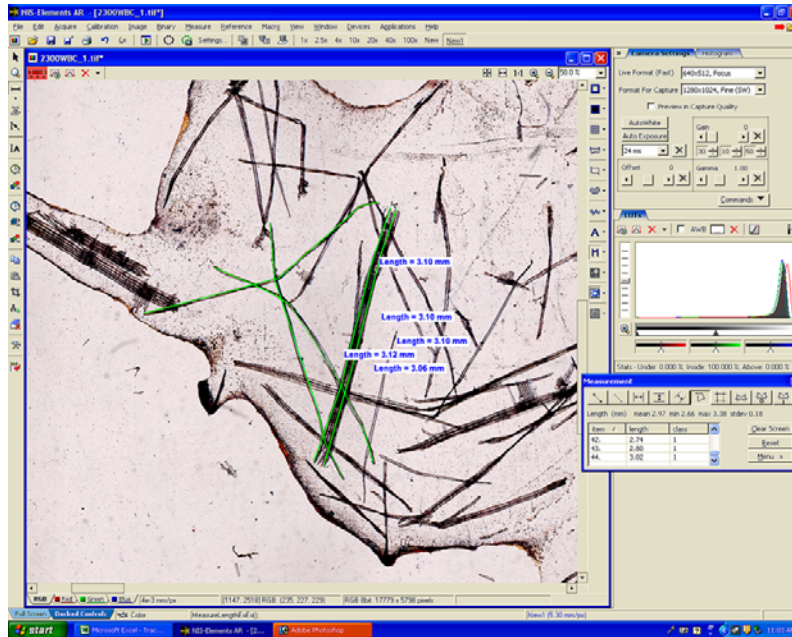
Figure 5.8 Screenshot of the NIS-Elements measuring tools. Suitable tracheids were traced and the lines and measurements were added to the screen. This feature prevented the re-measuring of tracheids. Lengths were compiled by the program and were imported to an Excel spreadsheet.

both slides, the lengths of 140 tracheids were measured and the data compiled and analyzed to determine a sample size that would provide 95% confidence in the mean.

In addition, 10, 20, 30, 40, 50, 60, and 70 tracheids were independently measured from each test slide to provide visual confirmation of the projected number of tracheids. The means of each group were graphed vs. the number of tracheids measured for each slide. Error bars, ± 2 standard errors, were added to bracket an approximate 95% confidence interval for each point.

5.3.6 Study to Determine Consistency of Measurements Along One Ring

In order to confidently combine the data from both the W and E sides, it was necessary to determine the tracheid length variation in a single annual ring of Prometheus. Fortuitously, the side edge of one of the main slab pieces (#1) exposed the entire length of one ring, dated 638. Five samples at even intervals were removed from ring 638 and prepared for measuring using the chemical and mechanical separation techniques detailed in sections 5.3.3 and 5.3.4. Fifty

56

tracheid lengths were measured from each of the five samples and the data was inputted into an Excel spreadsheet. An one-way ANOVA was performed to test the hypothesis that the means were equal between the five samples. If a difference was detected ($p < 0.05$), pairwise t-tests were run between all possible pairs of samples.

5.3.7 Analyses of Assumptions for the Primary Study Data

Systat 10 was used for generating histograms, normality plots, and Kolmogorov-Smirnov one-sample tests for the W and E data, and the combined data (W + E). Scatterplots of the all sample means along with error bars relating to 95% confidence intervals were constructed for the W and E data, and the combined data.

5.3.8 Statistical Analyses

With Systat 10, a paired t-test was performed with the W and E data sets. Both tracheid length data sets (W and E) were regressed against ring number from the pith. TableCurve 2D produced graphs for all data sets along with polynomial curve equations. A regression tree was performed in Systat 10 to determine improved correlations in subsets of the data.

<u>5.4 Additional Studies</u>

Mean tracheid lengths from the combined data set were compared to extreme periods of warm, dry, wet, and cool conditions (Salzer and Kipfmueller 2005).

From a 1000 dpi scan of the main slab, the mean widths of 100-year intervals were measured, from the youngest complete century 1900 to 1800, to the oldest complete century on the slab, -2400 to -2500.   Each century was measured at equidistant points at least six times up to a maximum of thirteen times. Mean widths were compared to historical long-term temperature events.

Using the same scan, the width of individual rings were measured at the W sampling sites. The number of rings measured at each century mark sample was variable (two to thirteen) (Figure 5.9).   The widths were averaged and compared to associated tracheid lengths.
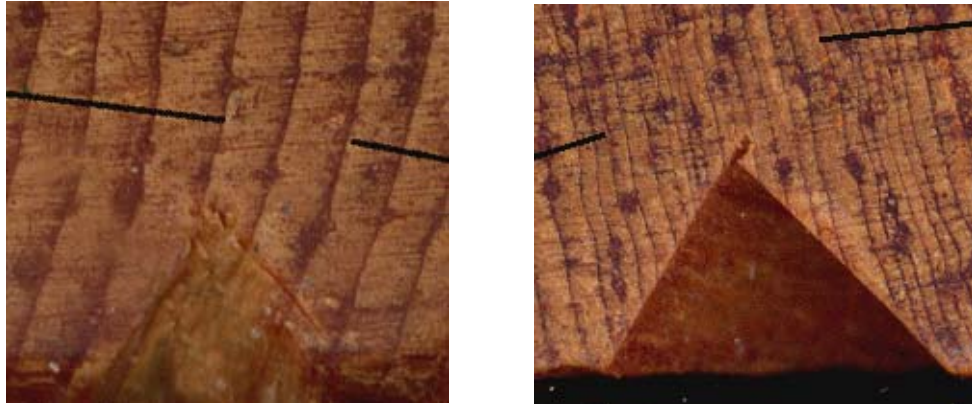
Figure 5.9 Two tracheid length sampling sites on Prometheus. Black lines enclose the rings chosen for measuring. A. -600 sample site. The width of two rings were measured. B. -1600 sample site. The widths of thirteen rings were measured.

CHAPTER 6

RESULTS

6.1 Overview

This chapter will present results in the order that the methods were explained in Chapter 4. Cross dating results will be followed by the tracheid length studies.

6.2 Crossdating Results

6.2.1 Overlapping Main Slab and Pith Piece of Prometheus

The main piece required 57 Proscope micrographs to cover 270 rings, encompassing the years between -2295 and -2564. Pith section #1 required 151 Proscope shots, to cover 1056 rings. The CrossDate program successfully matched the rings measured on the #5 main section with the rings on pith piece #1. The program reported a correlation value of 0.805. A montage of screenshots of the CrossDate program results illustrates the ability of the program to take numerical measurements and project a skeleton plot to demonstrate the matchup of the rings (Appendix A). The absence of a line for a ring indicates a value that falls in a medium range of widths. Longer lines indicate wider rings than the medium values and shorter segments are shorter than the medium values. In addition, it was possible to match all three pith sections to each other. The overlap of the main slab and pith pieces confirms that there are at least 4798 unique annual rings between the combination of the pith sections and the main slab sections.

6.2.2 Crossdating Prometheus to Local Bristlecone Chronologies and to Buddy

Master tree chronologies were available for download at the International Tree Ring Data Bank (World Data Center for Paleoclimatology 2008). Data for each year in the chronology had been averaged and standardized. These chronologies are used to match against a single tree to

59

find missing rings and to definitively date the single tree. Hill 10842 (Graybill) is a compilation of the tree ring sequences of 45 trees and it spans the years between 0 AD and 1984. The Indian Garden (Graybill) chronology used 54 trees to complete the series, spanning the years between - 2370 and 1982 AD. Prometheus and Buddy rings 1900 – 1600 were crossdated with the two master chronologies, with correlation values between 0.520 and 0.650 (Table 6.1). Buddy and Prometheus were crossdated, resulting in a similar value, 0.619.

Table 6.1 Crossdating Correlation Results for Matches Between Prometheus, Buddy, Hill 10842 Master Chronology, and Indian Garden Chronology. Correlation values are similar, ranging from 0.520 to 0.650.

CrossDate matches	Correlation value
Prometheus v. Buddy	0.619
Prometheus v. Hill 10842	0.591
Prometheus v. Indian Garden	0.650
Buddy v. Hill 10842	0.520
Buddy v. Indian Garden	0.647

6.3 Tracheid Length Measurements

6.3.1 Preliminary Study for Determining Sample Size

The collective mean of the pilot study tracheids was 2.70 mm and the standard deviation was 0.379 (n=140). For a 95% confidence in the mean, the projected number of tracheids to measure per wood sample was 31.4. With each 1% increase in the confidence level, the number of measurements increased dramatically. It was decided to measure 50 tracheids per sample. This sample size produces measurements in excess of the 96% confidence level (Table 6.2). Increasing the number of tracheids counted over 50 follows a path of diminishing returns.

Table 6.2 Percentage Confidence in the Means of Prometheus Preliminary Study Tracheid Lengths. The sample size of 50 tracheids to measure was selected. This number slightly exceeds 96% confidence in the mean.

% Confidence in the Mean	Number of tracheids to measure per sample
95	31.4
96	49.1
97	87.3
98	196.4
99	785.5

The pilot study of tracheid lengths had a normal distribution. A Kolmogorov-Smirnov one sample test for normality returned a $p = 0.404$, well above the 0.05 significance level. The histogram and the normal probability plots confirm that the data appears normally distributed (Figure 6.1).
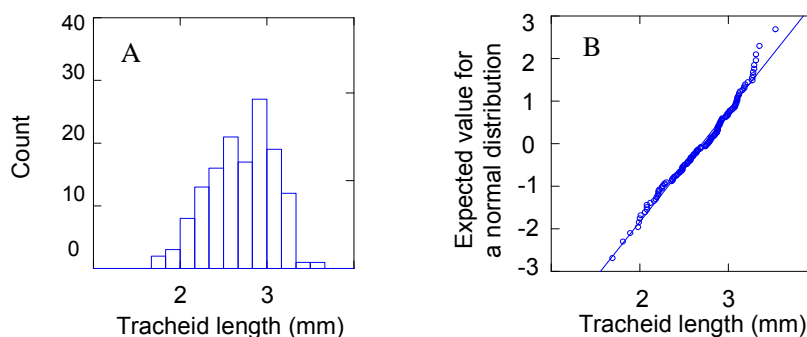
Figure 6.1 Investigating the normality of the preliminary study tracheid lengths (n = 140). A. Histogram. The shape of the data resembles a normal distribution. B. Normal probability plot. The lengths match up with the expected normal values, producing a straight line relationship.

From each of the two slides prepared in the preliminary study, 10, 20, 30, 40, 50, 60, and 70 tracheids were measured. Because the group sizes were unequal, a Levene's test for equality of variances was run. An one-way ANOVA was performed with the residuals of the data, testing the hypothesis that the variances of the groups were equal. With a $p = 1.0$, the variances were

determined to be statistically equal. The one-way ANOVA of the slide #1 preliminary study tracheids, testing the hypothesis that the means of each set are all equal to each other, confirmed that all the group means were equal to each other (p = 0.95).

The one-way ANOVA of the slide #2 pilot study tracheids determined that some or all the group means were not equal to each other (p = 0.036). Because the group sizes were unequal, a Levene's test for equality of variances was run. An one-way ANOVA was performed with the residuals of the data, testing the hypothesis that the variances of the groups were equal. With a p = 1.0, the variances were determined to be equal. After verifying homoschedasticity (an important assumption for post hoc tests), it was acceptable to determine which group means were unequal. Post-hoc pair-wise tests using least square means were performed. The means were determined to be different between the 10 and 70 tracheid groups (p = 0.014).

Graphically, the statistical tests were supported (Figure 6.2). For slide #1 tracheids, all confidence intervals overlapped. For slide #2, the error bars of the 10-tracheid group overlapped all of the groups, except for the 70-tracheid group. Based on the calculation of the 95% confidence value and the statistical and graphical evidence, the choice of fifty tracheids to measure per sample appeared justified.

6.3.2 Study to Determine Consistency of Measurements Along One Ring

A one-way ANOVA, testing the hypothesis that the means of two or more of the sample groups along ring #638 were not equal, returned p = 0.000000 - there were strong differences detected between some or all of the sample groups. Homoschedasticity and normality were confirmed with a Levene's test (p = 1.00) and five Kolmogorov-Smirnov tests for normality. Post-hoc pairwise t-tests (Bonferroni), testing for individual differences between each set of samples found that eight out of ten pairs of sample means were not equal to each other (Table 6.3). The means were statistically identical between groups 1 and 5 and 4 and 5. Graphically, this result is also supported (Figure 6.3). Error bars do not overlap for any groups, except between 1 and 5 and 4 and 5.

62
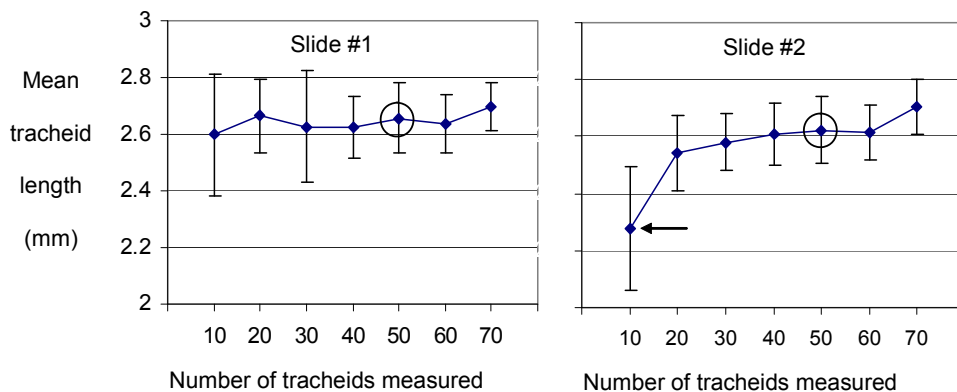
Figure 6.2 Mean tracheid length of preliminary test tracheids versus the number of tracheids independently counted on slides #1 and #2. Error bars equal +/- 2 standard errors. The groups that contained fifty tracheids are circled. On slide #2, an arrow points to the group containing ten tracheids. The pairwise tests determined a significant difference between the means of the 10 and 70 tracheid group.

6.3.3 Tracheid Length Measurements From Prometheus

132 of 135 Kolmogorov-Smirnov tests for the normality of all sets of data within the three groups, W, E, and combined W + E, were not significant (p > 0.05). Since the K-S test compares the distribution of your data to a known distribution (in our case, a normal distribution), finding significance means that the distributions are significantly different from each other. Three years in the combined group did not statistically resemble a normal distribution. For the years 1964C, 800C, and 500C, the K-S p-values were 0.0, 0.011, and 0.036, respectively. When the histograms and normality plots were drawn for all 135 sets of length data, the reason became clear for the deviation from normal; the distribution of the combined data for these three sets became bimodal (Figure 6.4). The means from these three years were different enough that they couldn't combine to form a normal distribution.

Table 6.3 Pairwise T-tests Between the Five Tracheid Length Groups of Ring #638. All group means were significantly different, except for groups 4-5 and 1-5 (shaded in gray).

Groups tested	p	Significant difference Yes/No
1 – 2	0.000	Yes
2 – 3	0.006	Yes
3 – 4	0.000	Yes
4 – 5	1.000	No
1 – 3	0.000	Yes
1 – 4	0.031	Yes
1 – 5	0.111	No
2 – 4	0.000	Yes
2 – 5	0.000	Yes
3 - 5	0.000	Yes
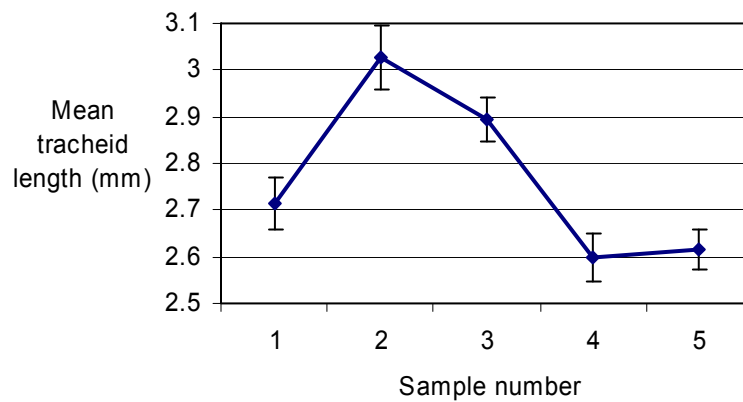
Figure 6.3 Mean tracheid length of Prometheus wood samples 1-5 taken along the edge of the ring dated 638. Fifty measurements were collected from each sample. Bars indicate a 95% confidence interval around each mean. Significant differences were found between all groups, except for between 1 and 5 and 4 and 5.
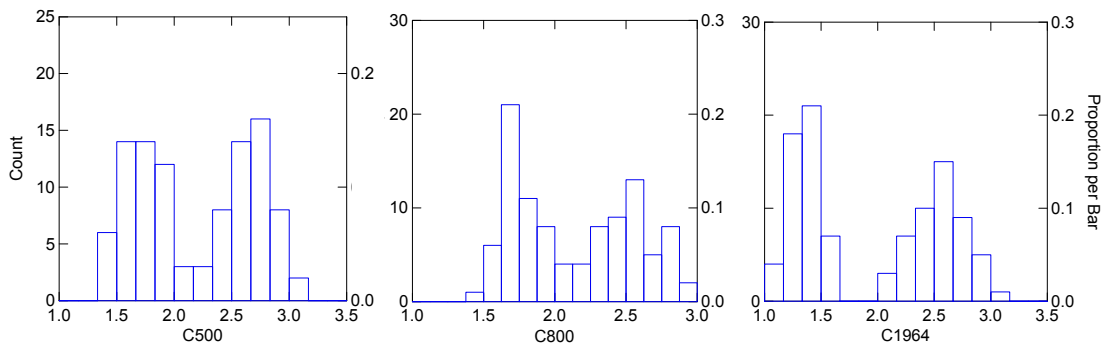
Figure 6.4 Bimodal distributions for the combined W + E data for the years 500, 800, and 1964. For 6 out of the 85 sets of data (W and E), the initial normal distributions became bimodal in the combined distribution.

When the W and E group means were graphed vs. ring number from pith, the deviations and commonalities in tracheid lengths were apparent between the sets (Figure 6.5). A common sharp drop in length is visible between the ring numbers 1978 and 2078 (corresponding to the years -800 and -900). Between the rings 3078 to 3678, the sequences diverge the greatest amount from each other. After 3678, there are seven missing E points, which makes determining the closeness of the series difficult to ascertain.

A paired t-test was performed between the W and E groups, to determine the extent of the differences between the paired sets of data. The test addressed the hypothesis that the accumulative differences between the means of each series would equal zero. If the p-value is low (< 0.05), this would be evidence that the means are different and that the two sides of Prometheus are different from each other. The data was balanced; there had to be W and E data from the same year. Thirty-five samples of forty from the W set and thirty-five samples of forty-five from the E set were used for the paired t-test. The paired t-test returned a $p = 0.07$. This is close to an alpha of 0.05, but exceeds it, therefore the hypothesis was accepted; the test found significant differences between the two edges of Prometheus. A paired t-test between the rings 0 to 1978 (just before the sharp decrease in tracheid length at 2078) returned a $p = 0.77$. This test

65
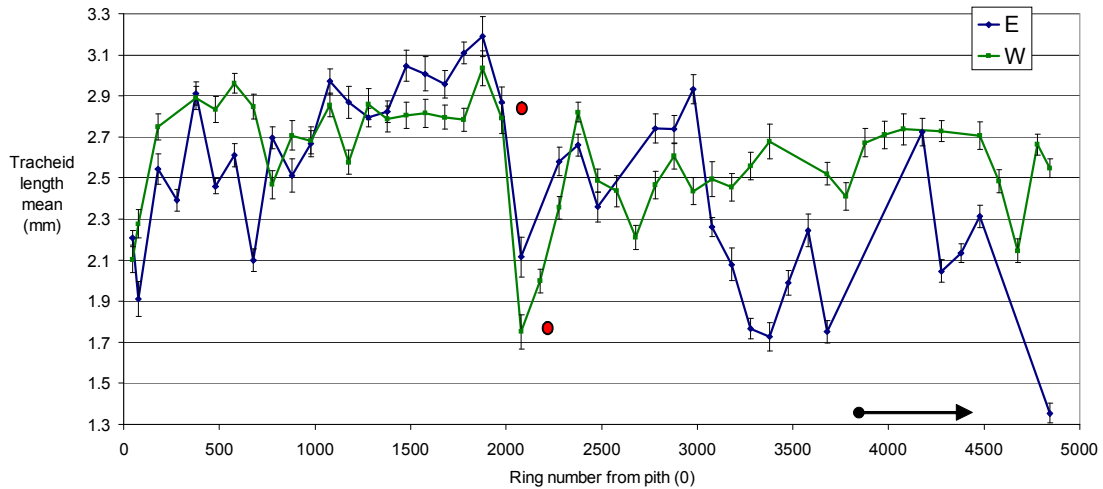
Figure 6.5 Scatterplot between the tracheid length means of the W and E groups and ring number from the pith. Red dots indicate the identical sharp decrease in tracheid lengths between the rings 1978 and 2078 (-900 and -800). The arrow indicates a point where the absence of seven means for the E group makes interpreting any relationship between the series difficult.

presented even stronger evidence that the sides are different from each other. While the preliminary study along ring 638 detected no difference between groups 1 and 5 (the two edges of Prometheus), the balanced series of W and E detected difference between the two sides in the pair t-test. These results do not support the concept of combining and averaging the two groups (W and E); therefore the remaining tests will examine the W and E sides separately.

TableCurve 2D is a curve-fitting software that generates linear or nonlinear equations best fitted to your data. It graphically presents the equations and graphs in order of descending correlations. For the W data set, TableCurve 2D presented an eighth order polynomial with a R^2 correlation of 0.39 (Figure 6.6). The program regarded the shortened tracheid lengths at ring 2078 and 2178 as outliers; therefore the curve does not react to those points. What is evident is a sharp increase in lengths between the rings 44 to 378, a decreased rate of growth between 378 and 478 and fluctuating curves after that.
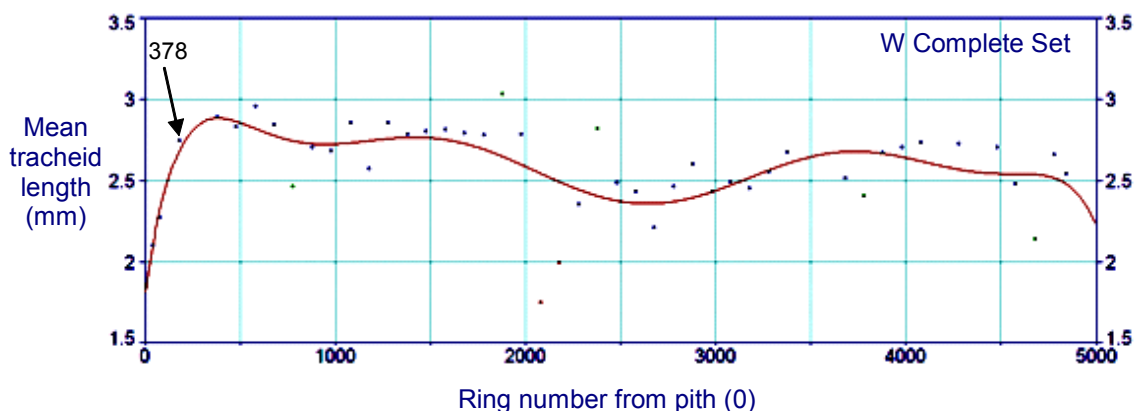
Figure 6.6 TableCurve 2D graph of mean tracheid length vs. ring number from pith for the Prometheus W data set - ring numbers 44 through 4842. The arrow points to ring 378. The lengths from 44 to 378 appear to increase at a greater rate than any others after that. The polynomial curve has an equation of $MeanW = 1.81 + 0.008\ Ring - 2.15 \times 10^{-5}\ Ring^2 + 2.75 \times 10^{-8}\ Ring^3 - 1.90 \times 10^{-11}\ Ring^4 + 7.47 \times 10^{-15}\ Ring^5 - 1.64 \times 10^{-18}\ Ring^6 + 1.92 \times 10^{-22}\ Ring^7 - 9.19 \times 10^{-27}\ Ring^8$ ($R^2 = 0.39$)

For the E data set, TableCurve 2D presented an eighth order polynomial with a R^2 correlation of 0.64, nearly twice the correlation of the W data set (Figure 6.7); the curve fit the data more closely, but it also decided that rings 2078 and 2178 were outliers, therefore the curve does not react to those points. What is evident is a shorter sharp increase in lengths between the rings 44 to 278, another rise in tracheid lengths to the 1878 and a large gradual decrease in lengths after that point.

Regression trees partition independent variables and their responses into subsets. With the Prometheus W and E data sets, the use of a regression tree could point out splits in the data; natural breaks where the correlation improves for the subset. For the W data, the program first targeted the major drop in tracheid length at 1978 (the year -800) (Figure 6.8). The lengths in the rings greater than 1978 were then partitioned into two groups, the split occurring between rings 2678 and 2778 (-200 and -100). The lengths in the rings less than 2078 (-700) were also broken into two groups, the split occurring between rings 578 and 678 (-2300 and -2200) . A graphical representation of the regression tree analysis displays the subsets chosen by Systat (Figure 6.9).

67
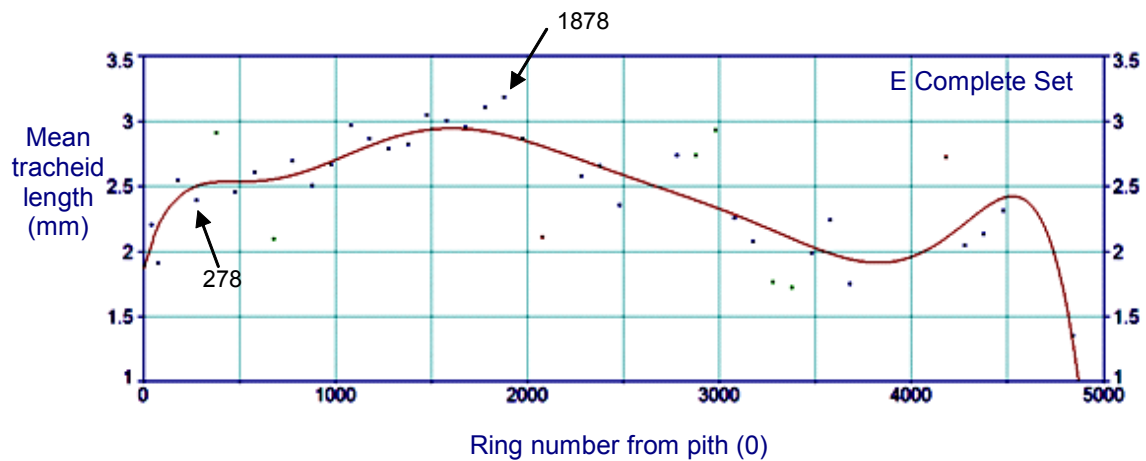
Figure 6.7 TableCurve 2D graph of mean tracheid length vs. ring number from pith for the Prometheus E data set - ring numbers 44 through 4842. The arrows point to rings 278 and 1878, the peaks of two strings of tracheid length increases. The polynomial curve has an equation of MeanE = $1.86 + 0.005$ Ring $- 1.56 \times 10^{-5}$ Ring$^2 + 2.28 \times 10^{-8}$ Ring$^3 - 1.76 \times 10^{-11}$ Ring$^4 + 7.56 \times 10^{-15}$ Ring$^5 - 1.84 \times 10^{-18}$ Ring$^6 + 2.38 \times 10^{-22}$ Ring$^7 - 1.26 \times 10^{-26}$ Ring^8 ($R^2 = 0.64$)

For the E data, the program first broke the data set at 3078 and 3178 (Figure 6.10). The lengths in the rings greater than 1978 were then partitioned into two groups, the split occurring between rings 2678 and 2778. The lengths in the rings less than 2078 were also broken into two groups, the split occurring between rings 478 and 578 (Figure 6.11).
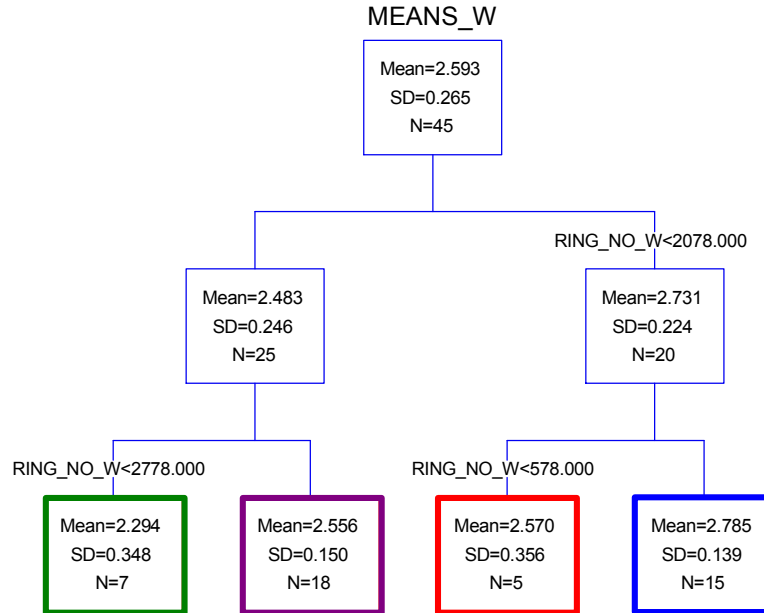
Figure 6.8 Regression tree for the W data set. The first major split occurred between rings 2078 and 2178. This corresponds to the sharp decrease in tracheid length previously noted. Four subsets were ultimately created. The box colors correspond to the data segments in Figure 6.9.
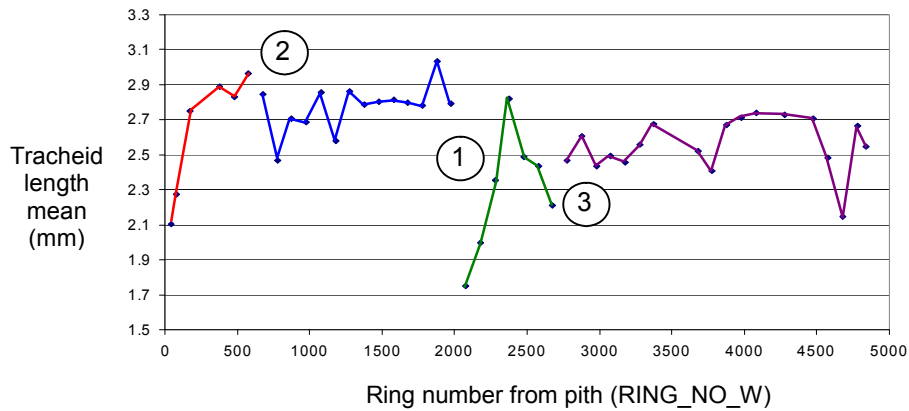
Figure 6.9 Scatterplot of tracheid length means vs. ring number from pith with regression tree subsets for the W data set. The segment colors correspond to the boxes in Figure 5.8. The first break in the data occurred between rings 2078 and 2178, the years -800 and -900, respectively (circled 1). The other two breaks were between -2300 and -2200 (circled 2) and between -200 and -100 (circled 3). The segment colors correspond to their matching boxes in Figure 6.8.

69
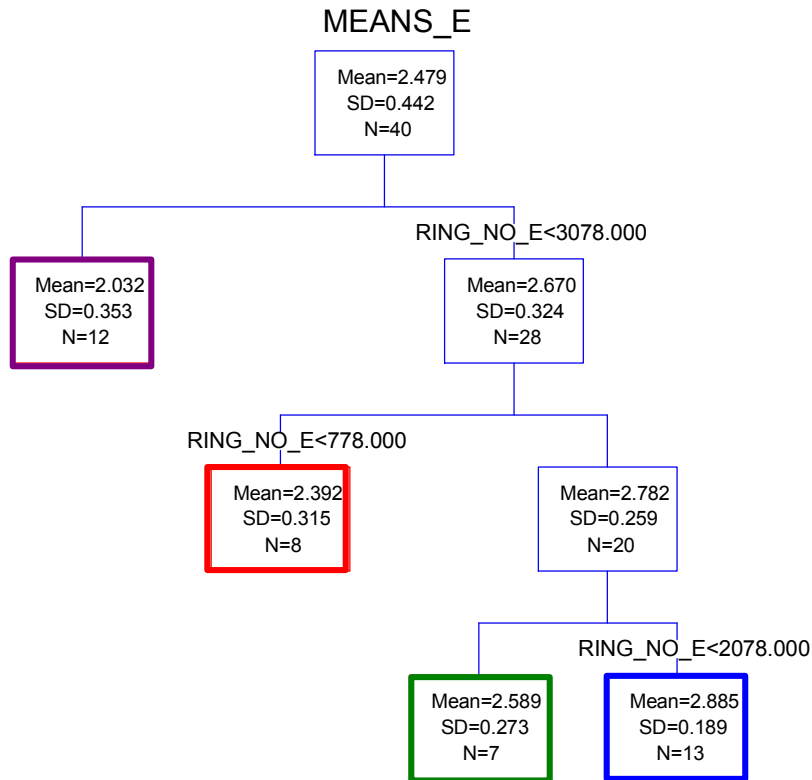
Figure 6.10 Regression tree for the E data set. The first major split occurred between rings 3078 and 3178. Four subsets were ultimately created. The box colors match to the corresponding line segments in Figure 6.11.
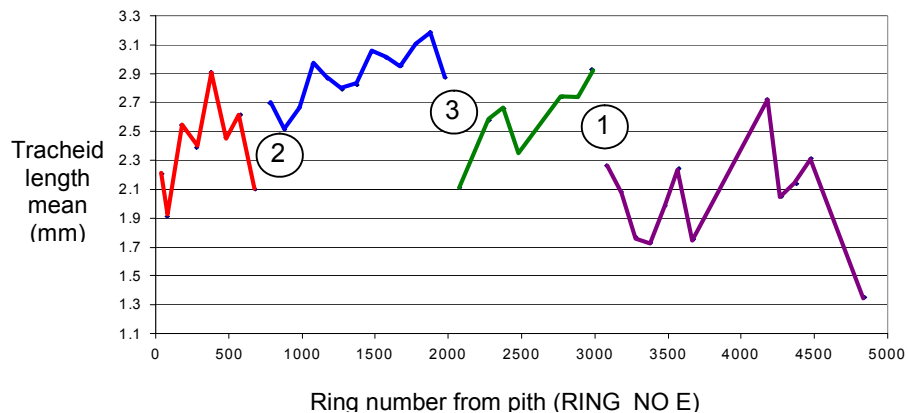
Figure 6.11 Scatterplot of tracheid length means vs. ring number from pith with regression tree subsets for the E data set. The segment colors correspond to the boxes in Figure 5.8. The first break in the data (circled 1) occurred between rings 2978 and 3078 (years 100 and 200). The second (2) and third (3) breaks occurred between rings 678 and 778 (years -2200 and -2100) and between rings 1978 and 2078 (years -800 and -900). The segment colors correspond to their matching boxes in Figure 6.10.

70

6.4 Complimentary environmental studies

Six extreme warm periods intersected the tree rings where tracheids had been measured. During the warm intervals, the mean tracheid lengths decreased from the preceding century. Six extreme cool periods intersect the century marks. During those cooler intervals, the mean tracheid lengths increased from the preceding century (Table 6.4). Twice, wet periods crossed the sampling points and during those periods the mean tracheids length decreased (year 800) and increased slightly (1200). The 1200 site was also experiencing a cool period. Four dry periods intersected sampling points and all tracheid length means increased from the preceding sample sites (1000, 1100, 1300, 1900). One of the four sites was associated with a cool interval (1100) (Figure 6.12).
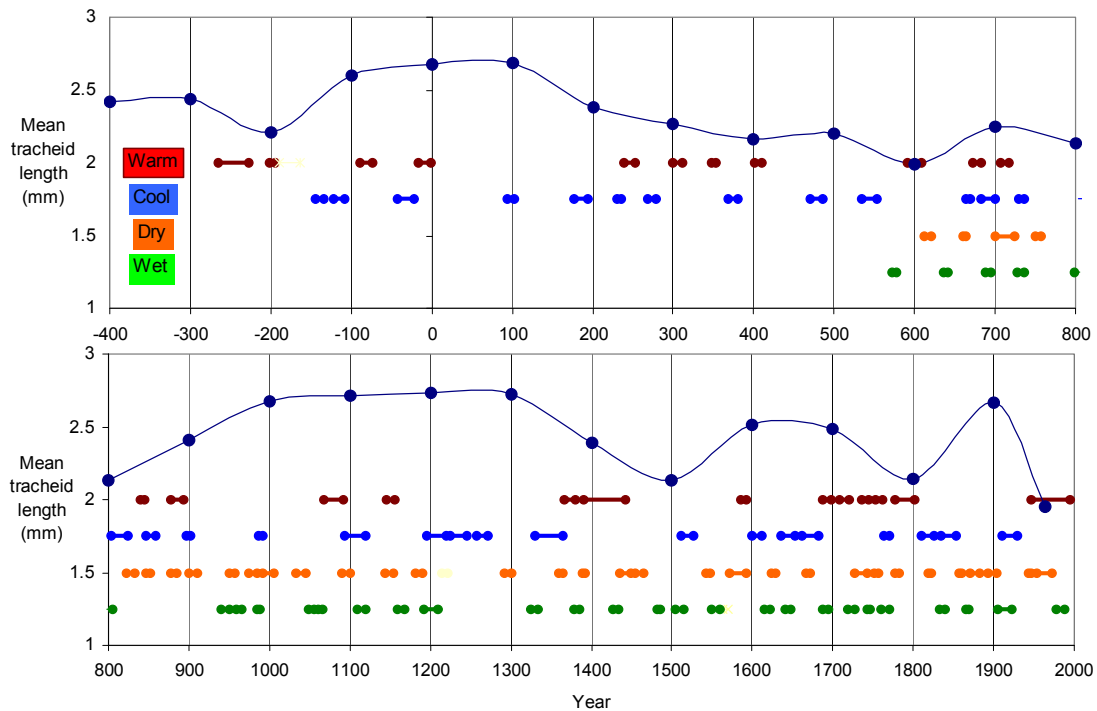
Figure 6.12 Mean combined tracheid length over time associated with periods of climatic extremes. The intervals of warm, cool, dry, and wet range from 5 to 49 years (From Salzer and Kipfmueller 2005).

71

Table 6.4 Increases or Decreases of the Mean Length of Tracheids During an Extreme Warm or Cool Period. Data corresponds to Figure 6.12 (From Salzer and Kipfmueller 2005).

Years that a warm period crosses where tracheids were measured	Tracheid length relative to preceding century mark	Years that a cool period crosses where tracheids were measured	Tracheid length relative to preceding century mark
-200	Decrease	100	Increase
300	Decrease	700	Increase
600	Decrease	900	Increase
1400	Decrease	1100	Increase
1800	Decrease	1200	Increase
1964	Decrease	1600	Increase

Mean width of one hundred year intervals were the widest of all the intervals at the beginning of the Little Ice Age (90.1 mm), with widths decreasing to a width less than half of the start of that period (44.2 mm). The century widths during the Medieval Warming Period were consistently low (below 40 mm) throughout the five centuries.

The beginning of two of the Bond temperature fluctuation events (Bond *et al* 1997) preceded two of the three widest ring intervals at -800 (67.4 mm) and -2200 (74.2 mm). The third Bond event (450) did not vary in size from the centuries preceding and following it (Figure 6.13).

Individual rings were measured and compared to associated mean tracheid lengths of the W data set (Figure 6.14). No correlation was detected between hundred year ring width and tracheid length (R^2 = 0.01). The mean ring width related to the -800 sampling site was the widest of all those measured.
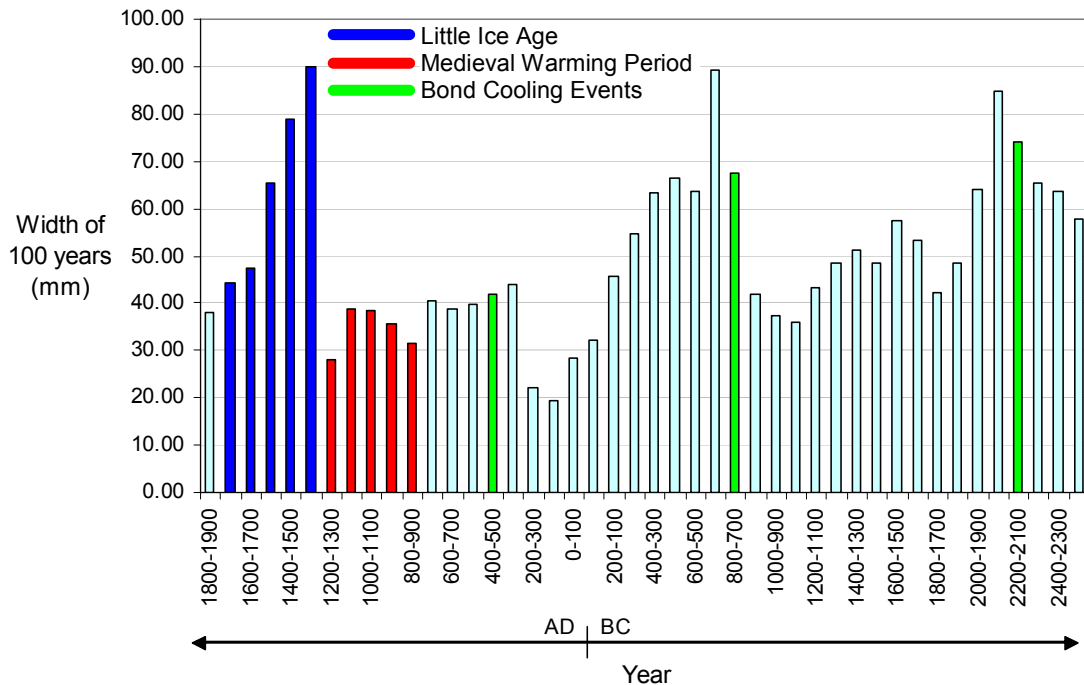
Figure 6.13 Mean width of one-hundred-year intervals of Prometheus associated with historical temperature events. The Little Ice Age lasted from approximately 1300-1800, the Medieval Warming Period from 800-1300, and the three Bond cooling events occurred 1400, 2800 and 4200 years before present (450, -800 and -2200).
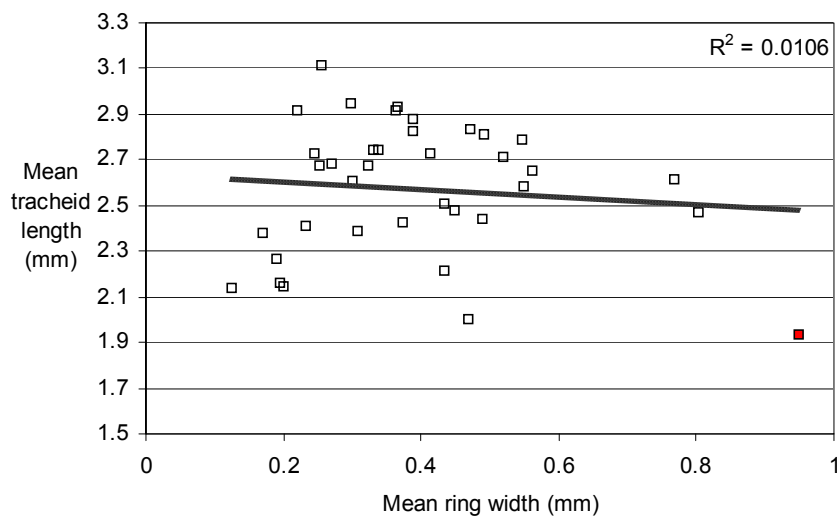
Figure 6.14 Mean ring width at tracheid sample sites compared to the associated mean tracheid lengths. No correlation was observed ($R^2 = 0.01$). The point in red corresponds to the -800 sampling site. The mean width of the rings (2) were the widest measured and the tracheid lengths were the shortest (1.91 mm).

73

CHAPTER 7

DISCUSSION

7.1 Overview

Evaluation of materials and methods used in this study and alternative ones will be discussed. A discussion of my research on crossdating, tracheid lengths versus age, ring widths, and climate are reviewed. This study mainly deals with Prometheus and generalizations about bristlecones or other species of pine should be carefully considered.

7.2 Evaluating Methods

7.2.1 Measuring the Width of Rings

The Proscope was a useful tool for photographing tree rings on a subject too large to be placed on a standard microscope stage (such as the main slab of Prometheus). The downside of the Proscope is the resolution. There is a very substantial difference in resolution between a Nikon scientific microscope and the Proscope. This difference is visible in Figure 7.1. The -2100 ring from pith piece #2 was captured with the Proscope and its proprietary software and with the Eclipse 80i microscope and ACT-1 software (Nikon). The micrographs were not altered in any way. Differences in the two images is obvious. The Eclipse 80i image is sharper and contains more details. Increasing the magnification (7.1C and 7.1D) reveals that the Proscope picture is blurry and the Eclipse 80i image is still in focus. While the Proscope image can be enhanced using an image processing program (filters to sharpen edges or the adjustment of histogram levels), this practice can introduce unwanted artifacts (features not present in the wood). The Proscope is adequate for photographing rings for measuring. Beyond that, its usefulness is questionable.

74

Since tree rings vary in density between early and latewood (latewood cell walls are thicker and lumens are smaller), methods to accurately discern ring boundaries using density differences have been developed by dendrochronologists. Photometers can record and display densities when a light is shown through a thin section of wood (Kuniholm 2001). X-ray densitometry can discern between earlywood and latewood by displaying the density of the cells. Photometry and x-ray densitometry also have the added benefit of quantifying earlywood and latewood widths within one ring – a measurement that has been shown by some to be as sensitive to climatic conditions as ring widths or tracheid dimensions (Jagels and Telewski 1990).
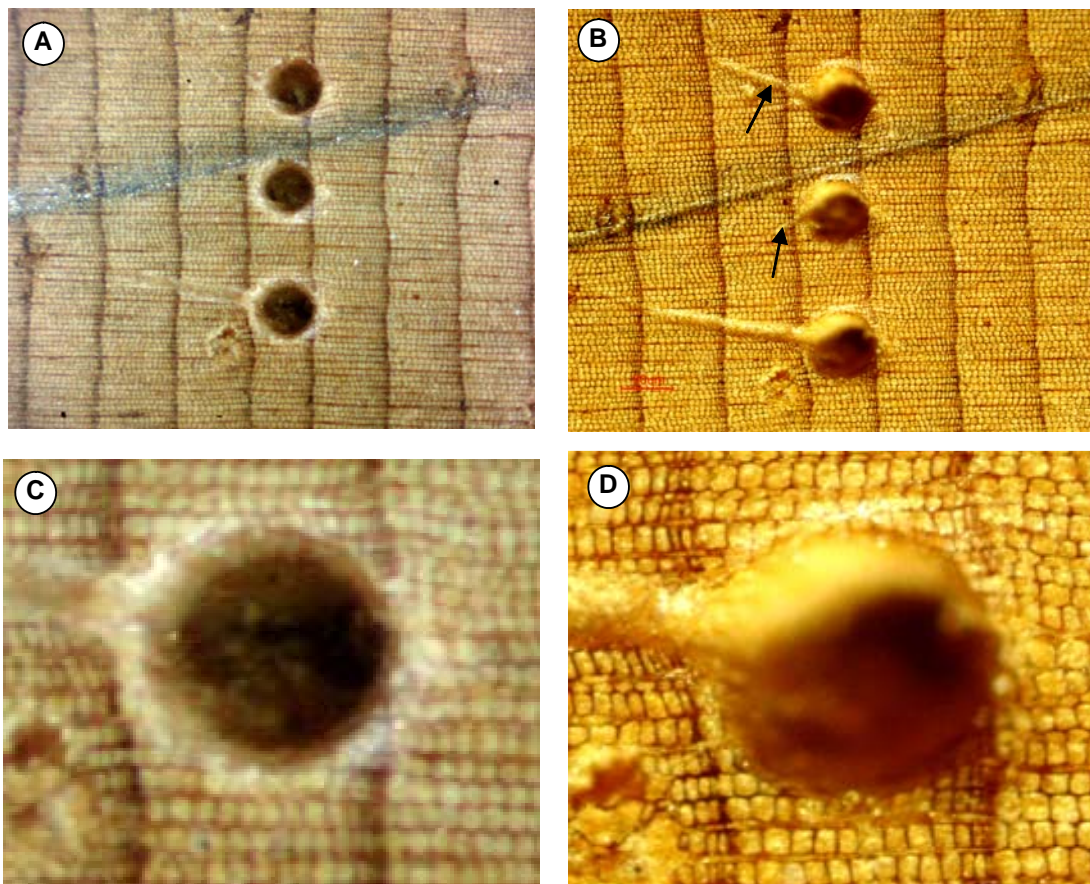
Figure 7.1 Unadjusted digital captures of Prometheus pith ring -2100, examined for resolution differences. A. Digital capture with the Proscope. B. Digital capture with the Eclipse 80i research microscope. Arrows indicate details not visible in A. C. Close-up of the Proscope picture. Note the blurring of the image. D. Close-up of the Eclipse 80i picture. The individual tracheids still have sharp edges.

Rather than measurements, original tree ring dating techniques rely upon a visual inspection of rings, followed by a judgment as to the nature of the ring; is the ring wider than the majority of rings around it or is it narrower? Is the ring a full complete ring (continuous) or is it a partial ring (discontinuous). Has the ring been damaged by some environmental event—fire or frost? Measuring rings with a computer program like Image Pro Plus is fast, but the attention of the user is on measuring rings, not actually looking closely looking at the rings. In this respect, drawing skeleton plots may produce a superior analysis of the rings.

7.2.2. Separating Tracheids for Measurement

For separating tracheids, the chemical maceration technique developed by Franklin (1945) was used. He used a solution of one part glacial acetic acid to two parts 30% hydrogen peroxide to separate the fibers in cured wood composites. He suggested that equal volumes of glacial acetic acid and 30% hydrogen peroxide could be used to separate the tracheids of untreated wood for microscopic examination. The release of wood fibers from each other was originally accelerated with 24-48 hours in a 60° C oven. The Franklin technique is time consuming in this study, considering that the maceration of bristlecone pine wood can take anywhere from one to three weeks. The amount of time needed to dissolve the pectins holding tracheids together is variable. The failure of four of the samples is directly attributable to the samples being in the maceration solution for too long. These samples were located along an uncut edge of Prometheus, where the wood was weathered and the edges were naturally "decayed." The standard two week protocol disintegrated these weathered samples, leaving no intact tracheids to measure.

Other than the fact that four samples were destroyed, the chemical separation method worked well. By the last water rinse, the tracheids were falling apart from each other and it was easy to tease them apart on the microscope slides. One problem occurred after the tracheids were individually spread apart on the slides. As the water evaporated from the slides, the tracheids migrated inward with the receding water edge and their number became denser than intended. Future macerations using Franklin's technique could experiment with additives (ethanol,

76

for example) or mechanical techniques (like drawing water off with the corner of a paper towel) in an attempt to fix the tracheids on the slides where they were initially placed.

7.2.3 Measuring Tracheids

After chemical separation, tracheid measurements can be made using optical microscopes. However, more precise measurements can be obtained using image analysis software (Kuniholm 2001). In the current study, images of the tracheids on the slides were captured with the Nikon Elements software. This is a powerful program, capable of merging over one hundred images together using the "big picture" feature. The drawback to an advanced feature like this is that the computer needs to have a large amount of available physical memory. In addition, it was discovered that temporary files need to be periodically deleted to avoid crashes of the program. The resulting montages of the slides are the physical size of the microscope slides (1 X 3 inches), with an automatic resolution of 7045 pixels per inch, and a file size of 350 to 400 megabytes apiece (Figure 7.2). 185 slide composites created a file of 57.5 gigabytes (See Appendix C for thumbnails). The very important upside of these large files is that they contain an amazing amount of information. After saving the montages, Nikon Elements was used to measure the tracheids. The program has a large variety of measurement tools and one of these, linked line segments, was able to measure both straight and curved tracheids. An example of the utility of the large files was seen in the inspection of tracheid tips. This step is necessary to validate that the whole tracheid is present for measurement (Figure 7.3). Since the images had already been calibrated by the capture feature (by inputting the magnification of the objective lens), the tracheid lengths were compiled and easily imported to Excel. The measuring tool also drew lines over the measured tracheids, avoiding the remeasure of any tracheids (Figure 7.4).
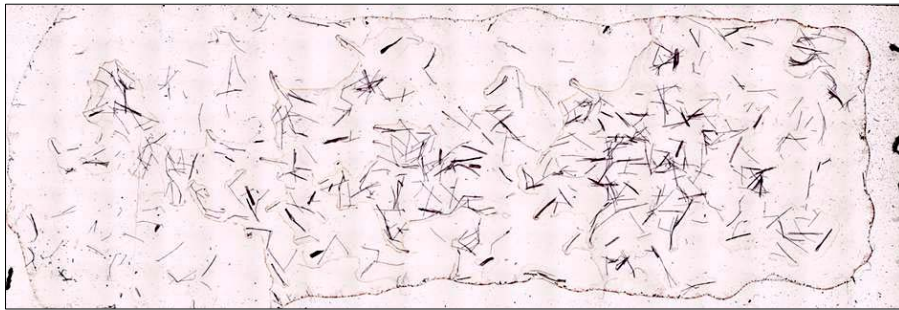
Figure 7.2 Sample year 100W composite slide of tracheids.

Figure 7.3 Three micrographs of the tips of Prometheus tracheids. A. From the sample year -1400W, undamaged and intact tracheid tips. B. Also from the sample year -1400W, broken tracheid tips. C. From the sample year -2400E, close-up of a shredded tracheid tip.
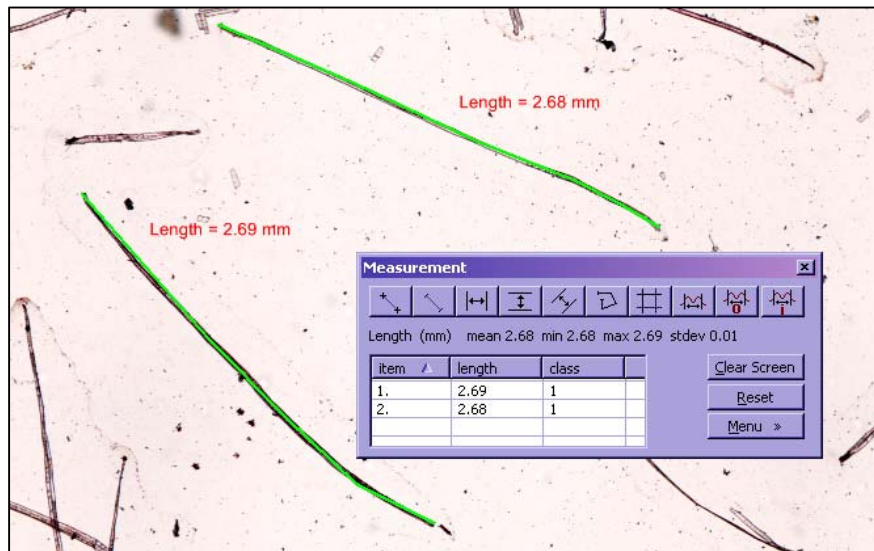
Figure 7.4. Prometheus tracheids (-2700W) with marked lines and compiled measurements.

The Ladell technique (1959) allows the measurement of tracheid lengths and is not dependent upon chemical maceration. His method projects an image of a tangential microscope section on a surface. This image shows the vertical length of the tracheids. Two parallel lines at a known distance would be drawn perpendicular to the long axis of the tracheids. Cell tips of a predetermined number of contiguous cells would be counted and mean tracheid length would be deduced by multiplying the number of cells by the ratio of the distance between the lines and the numbers of cell tips. This technique, of course, requires sectioning of the wood, which is a formidable project in itself.

The need for a fast and simple method for classification of tracheid lengths is sorely felt by pulp and paper manufacturers. The elasticity and tensile strength of finished paper products is directly related to tracheid length (Hauksson *et al* 2001). Near infrared spectroscopy (NIR) is currently being investigated as an alternative both to the Ladell method and to the chemical separation of tracheids. When infrared radiation is applied to a surface, some of it is reflected and some of it is absorbed. The amount of radiation reflected from the sample is called the reflectance value (R) of the sample. The reflectance values can identify compounds or determine sample composition. NIR produces a spectrum that represents the lignin, cellulose, and hemicellulose proportions of the secondary walls of tracheids (Schimleck *et al* 2004). As tracheid lengths increase through time, the concentration of cellulose increases and the amount of lignin decreases (Bendtsen and Senft 1986; Shupe *et al* 1997). Via *et al* (2005) tested NIR versus Franklin's method of chemical separating tracheids. For longleaf pines (*Pinus palustris*), correlation was the highest (r = 0.72) with the wood nearest the pith, rings 1 to 8. The correlations gradually decreased to 0.40 by ring 30. The low correlation values indicate that the method needs refining, but the use of sophisticated statistical techniques in conjunction with the NIR spectrums is being explored (Hauksson *et al* 2001).

Raczkowski *et al* (2004) evaluated the use of ultrasound transmission rates – measuring the time it takes for 0.5 MHz sound waves to travel through samples of twelve different conifer species. With an increase in tracheid length, the ultrasound transmission rate increased from 4.5

km/second to 6.6 km/sec. Tracheids were also measured using Franklin's maceration method. Correlation values were low between the predicted and actual lengths of tracheids (R = 0.413 – 0.480). The authors considered these values unreliable but expressed hope that ultrasound techniques could be refined and improved to yield more accurate results.

<p style="text-align:center">7.3 Evaluation of Results</p>

7.3.1 Crossdating

CrossDate, the program, reported a correlation value of 0.805 for the relationship between the main slab and the pith piece of Prometheus. This value was verified by Tom Harlan of the Laboratory of Tree Ring Research (University of Arizona) as being a strong match. Because the matchup of the main slab and pith piece was successful, it allowed the sampling of an additional four hundred annual rings or four more century rings beyond the 46 sampled on the main slab. These early century rings were critical in determining that a juvenile growth phase was present in Prometheus.

The purpose in crossdating Prometheus to Buddy and to master tree chronologies was to discover if it was possible to establish a correlation between them. A relationship between the two chronologies and Prometheus for the years between 1600 and 1900 was discovered. Correlation values of 0.520 to 0.650 for the Indian Garden and Hill 10842 chronologies (Table 7.1) were acceptable, especially in light of the fact that the Prometheus and Buddy raw data were not standardized. Ring widths, like tracheids, can vary within a tree because of fluctuations in the environment, with age, and with the anatomy of the tree. Variation in ring widths can occur between trees in the same stand due to geographic site differences. Buddy and Prometheus, although approximately one hundred meters from each other, generated a correlation of 0.619. Standardizing a ring width sequence smoothes out the data, removing short term growth events. To standardize a ring width sequence, a curve is fitted to the ring widths, such as the one generated with TableCurve 2D for the Prometheus tracheid lengths. The value of the curve at each year is divided into the ring width to remove short term growth effects. The standardized ring width sequence is then referred to as a ring width index. The indices for multiple trees are

averaged and the results become a master tree chronology, such as that for Hill 10842 and Indian Garden (Fritts 1976). These two chronologies were chosen for their proximity to Prometheus. Prometheus is located 98 kilometers from Indian Garden and 8.7 kilometers from Hill 10842 (Figure 7.5). Hill 10842 is located within the boundaries of the Great Basin National Park. Prometheus is located at 10780 feet (3316 meters) in altitude, the Indian Garden stand at 9500 feet (2896 meters), and the Hill 10842 grove at 9600 feet (2926 meters). It makes sense that correlation should occur between Prometheus and Hill 10842 (0.591) – they are only 8.7 kilometers apart – but, it is interesting that the correlation was stronger between Indian Garden and Prometheus (0.650).

Future crossdating attempts of Prometheus with tree ring chronologies would be very beneficial to discovering a closer estimation of the exact age of Prometheus. As mentioned earlier, the strength of a master chronology is in its collection of the ring width sequences of many trees. Hill 10842 (Graybill) is a compilation of the tree ring sequences of 45 trees and it spans the years between 0 and 1984. The Indian Garden (Graybill) chronology utilized 54 trees to complete the series, spanning the years between -2370 and 1982. In Chapter 3, it was related that Donald Currey had counted 4842 unique rings on Prometheus. Based upon the fact that the slab was removed two feet above the original base of the tree, he went on to tentatively say that Prometheus probably started growing around 4900 years ago. In this study, 4844 rings were counted on Prometheus, but, after spotting fourteen partial rings within a 400 year span, many of which had not been counted by Currey, it is obvious that the estimation of the age of Prometheus is low. Since a relationship between the rings of Prometheus and two master tree chronologies for the years between 1600 and 1900 has been established, all of the rings of Prometheus covering the years of the chronologies should be crossdated with Indian Garden and Hill 10842 chronologies. Other tree ring chronologies are available that could also be used to crossdate Prometheus; for example, Mount Washington within Great Basin National Park, while a shorter chronology, 825 to 1980, is another chronology that could be utilized.
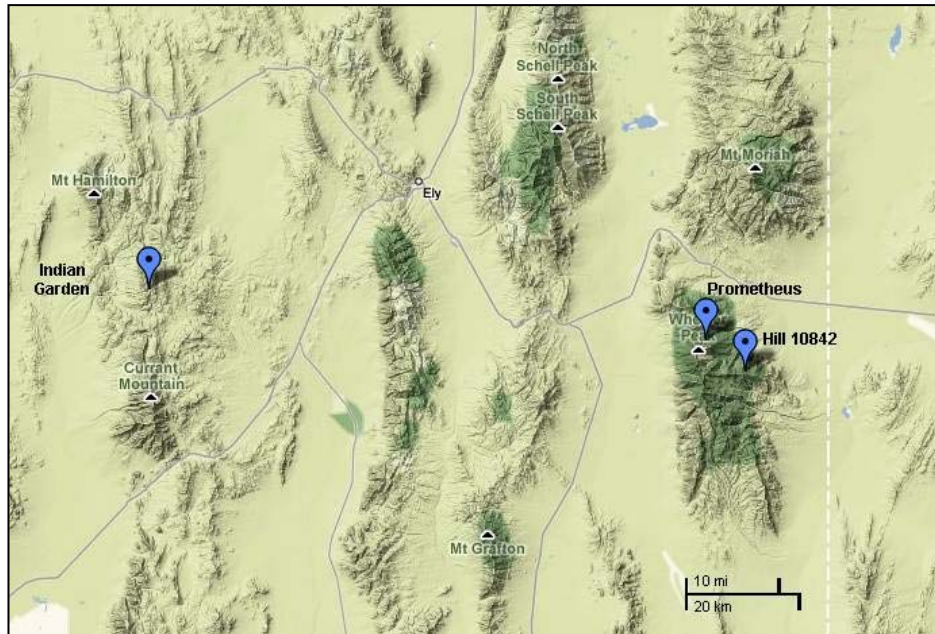
Figure 7.5 Map of the locations of Prometheus, Hill 10842 master tree ring chronology and Indian Garden master tree ring chronology. Indian Garden is 98 kilometers from Prometheus and Hill 10842 is 8.7 kilometers from Prometheus. Their altitudes are similar: Prometheus is located at 10780 feet in altitude, Indian Garden is at 9500 feet, and Hill 10842 is at 9600 feet. (Google Maps 2008)

7.3.2 Tracheid Length Variation

In two previous studies, the lengths of bristlecone pine *(Pinus longaeva)* tracheids have been correlated to tree age. Baas *et al* (1986) measured tracheid lengths in cores taken from three trees located in the Methuselah Walk area (Inyo National Forest, California). One tree was over 2200 years old, and the other two were 500 and 600 years old. Wood samples were removed at 10, 50 or 100-year increments. The oldest stem demonstrated a steady increase in the length of the tracheids over the 2200 years, not exhibiting any changes in the rate of tracheid growth. In the current study, the maximum tracheid length occurred at -1000, 1878 rings from the pith, with tracheid lengths fluctuating after that point. Despite the larger amount of samples taken at ten-year intervals during the earliest years present in the 2200-year-old tree, the authors did not note a rapid rate of tracheid length increase resembling a steep juvenile growth curve. This

may be due to the fact that the authors estimated that 100 to 200 years were missing between the pith and the beginning of their core. Steep juvenile increases were observed within the first several centuries of the two younger stems, age 500 and 600-years-old. Their growth curves leveled off, but were still slightly increasing over the last 200 years (Figure 7.6).
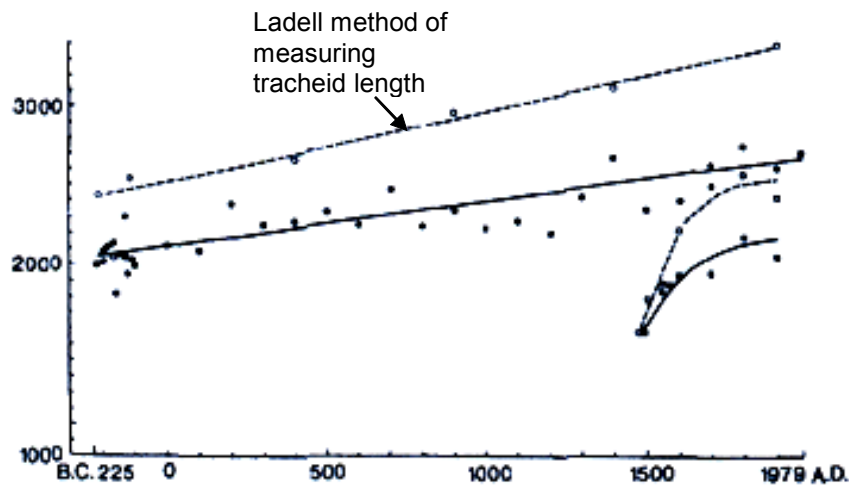
Figure 7.6 Tracheid length (microns) vs. year for two cores of *Pinus longaeva*. Solid correlation lines are from measurements obtained from maceration techniques and broken lines are for calculated values using Ladell's method. For the 2200-year-old core, tracheid lengths increased uniformly. For the 500-year-old core, a steep juvenile growth rate was noted until the growth rate decreased after a few centuries. (After Baas *et al* 1986)

In the spring of 2008, Kelsey Pendley conducted a study to correlate Little Ice Age temperatures with tracheid lengths in Prometheus. She also investigated the changes in tracheid length related to age. Samples were removed from the pith piece of Prometheus at the rings from pith numbered 0, 10, 50, 100, 200, 300, and 400. No relationship between Little Ice Age temperatures and tracheid lengths was detected. However, she observed a sharp rate of growth in tracheid lengths between ring 0 and 100 (four samples). Tracheid lengths dropped in length between rings 100 and 300, but increased slightly from ring 300 to 400 (Figure 7.7). The conclusion reached was that a juvenile growth phase was likely present between rings 0 to 100. After that ring, it was suggested that the wood had been damaged in some way, resulting in the reduction of the tracheid lengths. When her data is compared to this study (Figure 7.8A), the

83

tracheid lengths from this study are shorter than the Pendley ones, except for the last sample at 378. This could be due to differences between the locations of the samples. Ms. Pendley's wood samples were removed from the pith piece containing the rings closest to the absent pith (#3). The wood samples for this study were removed from the largest pith piece (#1). There may have been slight differences in tracheid lengths between the two pieces. When the two data sets are combined and treated as one set of data, a third order polynomial curve fits the data better (R^2 = 0.71) than a second order curve (R^2 = 0.40) (Figure 7.8B; Figure 7.8C). The third order curve has a stronger increase in tracheid length from 0 – 100 years than the shallower second order curve. This may be the juvenile growth phase as Ms. Pendley observed in her data.

An interesting sidenote was that, when Ms. Pendley ran test studies of tracheid macerations using Franklin's method, she added additional steps; she followed the last water rinse with an ethanol dehydration series and a final rinse in xylene. The tracheids were observed to separate easily after the water rinses but were difficult to separate after the ethanol and xylene rinses. After collaboration with her advisor, Dr. Arnott, she abandoned the ethanol and xylene steps. Her experiences and advice were the basis of my choice to use the Franklin maceration process without the added steps. In addition, she noted that paper slips identifying the sample year that had been placed into the solution vials would disintegrate and that the maceration solution would remove any pen markings written on the outside of the vials. This led to my decision to etch the outside of the glass vials with a dremel tool.

For this study, a preliminary test that measured 140 tracheids from a sample of Prometheus, age unknown and irrelevant, was conducted to determine a sample size for the primary study. The data for the sample were normally distributed. A conservative sample size of fifty tracheids was selected because the confidence in the mean exceeded 96%. To further explore the suitability of the chosen sample size, groups of tracheids were measured from the two prepared slides. 10, 20, 30, 40, 50, 60, and 70 tracheids were independently measured (no tracheid was measured twice). The data of the groups were tested for normality and homoschedasticity with Kolmogorov-Smirnov tests and Levene tests, respectively.

84
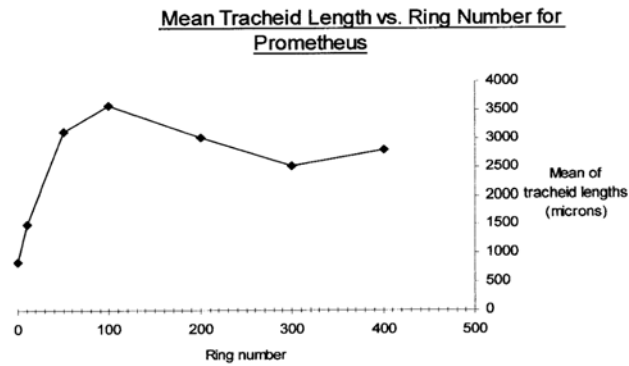
Figure 7.7 Mean tracheid lengths versus Prometheus ring number (Pendley 2008).
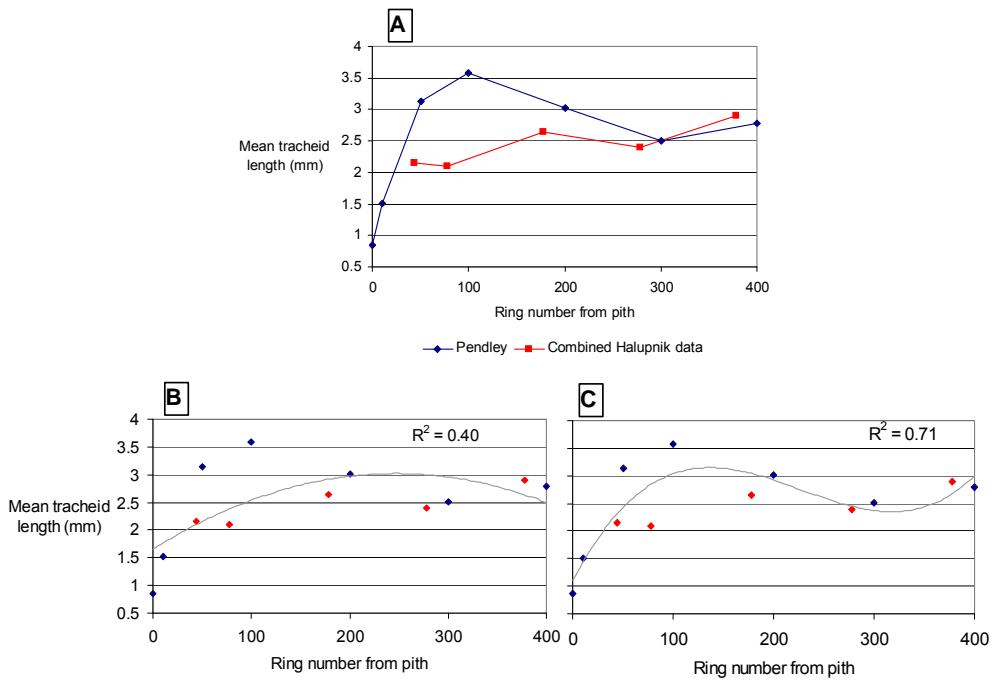
Figure 7.8 Three scatterplots of Pendley and Halupnik mean tracheid length versus ring number from pith. A. Pendley and Halupnik data with point-to-point lines drawn separately. B. Pendley and Halupnik data combined, with a second order polynomial curve ($R^2 = 0.40$). C. Pendley and Halupnik data combined with a third order polynomial curve ($R^2 = 0.71$).

85

A one-way ANOVA tested the hypothesis that the means of the groups were equal to each other. Statistically, slide #1 groups were normally distributed, had equal variances, and the group means were determined to be equal to each other (p = 0.95). Slide #2 groups were normally distributed and had equal variances, but the ANOVA detected differences in the means (α = 0.05, p = 0.036). Post hoc pair-wise t-tests revealed significant difference in the means between the 10 and 70-tracheid groups (p = 0.014). All other pair-wise t-tests were not significant, therefore their group means were statistically equal.

The primary study samples were removed along the two long edges of Prometheus, designated W and E. Concern was expressed that it wasn't proper to combine the measurements from the two edges without knowing the variability of tracheid lengths between the two sides. Fortuitously, a main slab piece exposed one entire edge from W to E. This ring, 638, was sampled five times along its length and fifty tracheids were measured from each group. Normality and homoschedasticity were confirmed with Kolmogorov-Smirnov tests and Levene tests. A one-way ANOVA detected significant differences between some or all of the means (p = 0.000000). Pairwise t-tests found that eight of the ten pairs of sample means were not equal to each other. The means were statistically equal between groups 1 and 5 and 4 and 5. Groups 1 and 5 were the ones removed from the extreme ends of the ring, therefore they corresponded to the E and W sides, respectively. These results produced conflicting conclusions. Significant variation in tracheid length occurred along the ring, but the edge means were equal. It was still possible that the E and W side data could be combined. Unfortunately, when the primary data was analyzed, a pairwise t-test conducted between the W and E data produced a p-value of 0.07, close to but still exceeding the 0.05 significance level. Significant differences between the two sets of data were detected.   Some evidence prior to the pairwise t-test hinted at this eventuality. Kolmogorov-Smirnov tests for normality were significant for three sets of combined (W + E) data – the distributions were not normal.   The histograms revealed that six previously normal distributions from W and E had combined to form three bimodal distributions (Figure 6.4). Scatterplots of the means versus the ring numbers for the W and E sets that were placed

86

together on one plot revealed similarities and differences in trends (Figure 6.5). After seeing all the evidence pointing to the differences between the W and E sides, it was decided to analyze the two sides separately.

For the W set of tracheid lengths, the most rapid growth in tracheids occurred from ring 44 to 378 (Figure 6.6), a period of 334 years. This could be a juvenile growth phase lasting over 300 years. For the E set of tracheid length means, a potential juvenile growth phase is not as apparent. From 44 to 378, the lengths decrease and increase two times, with an overall increase in length. In fact, the lengths continue to increase, with some fluctuations, up to ring 1878. For the studies cited in Chapter 4, the juvenile growth phase lasted between ten and forty years. Possibly, for a tree that may live thousands of years, the juvenile phase can last hundreds of years, as Baas *et al* (1986) suggested when they analyzed their bristlecone pine cores.

The most surprising sample had to be the one removed at ring number 2078 (year -800). For the W group, the mean tracheid length decreased from 2.79 to 1.75 millimeters between the century marks of -900 and -800; this was a 37% decrease in mean length between the two century points. The drop in length was so extreme that TableCurve 2D assumed that it must be an outlier when it was graphing the data. When that sample was being measured, it was also thought that there must be a mistake for the low values – something that amounted to experimental error. Accordingly, those two slides were re-measured and the tracheids carefully re-examined for broken ends. The measurements of the tracheids were the same as the first set. The fact that the next three centuries increased steadily from that low point also validated the measurements at -800. A scatterplot of the tracheid lengths lined up to the image of the slab and pith pieces of Prometheus may provide a clue for the drop in tracheid length (Figure 7.9). On the E side, between the years -1500 to -500, a part of the wood is absent. When Dr. Arnott was visiting the site of Prometheus in 2003, he matched a scan of the main slab to the stump (Figure 7.10). It shows absent wood in that and other areas, but it also shows that trunk surrounds the gaps. It may be a coincidence that the tree is missing wood during the period where the tracheid lengths decrease sharply, but it is in the realm of possibility that the tree was damaged along that

87

growing edge; for example, a rock fall could have impacted the bark with enough force to damage the cambium. Unfortunately, that is a topic that has not been researched; an event that physically damages the tree but doesn't kill it – such as a rock fall, a tree fall, excessive snow or ice load, or lightning strikes. Tracheid length responses in relation to wound responses have been researched, but the wounds are generally caused by pinning – inserting a pin into a tree. Kuroda (1986) observed an increased rate of cambial divisions after wounding. Coupled with the fact that increasing the rate of the divisions of initials leads to decreased tracheid lengths (Bailey 1923), a wound might lead to seriously decreased tracheid lengths. An investigation into avalanches and rock falls and their effect on wood properties did not yield any useful information. The articles about conifer trees that survive these damaging events focus mainly on the formation of vertical trauma resin ducts and callus tissue (Stoffel and Hitz 2008; Lev-Yadun 2002; Bollschweiler *et al* 2008) – features that were not observed in the Prometheus wood.

The current results of tracheid lengths versus age did resemble another study concerning tracheid length in conifers. Bailey and Shepard (1915) measured tracheid length for four different conifers (white fir, longleaf pine, white pine, and hemlock). They observed a juvenile growth phase for all four species. After the grow rate of tracheids slowed down, tracheid lengths fluctuated, increasing and decreasing several times.   Figure 4.8, the graph of the tracheid lengths of the four conifers, resembles the pattern of growth exhibited by Prometheus. The other studies of tracheid length versus age did not report the dramatic fluctuations exhibited by the Bailey and Shepard study and this current study.

Regression tree analysis in this study did not supply any useful information. The routine did recognize the sharp decrease in tracheids at ring number 2078 (year -800). It seems that the utility of this tool would be increased if multiple subjects were studied and the regression trees analyses found the same subsets of data. The discovery of common breaks in many sets of data could guide the researcher to investigate subsets of data that might not have otherwise been identified.
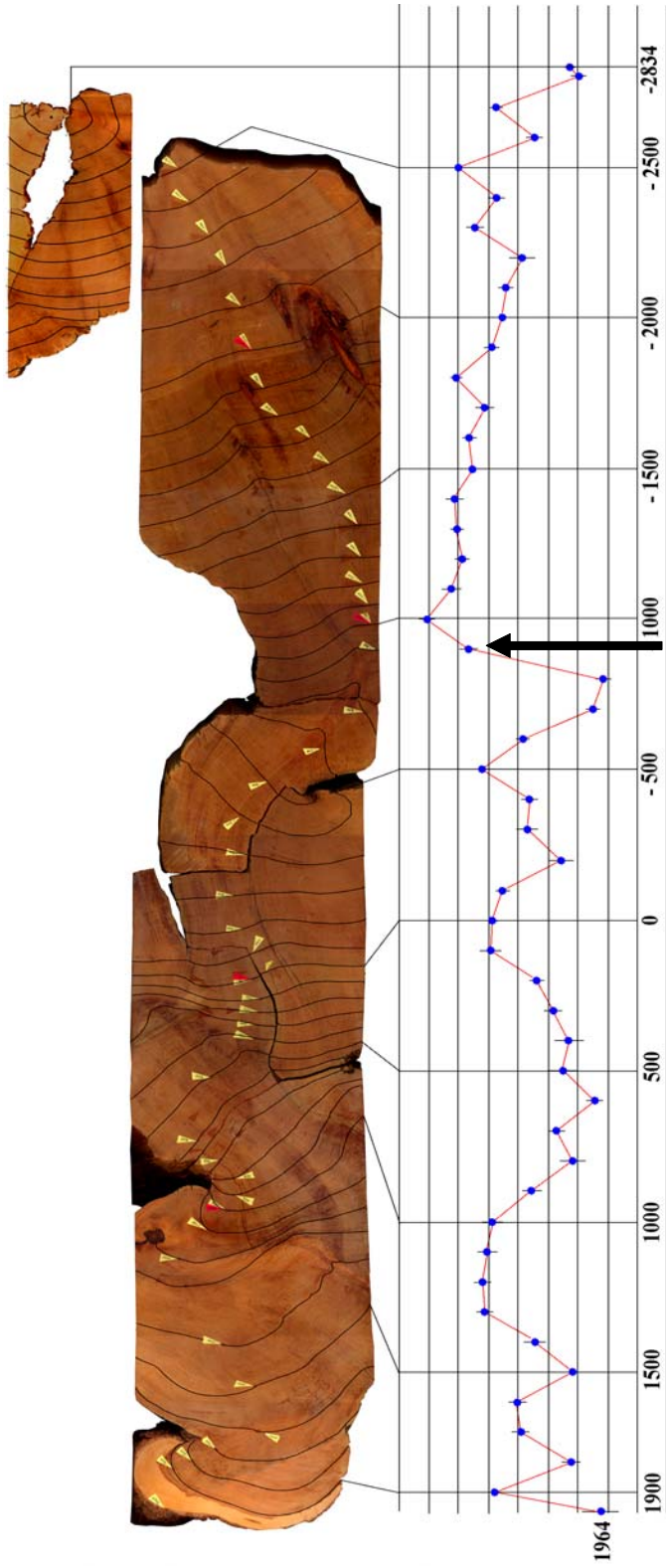
Figure 7.9 Scatterplot of the combined mean tracheid lengths vs. year lined up to the main slab and pith pieces of Prometheus. An arrow points to -800, the century sample point where the dramatic decrease in tracheid length was noted.

89

Figure 7.10 Prometheus stump with scanned image of the main slab laid overtop. An arrow points to the approximate location of -800 century ring where the unexpected drop in tracheid length occurred. Note the absent wood and how the stump surrounds the gap (HJ Arnott).

7.4 Complimentary environmental studies

The Salzer and Kipfmueller (2005) study identified extreme periods of wet, dry, cool, and warm in the southwestern United States. Six periods of warm and six periods of cool related to the century points where tracheids were sampled on the main slab. Relative to the preceding sample sites, mean tracheid lengths decreased during the warm periods and increased during the cool periods. This correlation supports the tenet that the mean temperature of a growing season affects ring width and tracheid length. Temperature is the primary determinant of the length of the growing season at high altitudes (Daubenmire 1954; Wardle 1965; Grace 1977). During a warmer than usual season, more time would be available for ring growth. Following that reasoning, a greater frequency of pseudotransverse divisions leads to shorter initials during expansion of the cambium (Bannan 1960; Philipson and Butterfield 1967). When a tree

90

experiences a period of rapid growth during a favorable growing season, the rate of pseudotransverse divisions is the greatest. The reverse would be true — a cooler period would produce longer tracheids due to the slowdown in pseudotransverse divisions of the cambial initials. This relationship, of course, works only if no other limiting growth factors (moisture) are negatively affecting the growing season.

Four unique long-term temperature events were compared to the mean width of one-hundred-year intervals from the main slab (Figure 6.13). The Little Ice Age (LIA) (~1300-1800) was a period of cooling that occurred after a warmer period of time known as the Medieval Warm Period (MWP) (~800-1300). Mann *et al* (1998) and Jones *et al* (1998) agreed that the 15th through 19th centuries were the coldest of the millennium over the Northern Hemisphere, but that the cooling amounted to no more than one degree C relative to late 20th century levels. In addition, the MWP temperatures were only 0.2 degrees C warmer than those temperatures from the LIA (Crowley and Lowery 2000). After examining the mean 100-year ring widths during the LIA and the MWP, the widest and the narrowest century rings were observed between the two periods. The mean width of the combined intervals was 50.3 mm. Three of the five LIA widths exceeded the mean value and all five of the MWP widths were less than the mean value. The simplest hypothesis would suggest that the narrow rings would belong to the cooler period (similar to what was discovered with the Salzer and Kipfmueller correlation above), but this was not the case when examining climate on a wider scale. The widest rings, suggesting vigorous growth and/or a longer growing season, matched the LIA. The temperature is likely a proxy for another variable, moisture, that is then coupled (cause and effect) with ring width. Stine (1994) maintains that the MWP was accompanied by severe drought conditions in California and the Great Basin. This is further evidence that the reduction in ring width during the warm period was more influenced by water stress than by the warmer temperatures causing longer growing seasons. These results conflict with LaMarche (1974) and his study of White Mountain, California bristlecone pines. Narrow rings correlated with low temperatures for trees at the upper tree line. Moisture limited growth more frequently in low altitude bristlecone pines. For a 5405 year record

91

of mean annual ring widths at the upper tree line, all growth trends positively related to temperature. LaMarche suggested that intersite differences could identify the factors influencing a region. One of the four combinations of temperature and moisture (warm/moist, warm/dry, cool/moist, and cool/dry) can be determined to be the prevalent growing condition when the ring widths of high altitude trees are compared to low altitude trees. Warm/moist conditions would produce wide rings at both locations. Warm/dry conditions would produce wider rings in the high altitude trees (which are more drought resistant) and narrower rings in the low altitude trees. Cool/moist conditions would result in narrower rings in the high altitude trees and wider rings in the lower altitude trees. Cool/dry conditions would result in narrow rings for both locations. Following that line of reasoning, the Little Ice Age did not reduce temperatures enough to affect ring width and also must have been accompanied by sufficient moisture for the growing season. As Stine (1994) determined, the MWP was a time of drought, severe enough to influence growth. This would account for the reduced ring widths in this study during the MWP. Bond *et al* (1997) examined sediment layers from North Atlantic deep sea cores and deduced that abrupt shifts in temperature lasting a few hundred years had occurred periodically every 1470 years +/- 500 years during the Holocene period. During the last 5000 years, three Bond events were described as taking place 1400, 2800, and 4200 years before present. These events would correspond to the years 450, -800, and -2200. Spikes in ring widths around -800 and -2200 could be the Bond temperature fluctuations influencing those growing seasons. As an interesting correlation, the regression tree analyses of Prometheus tracheid length data separated the W and E data sets between -900 and -800 and between -2200 and -2300. The most recent Bond event at 450 is less clear as to its influence on ring widths. These events are said to have varied in intensity. The research into Bond events is ongoing and new reports may one day correspond more closely to the data provided in this study.

The LaMarche (1974) study offered two additional graphs for comparison with the Prometheus one-hundred-year ring width data. For two regions in the White Mountains, treeline and lower forest border, twenty year intervals of rings were measured and averaged and

compared to climatic conditions of cool-dry, warm-moist, cool-moist, and cool-dry. Generally, during periods of dryness regardless of the temperature, LaMarche noted differences in ring-width departure from the overall mean.   The trees in the two regions reacted in opposite ways concerning ring widths during the dry periods – lower forest trees decreased their ring widths and tree line trees showed an increase in ring widths. When Prometheus one-hundred year mean ring widths were added to the graph (Figure 7.11) and compared to the departure from the mean of the White Mountain trees (Table 7.1), the Prometheus tree followed the pattern of the lower forest border trees nine out of the eleven centuries examined. Prometheus followed the pattern of the tree line trees for four of the eleven centuries examined.
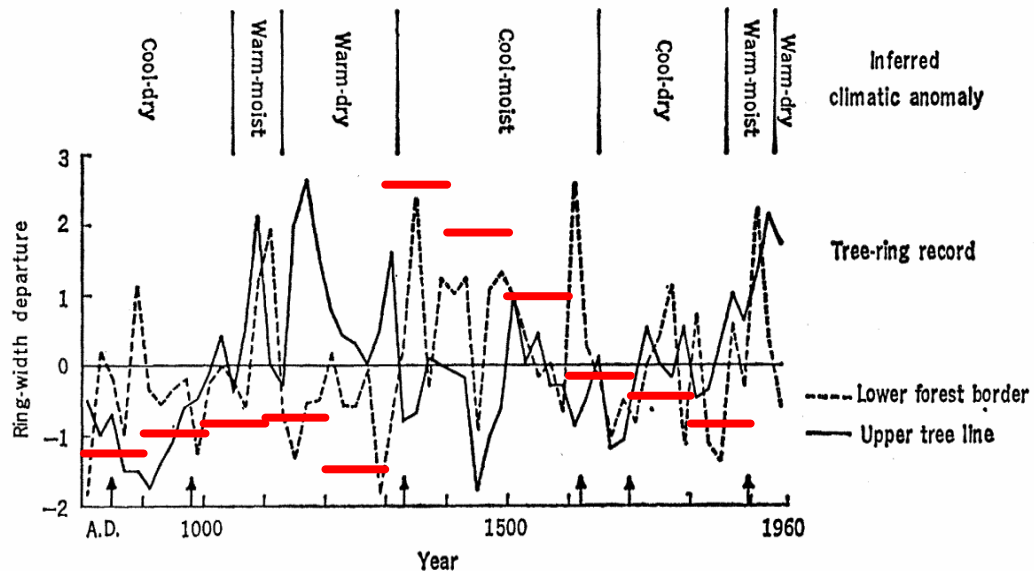
Figure 7.11 For White Mountain bristlecone pines, ring-width departure from the mean versus year for lower forest border trees and the upper tree line between the years 800 and 1950.   In the LaMarche study, twenty rings were measured and averaged and compared to the overall mean ring width (0). Red bars indicate the one hundred year mean ring widths of Prometheus from this current study, scaled to fit this graph (From LaMarche 1974)

The second LaMarche (1974) graph compared one-hundred year mean ring widths to year, exactly what was produced in this study (Figure 6.13), except that a line following the width values replaced the columns used herein. The LaMarche line was superimposed on the current study data (Figure 7.12). The LaMarche data contained widths from rings older than this study

93

(-3500 versus -2400), so the line was shortened to match up correctly. The two sets of data do not appear to vary together at most points, but there are intervals (500 to 1100, -900 to -1800) where the columns and line increase and decrease together.

Table 7.1 For White Mountain Bristlecone Pines and Prometheus, Ring-width Departure from the Mean versus Year. "Below" and "above" mean that the twenty-year mean ring widths were below or above the overall mean value for the White Mountain trees. The red text points out the White Mountain trees that followed the same trend as Prometheus (From LaMarche 1974)

	White Mountain Treeline	White Mountain lower forest border	Prometheus
800-900	**Below**	**Below**	**Below**
900-1000	**Below**	**Below**	**Below**
1000-1100	Above	**Below**	**Below**
1100-1200	Above	**Below**	**Below**
1200-1300	Above	**Below**	**Below**
1300-1400	Below	**Above**	**Above**
1400-1500	Below	**Above**	**Above**
1500-1600	**Above**	Below	**Above**
1600-1700	**Below**	Above	**Below**
1700-1800	Above	**Below**	**Below**
1800-1900	Above	**Below**	**Below**
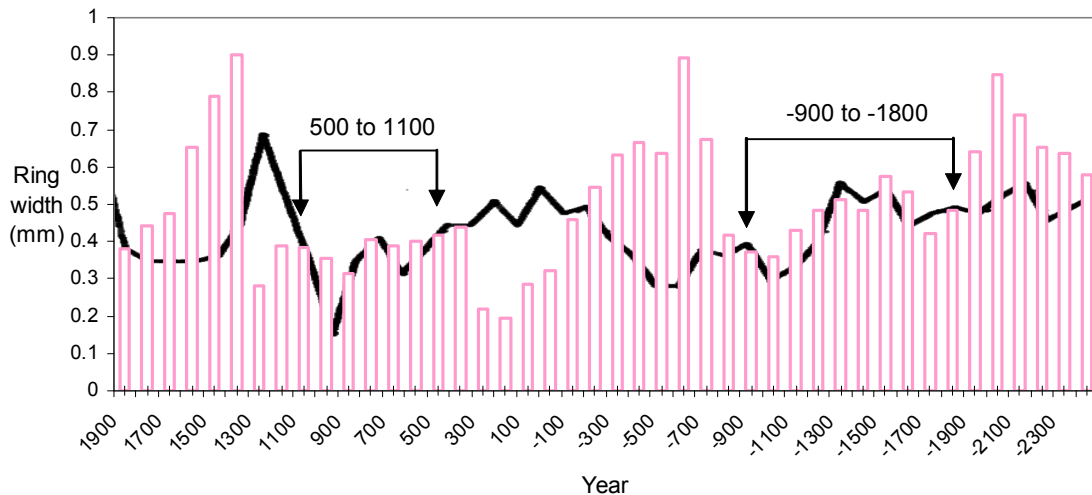
Figure 7.12 Mean century ring width versus age for Prometheus data and White Mountain bristlecone pines. Bar heights depicts the Prometheus mean century ring widths. The black line was copied from the LaMarche (1974) study and placed behind the column graph. Arrows indicate intervals where the two sets of data appear to vary together.

94

When mean tracheid lengths from the W data set were compared to the mean ring widths at the sampling sites (Figure 6.14), no overall correlation was found ($R^2 = 0.01$). At the sampling points, ring widths were variable and this may be the reason for the unclear results. In previous studies that found an inverse relationship between ring width and tracheid length (Bisset *et al* 1951; Strickland and Goddard 1966; Dinwoodie 1963), care was taken to consistently sample either the earlywood or latewood tracheids because the variability between those two areas within one ring could influence the relationship between ring width and tracheid length. The -800 sample that was previously shown to decrease sharply in length from the -900 site contained the widest rings measured in this study. Since tracheid length decreases with the rate of pseudotransverse divisions within the cambium during a favorable growing season, one or more extremely favorable growing seasons (seasons without moisture limitations or extreme cold temperatures) may be the cause of the decrease in tracheid length observed at -800. Multiple pieces of evidence (a Bond event, very short tracheids, the regression tree analysis splitting the data at this point, and the widest rings) suggest that a dramatic climate event may have affected Prometheus during that period of time.

CHAPTER 8

CONCLUSIONS

8.1 Methods

Franklin's method for the maceration of wood worked well for bristlecone pine tissue. The time in solution needs to be adjusted for weathered wood versus "cut edge" samples.

Nikon NIS Elements software combined with the Eclipse 80i research microscope provided 185 high resolution digital images using the "big picture" feature of NIS Elements. Using these images, it was possible to measure "complete tracheids" in which both ends were inspected. These digital images are available from the publisher. The tracheid length measurements are contained within Appendix B. Previous studies cannot be re-measured whereas the current study provides complete recall of the tracheids measured and of the measurements.

Images of tree rings were captured with either the Proscope handheld microscope, a HP scanner, or the Nikon research microscope mentioned above. The Proscope was used to capture images of rings for measurement, but the resolution of those images was inadequate for visualizing fine details. The captured images were also limited in size and would have to be merged together to provide larger continuous surface images. The scanner, capturing at 1000 dpi, also provided images suitable for measurement of ring width and, as an improvement on the handheld microscope, supplied images from one side of the Prometheus wood slab to the other. Nine scans of the main slab were merged together into a life size composite of Prometheus measuring 238 centimeters by 37 centimeters, with a corresponding file size of 1.26 gb. The research microscope provided the highest quality images, but the thickness of the wood became an issue. Only the thinner sections of the pith pieces could be viewed because they fit between the microscope stage and the objectives.

8.2 Crossdating

Prometheus sections (main slab and pith pieces), not previously clearly related, were crossdated with a strong correlation value of 0.80. Using these data, it was determined that 4842 rings can be found along the transect used by Currey (1965). Prometheus tree rings, dated 1600-1900, were crossdated with two master chronologies (Hill 10842 and Indian Garden) (World Data Center for Paleoclimatology 2008) and with a closely related tree called "Buddy." All matches produced a correlation value ranging between 0.52 and 0.65. Standardizing Prometheus and Buddy data would undoubtedly make the correlations stronger. Since the Indian Garden (Graybill) chronology spans the years between -2370 and 1982, it is suggested that future crossdating attempts with this master chronology would improve the estimation of the true age of Prometheus by identifying missing rings.

During crossdating and further examination of the surface of Prometheus, it was determined that the current assessment of the age of the Prometheus wood is an underestimation. The pith and two additional rings are missing from the "pith piece." During an examination of rings for a supplemental study, fourteen partial rings were observed between the years -1675 to -1575, -1500 to -1400, 140 to 240, and 1785 to 1885 (400 years). These rings had not been included in Currey's count. Assuming a constant rate of partial rings over the remaining 4444 years of Prometheus, 155 rings could be unaccounted for in the age of Prometheus. Adding the missing pith years (3) and the known (14) and unknown partial rings (155), the age of the Prometheus slab is closer to 5014. These data support the suppositions of Currey (1964) that Prometheus was at least 5000 years of age.

8.3 Tracheid Length

This study provided data on the oldest individual bristlecone pine, extending our knowledge of tracheid lengths from 2200 years (Baas *et al* 1986) to over 4850 years. Data were collected from two separate transects of the stem (W and E) and were shown to be statistically different from each other. A primary growth phase was demonstrated in this study. From the combined Pendley (2008) and current study, tracheid lengths increased from 1 to 3.5 millimeters

within one hundred years. A third order polynomial fit the data with a correlation R^2 = 0.70. The length of the Prometheus growth phase is in contrast to the finding of Baas *et al* (1986), where a primary growth phase lasting 250-500 years was identified in the 500 and 600-year-old cores. A maximum tracheid length (3.19 mm) was observed in the current study at -1000, 1878 rings from the pith. Baas *et al* observed that tracheids lengths steadily increased, with no sign of leveling off, over the entire 2200-year-old core. For the Prometheus wood, tracheid lengths, after the sharp decrease in length at -800, assumed a variable, but more or less constant length. That marked reduction of tracheid length at -800 was found in both transects. The cause or causes of the sharp decrease is unknown, but environmental factors (temperature or available water) or, less likely, direct physical damage to the cambium are among the possibilities.

In the additional study comparing mean tracheid length to mean ring width at the associated sample sites, the correlation between the two was inconclusive (R^2 = 0.01), but the -800 mean tracheid length matched the mean widest ring width of the study. This result suggests that very favorable growing conditions for the years sampled were present. While previous physical damage to the cambium is possible, there is no evidence that it occurred at the sampling point.

Six periods of extreme warm periods, five to fifty years in duration, intersected with tracheid sampling points on the Prometheus main slab. All of the tracheid lengths decreased in length from the prior sample. Six periods of extreme cool periods, five to fifty years in duration, intersected with tracheid sampling points. All of the tracheid lengths increased in length from the prior sample. These results agree with previous studies that determined that warmer seasons (without other limiting factors) promote vigorous activity of the vascular cambium. Rapidly dividing to increase the circumference, initials are shorter and thus produce shorter tracheids. The reverse situation is also true — a reduced rate of pseudotransverse divisions for initials leads to longer initials and thus longer tracheids (Bannan 1960; Philipson and Butterfield 1967). Mean tracheid lengths did not correlate with associated mean ring widths at their sampling points, although the shortest tracheids (-800) did match the widest rings measured.

98

8.4 Ring Width

The mean width of one hundred rings across the surface of the main slab were compared to five different long-term temperature events spanning 4200 years before present. During the Little Ice Age (~1300-1800), the majority of the century intervals (three of five) were wider than average width. The first century, 1300-1400, exhibiting the widest interval measured (90.1 mm). During the Medieval Warming Period (~800-1300), all five of the century widths were less than the mean width. This appears contrary to the concept that warmer growing seasons promote wider rings and cooler seasons produce narrower rings. But, evidence exists that the Medieval Warming Period was also a period of severe drought and water stress limits wood growth. The Little Ice Age temperatures were reported to be a reduction from normal temperatures of one degree C or less. This was likely not enough to affect physiological growth processes. The increase in ring width during the Little Ice Age is probably due to the presence of abundant water in an area (upper treeline) that normally receives very little water during the growing season, one inch or less a month. Two of the three Bond events (-800 and -2200) were associated with spikes in the century widths, possibly a reaction to the fluctuation in temperatures and/or precipitation.

When mean century ring widths of Prometheus were compared to the deviation from the average ring width for White Mountain bristlecone pine trees at treeline and lower forest border (LaMarche 1974), the Prometheus data followed the pattern of the lower forest border trees nine of the eleven measured intervals (800-1950). When mean century ring widths of Prometheus were compared to mean century ring widths of White Mountain bristlecone pines, the data did not vary together over the entire set of years, -2400 to 1900, but groups of years (500 to 1100, -900 to -1800) appeared to relate to each other, rising and falling together.

APPENDIX A

CROSSDATE PROGRAM RESULTS

CROSSDATE

A Tool for Tree Ring Dating

by Greg D. Lazear and Thomas P. Harlan

Version 2.1 Copyright 2001-2003

SCROLL Skeleton Plots:
Clicking a ring moves it to the CENTER
Clicking outside plots scrolls BOTH

SEARCH CONTROL PANEL

SELECTION Cross Date Years: 282 to   551

SELECTION Correlation: 0.805

Scroll

Done

— Search Pattern SELECTION —
Starting Ring: 1
Ending Ring: 270

— Match Method —
Correlation Coef.
Absolute Difference

— Incremental Search —
Minimum Correlation 0.5
Find Next Match
Find Best Match

— Global Segment Search —
No. Rings in Segment 40
Find Best Segment

Specimen: Copy of MainSection

Specimen: Copy of PithSection

Specimen: Copy of MainSection

Specimen: Copy of PithSection

CROSSDATE
A Tool for Tree Ring Dating
by Greg D. Lazear and Thomas P. Harlan
Version 2.1 Copyright 2001-2003

SCROLL Skeleton Plots:
Clicking a ring moves it to the CENTER
Clicking outside plots scrolls BOTH

SEARCH CONTROL PANNEL

Specimen Cross Date Years: 1 to 251

Scroll

Current Pattern Correlation 0.591

Match Method

Incremental Search
Minimum Correlation 0.5

Search Pattern Selection

Starting Ring 1
Ending Ring 251

Correlation Coef.
Absolute Difference

Find Next Match
Find Best Match

Global Segment Search
No. Rings in Segment 40

Find Best Segment

Done

Specimen: prometheus

Specimen: hill10842

Specimen: prometheus

Specimen: hill10842

103

CROSSDATE

A Tool for Tree Ring Dating

by Greg D. Lazear and Thomas P. Harlan

SCROLL Skeleton Plots:
Clicking a ring moves it to the CENTER
Clicking outside plots scrolls BOTH

SEARCH CONTROL PANNEL

Specimen Cross Date Years: 1 to 251

Current Pattern Correlation: 0.520

Done

Global Segment Search

No. Rings in Segment 40

Find Best Segment

Scroll

Incremental Search
Minimum Correlation 0.5

Find Next Match

Find Best Match

Match Method
○ Correlation Coef.
○ Absolute Difference

Search Pattern Selection

Starting Ring: 1

Ending Ring: 251

Specimen: Buddy

Specimen: hill10842

Specimen: Buddy

Specimen: hill10842

104

CROSSDATE

A Tool for Tree Ring Dating

by Greg D. Lazear and Thomas P. Harlan

SCROLL Skeleton Plots:
Clicking a ring moves it to the CENTER
Clicking outside plots scrolls BOTH

SEARCH CONTROL PANNEL

Specimen Cross Date Years: 1 to 376

Current Pattern Correlation: 0.650

Scroll

Search Pattern Selection

Starting Ring: 1

Ending Ring: 376

Match Method

○ Correlation Coef.
○ Absolute Difference

Incremental Search

Minimum Correlation: 0.5

Find Next Match

Find Best Match

Global Segment Search

No. Rings in Segment: 40

Find Best Segment

Done

Specimen: prometheus300

Specimen: indiangarden

Specimen: prometheus300

Specimen: indiangarden

CROSSDATE
A Tool for Tree Ring Dating
by Greg D. Lazear and Thomas P. Harlan

SCROLL Skeleton Plots:
Clicking a ring moves it to the CENTER
Clicking outside plots scrolls BOTH

SEARCH CONTROL PANNEL

Specimen Cross Date Years: 1 to 251

Current Pattern Correlation: 0.647

Scroll

Search Pattern Selection
Starting Ring: 1
Ending Ring: 251

Match Method
- Correlation Coef.
- Absolute Difference

Incremental Search
Minimum Correlation: 0.5
Find Next Match
Find Best Match

Global Segment Search
No. Rings in Segment: 40
Find Best Segment

Done

Specimen: Buddy

Specimen: indiangarden

Specimen: Buddy

Specimen: indiangarden

106

APPENDIX B

TRACHEID LENGTHS (MM)

Preliminary study to determine sample size (n = 140)

3.09	2.9	2.08	2.63	3.53
2.57	2.58	2.08	3.08	3.31
2.28	2.61	2.54	2.36	2.42
2.01	2.93	3.01	2.66	2
3.01	2.06	2.78	2.54	3.28
2.38	2.12	2.26	2.68	3.29
2.88	2.78	1.81	3.13	2.47
2.3	2.74	3.07	2.48	2.53
2.75	2.89	1.99	2.8	2.81
2.64	2.92	3.29	2.49	2.64
2.6	3.19	2.85	3.09	2.99
2.21	2.48	3.08	2.41	2.79
3.12	3.18	2.87	2.65	2.97
2.37	2.21	2.87	2.16	3.27
2.51	2.08	2.58	2.5	2.55
2.83	2.57	2.76	2.84	2.79
2.64	2.99	3.27	3.1	2.88
1.69	3.31	2.9	2.39	2.57
2.45	3.18	2.8	3.1	2.91
2.37	3.04	2.25	2.48	2.91
2.22	2.21	2.2	2.45	
2.92	2.69	3.12	2.88	
3.22	2.61	2.25	2.43	
3.35	2.18	3.11	1.98	
2.88	3.16	2.93	2.97	
2.81	2.87	2.77	2.88	
3.02	2.86	2.9	2.48	
3.05	3.07	3.1	1.89	
3.28	2.28	2.6	2.75	
2.99	2.19	2.84	2.69	

Preliminary test to determine sample size - Slide 1

10	20	30	40	50	60	70
2.7	2.8	2.61	2.68	2.87	3	3.09
2.69	2.15	2.73	2.48	2.28	2.85	2.57
1.98	2.42	3.04	2.43	3.21	2.64	2.28
2.09	2.56	2.47	2.59	2.38	2.5	2.01
2.94	2.76	2.27	2.25	3.17	2.41	3.01
2.5	2.07	2.13	2.36	3.32	2.51	2.38
2.54	2.74	3.29	2.29	1.84	2.28	2.88
2.72	3.14	1.65	2.98	3.33	2.01	2.3
2.72	2.37	3.45	2.81	2.49	2.45	2.75
3.09	2.66	2.84	3.04	2.34	2.61	2.64
	2.38	3.05	2.6	2.37	2.89	2.6
	2.63	2	2.59	2.8	2.21	2.21
	2.89	2.19	2.5	2.89	3	3.12
	2.54	2.57	1.74	2.22	3.22	2.37
	2.91	1.9	2.51	2.75	2.15	2.51
	2.98	2.23	2.92	2.05	2.93	2.83
	2.57	2.56	2.23	2.43	2.2	2.64
	2.97	2.45	2.75	3.18	2.62	1.69

2.98	1.94	2.88	2.5	2.79	2.45
2.76	3.83	2.52	2.43	2.26	2.37
	2.98	3.05	3.36	2.05	2.22
	3.39	2.77	2.65	2.47	2.92
	2.06	2.77	2.42	3.31	3.22
	3.2	2.94	2.31	3.41	3.35
	3.12	3.4	1.51	2.73	2.88
	2.55	3.09	2.25	2.7	2.81
	2.15	2.71	2.72	2.57	3.02
	2.23	2.69	2.65	2.1	3.05
	3.21	2.51	2.45	1.88	3.28
	2.65	2.23	2.26	2.4	2.99
		2.51	2.96	2.15	2.63
		2.12	2.45	2.88	3.08
		2.38	2.58	2.3	2.36
		3.11	2.7	2.33	2.66
		2.74	2.35	2.68	2.54
		2.4	3.04	2.72	2.68
		2.84	3.24	2.4	3.13
		2.42	3.1	2.73	2.48
		3.1	2.54	2.39	2.8
		1.96	2.48	3.35	2.49
			2.92	2.31	3.09
			2.7	2.65	2.41
			2.07	2.45	2.65
			2.68	2.8	2.16
			3.79	3.27	2.5
			2.98	2.75	2.84
			3.23	3.57	3.1
			2.33	2.24	2.39
			2.89	2.73	3.1
			2.41	2.75	2.48
				2.86	2.9
				2.95	2.58
				2.91	2.61
				2.01	2.93
				3.18	2.06
				2.9	2.12
				2.11	2.78
				2.87	2.74
				2.39	2.89
				3.3	2.92
					3.19
					2.48
					3.18
					2.21
					2.08
					2.57
					2.99
					3.31
					3.18
					3.04

Preliminary test to determine sample size - Slide 2

10	20	30	40	50	60	70
2.34	2.81	2.81	2.11	2.91	2.91	2.21
2.29	2.94	2.94	2.91	3.26	2.62	2.69
2.35	2.98	2.98	2.22	3.14	2.68	2.61
3.01	2.61	2.61	2.53	2.85	2.46	2.18
2.06	2.5	2.5	2.1	2.15	2	3.16
1.71	2.52	2.52	3.05	2.85	2.36	2.87
2.15	1.9	1.9	2.23	2.92	2.92	2.86
2.19	2.03	2.03	2.6	2.85	3.37	3.07
2.57	2.65	2.65	2.5	3.09	2.39	2.28
2.09	2.68	2.68	2.78	2.26	2.09	2.19
	2.69	2.69	2.22	2.73	2.6	2.45
	2.61	2.61	1.92	2.81	2.19	2.88
	2.75	2.75	2.51	2.27	2.37	2.43
	2.53	2.53	2.8	2.52	2.18	1.98
	2.31	2.31	2.36	2.24	2.9	2.97
	2.52	2.52	3.23	2.21	2.7	2.88
	2.43	2.43	2.9	2.7	2.12	2.48
	2.12	2.12	2.31	1.87	2.96	1.89
	2.32	2.32	2.67	2.28	2.71	2.75
	2.92	2.92	2.7	3.21	2.66	2.69
		2.51	3.21	3.02	2.36	2.99
		2.75	2.36	3.07	3.02	2.79
		2.54	2.83	2.08	2.09	2.97
		2.98	2.41	3.09	2.14	3.27
		2.9	2.27	2.29	2.18	2.55
		2.57	2.88	2.49	2.14	2.79
		2.23	2.77	2.5	3.04	2.88
		2.58	2.72	2.9	2.27	2.57
		2.96	2.64	2.1	2.54	2.91
		2.59	2.2	2.87	3.08	2.91
			3.16	2.51	2.57	2.08
			2.47	2.08	2.26	2.08
			3.11	3.3	2.86	2.54
			2.89	2.21	2.59	3.01
			2.82	3.19	2.81	2.78
			2.92	2.81	2.29	2.26
			2.3	1.54	2.17	1.81
			2.74	2.17	2.64	3.07
			2.15	2.35	2.71	1.99
			2.79	2.8	3.01	3.29
				3.02	3.04	2.85
				2.91	2.08	3.08
				3.19	2.15	2.87
				2.67	2.89	2.87
				2.76	2.9	2.58
				2.18	3.09	2.76
				2.08	3.32	3.27
				2.59	2.89	2.9
				2.24	2.48	2.8
				2.99	3.15	2.25

2.79	2.2
2.77	3.12
3.26	2.25
2.01	3.11
2.59	2.93
2.81	2.77
3.13	2.9
2.54	3.1
1.98	2.6
2.94	2.84
	3.53
	3.31
	2.42
	2
	3.28
	3.29
	2.47
	2.53
	2.81
	2.64

Tracheid lengths along one ring -638 (mm)

1	2	3	4	5
2.35	2.67	2.51	2.14	2.27
2.37	2.69	2.54	2.31	2.31
2.39	2.7	2.63	2.32	2.33
2.41	2.7	2.65	2.34	2.34
2.41	2.7	2.65	2.37	2.38
2.48	2.71	2.67	2.39	2.39
2.51	2.73	2.67	2.4	2.41
2.51	2.74	2.69	2.42	2.43
2.51	2.74	2.73	2.42	2.43
2.53	2.75	2.77	2.45	2.47
2.53	2.75	2.79	2.46	2.48
2.55	2.76	2.79	2.46	2.49
2.57	2.78	2.8	2.46	2.49
2.57	2.85	2.8	2.47	2.53
2.58	2.87	2.8	2.48	2.54
2.59	2.89	2.81	2.5	2.57
2.59	2.89	2.81	2.51	2.57
2.61	2.91	2.82	2.52	2.57
2.61	2.96	2.83	2.52	2.58
2.63	2.97	2.84	2.53	2.59
2.65	2.97	2.87	2.54	2.6
2.68	2.98	2.87	2.56	2.6
2.68	2.98	2.88	2.56	2.62

111

2.7	2.99	2.89	2.57	2.62
2.71	3	2.9	2.58	2.63
2.74	3.01	2.91	2.59	2.63
2.76	3.01	2.91	2.59	2.65
2.76	3.02	2.92	2.6	2.66
2.77	3.02	2.93	2.63	2.67
2.77	3.04	2.93	2.63	2.67
2.8	3.05	2.93	2.64	2.68
2.8	3.05	2.94	2.65	2.69
2.81	3.06	2.95	2.67	2.69
2.83	3.11	2.95	2.68	2.7
2.83	3.15	2.98	2.7	2.71
2.84	3.21	2.98	2.71	2.71
2.84	3.21	3.01	2.73	2.73
2.84	3.29	3.02	2.74	2.74
2.84	3.29	3.03	2.75	2.74
2.87	3.31	3.04	2.76	2.75
2.9	3.32	3.05	2.76	2.76
2.92	3.35	3.06	2.79	2.76
2.93	3.36	3.08	2.81	2.76
2.94	3.37	3.09	2.82	2.76
2.95	3.38	3.12	2.83	2.77
2.97	3.39	3.13	2.85	2.79
2.99	3.39	3.13	2.86	2.79
3.05	3.4	3.15	2.87	2.8
3.1	3.41	3.16	2.88	2.93
3.15	3.54	3.28	3.11	2.98

Year Ring No.	1964W 4842	1964E 4842	1900W 4778	1800W 4678	1700W 4578	1600W 4478	1600E 4478	1500E 4378	1400W 4278
	2.33	1.31	2.42	2.17	2.39	2.64	2.22	2.89	2.57
	2.24	1.31	2.31	2.35	2.08	2.81	2.1	2.5	2.6
	2.16	1.2	2.74	1.8	2.16	2.56	2.06	2.49	2.53
	2.64	1.19	2.51	2.4	2.39	2.44	1.93	2.07	2.7
	2.56	1.09	2.93	1.97	2.25	2.44	1.98	2.15	2.73
	2.21	1.27	2.29	2.19	2.48	2.43	1.77	2.55	2.73
	2.28	1.3	1.98	2.18	2.54	3.05	2.44	2.35	2.85
	2.61	1.36	2.17	2.07	2.51	2.28	2.04	2.03	3.11
	2.03	1.36	2.36	2.19	2.46	2.45	2.25	2.02	2.82
	2.07	1.16	2.3	2.27	2.34	2.88	2.12	2.3	3.02
	2.54	1.35	2.32	2.29	2.34	3.15	2.32	2.16	2.79
	2.54	1.08	2.43	2.35	2.32	2.43	1.83	2.18	2.64
	2.95	1.26	2.47	1.87	2.47	2.39	2.22	2.27	2.43
	2.89	1.19	2.72	2.07	2.12	3.13	2.31	2.39	2.57
	2.31	1.14	2.98	2.07	2.28	2.58	1.94	2.12	2.71
	2.49	1.38	3.04	1.94	2.53	2.65	1.93	2	3.05
	2.65	1.39	2.71	2.15	2.25	2.85	1.95	1.92	2.66
	2.94	1.33	2.97	2.13	2.18	2.66	2.16	2.27	2.65
	2.64	1.36	2.86	2.12	2.95	2.85	2.19	2.39	2.59
	2.71	1.43	2.76	2.53	2.81	2.56	2.36	2.12	2.7
	2.5	1.4	2.93	1.95	2.19	2.63	2.32	1.97	2.94
	3.04	1.34	2.77	1.97	2.81	2.49	2.09	2.68	2.95
	2.54	1.3	2.39	2.13	2.68	2.56	2.18	2.24	2.56
	2.65	1.3	2.73	2.24	2.62	2.75	2.16	2.14	2.56
	2.81	1.28	2.47	2.29	2.62	2.82	2.31	2.11	2.85
	2.69	1.45	2.93	2.32	2.51	2.87	2.24	2.11	2.89
	2.73	1.39	2.47	2.09	2.72	2.89	2.61	2.08	2.77
	2.87	1.25	2.59	2.22	2.7	3.05	2.32	2.06	2.73
	2.43	1.28	2.83	2.42	2.39	2.64	2.56	2.15	2.69
	2.4	1.5	3.05	1.88	2.46	2.75	2.87	2.27	2.63
	2.67	1.53	2.69	1.8	2.42	2.12	2.64	1.64	2.66
	2.56	1.28	2.62	1.76	2.46	2.73	2.82	1.9	2.45
	2.67	1.34	2.61	2.12	2.75	2.58	2.84	2.15	2.45
	2.62	1.41	2.93	1.9	2.46	2.83	2.75	1.98	2.46
	2.84	1.26	2.82	2.6	2.38	2.87	2.06	1.97	2.92
	2.33	1.43	2.72	2.54	2.63	2.82	2.48	1.98	2.7
	2.49	1.58	2.5	1.91	2.99	2.85	2.47	1.93	2.86
	2.53	1.29	2.54	2.03	2.68	3	2.59	2.03	2.82
	2.78	1.42	3.02	1.85	2.39	2.91	2.37	1.96	2.82
	2.49	1.39	2.65	1.9	2.3	2.62	2.72	2.05	2.79
	2.4	1.48	2.76	1.74	2.49	2.89	2.84	2.22	2.83
	2.41	1.46	2.84	2.39	2.76	3.02	2.76	1.9	2.58
	2.64	1.38	2.81	2.43	2.4	2.54	2.53	2.89	2.46
	2.2	1.36	2.72	2.41	2.64	3.01	2.46	1.8	2.65
	2.43	1.31	2.69	2.09	2.43	2.32	2.16	2.05	2.84
	2.76	1.61	2.43	1.81	2.44	2.81	1.81	1.74	2.88
	2.6	1.56	2.77	2.43	2.48	2.65	2.49	1.68	3.01
	2.47	1.66	2.99	2.22	2.36	2.6	2.82	2.12	2.6
	2.72	1.58	2.76	2.52	2.38	2.8	2.06	1.7	2.68
	2.34	1.44	2.82	2.2	2.78	2.65	2.21	2.08	2.96

Year Ring No.	1400E 4278	1300E 4178	1200W 4078	1100W 3978	1000W 3878	900W 3778	800W 3678	800E 3678	700E 3578
	2.22	2.86	2.65	2.99	2.19	2.1	2.07	1.9	2.2
	2.03	2.47	2.88	2.91	2.45	2.13	2.54	1.86	1.81
	2.05	2.89	2.67	2.22	2.41	2.49	2.52	1.87	1.82
	2.21	3.06	2.68	2.73	2.65	2.51	2.51	1.86	2.24
	2.43	2.71	2.65	2.53	2.51	2.48	2.44	2.01	2.23
	2.44	2.67	2.67	2.97	2.55	1.92	2.27	1.88	1.87
	2.08	2.77	2.53	2.92	3.19	2.24	2.16	2.03	2
	2.17	2.54	2.93	2.99	2.59	1.79	2.6	1.91	2.27
	1.96	2.41	2.81	2.71	2.19	2.52	2.31	1.69	2.12
	2	2.61	2.89	2.93	2.51	2.38	2.25	1.61	2.15
	2.34	2.75	3.05	2.89	2.34	2.28	2.25	1.65	2.58
	2.04	2.8	2.51	3.02	2.61	1.79	2.45	1.7	2.18
	2.03	2.88	2.71	2.99	2.8	2.56	2.58	1.56	2.53
	2.06	2.98	2.63	2.38	2.83	2.59	2.54	1.68	2.52
	2.16	2.76	2.58	2.6	2.36	2.42	2.51	1.98	2.4
	1.99	2.91	2.6	2.94	2.74	2.46	2.53	2	2.32
	2.48	2.61	2.8	2.57	2.75	2.51	2.43	1.86	2.23
	1.93	2.62	2.88	2.97	2.77	2.16	2.44	1.68	2.63
	1.81	2.81	2.58	3.13	2.78	2.63	2.87	1.79	2.24
	1.51	2.75	2.88	2.7	3.24	2.41	2.55	1.67	2.21
	1.94	3.02	3.07	3.04	2.91	2.27	2.77	1.66	2.1
	2.01	2.7	2.6	2.6	2.59	2.46	2.57	1.72	2.32
	2.37	2.26	2.92	2.67	2.93	2.25	2.31	1.65	2.25
	1.79	2.8	2.73	2.98	2.82	2.47	2.21	1.71	2.31
	2.12	2.51	2.83	3.18	2.85	2.52	2.67	1.8	2.5
	2.03	2.39	2.5	2.78	2.78	2.29	2.45	1.9	2.32
	2.12	2.98	2.49	2.61	2.25	2.19	2.71	1.89	2.48
	2.09	2.94	2.64	2.78	3.1	2.7	2.73	1.78	2.31
	2	3.09	3.15	2.37	2.95	2.72	2.78	1.83	2.45
	1.99	2.42	2.52	2.5	2.33	2.5	2.29	1.84	2.18
	2.02	2.99	3.19	2.41	2.84	2.25	2.8	1.68	2.01
	2.05	2.72	2.35	2.45	2.63	2.55	2.54	1.63	2.05
	2.04	2.49	2.55	2.47	2.38	2.42	2.76	1.68	1.91
	2.16	3.01	2.84	2.57	2.87	2.29	2.67	1.64	2.05
	2.03	2.9	2.78	3.12	2.87	2.35	2.22	1.65	1.9
	2.12	2.74	2.92	3.11	2.36	2.98	2.19	1.45	2.36
	2.36	2.61	2.61	2.58	2.78	2.39	2.34	1.58	2.2
	1.89	2.67	2.49	2.58	2.42	2.49	2.46	1.79	2.56
	1.83	2.7	2.56	2.53	2.96	2.62	2.42	1.7	2.07
	1.97	2.76	2.56	2.42	2.56	2.65	2.76	1.66	2.42
	2.16	2.88	2.77	2.93	2.83	2.69	2.44	1.6	2.34
	1.89	2.51	3.32	2.79	2.56	2.89	2.44	1.74	2.33
	1.91	2.8	3.03	2.58	2.6	2.49	2.7	1.73	1.93
	1.97	2.89	2.75	2.57	2.51	2.41	2.92	1.73	2.26
	1.72	2.71	2.38	2.52	2.94	2.53	2.93	1.88	2.45
	1.78	2.55	2.99	2.45	2.26	2.38	2.61	1.51	2.27
	1.76	2.72	2.91	2.46	2.78	2.48	2.32	1.88	2.17
	2.26	2.44	2.75	2.55	3.01	2.11	2.59	1.67	2.3
	1.84	2.38	2.64	2.33	2.93	2.34	2.83	1.55	2.37
	2.19	2.75	2.44	2.47	2.55	2.45	2.75	1.82	2.54

Year Ring No.	600E 3478	500W 3378	500E 3378	400W 3278	400E 3278	300W 3178	300E 3178	200W 3078	200E 3078
	1.79	2.67	1.84	2.17	1.4	2.57	1.68	2.72	2.27
	2.14	2.6	1.87	2.33	1.5	2.87	1.88	2.76	2.37
	1.98	2.64	1.71	2.36	1.4	2.4	2.18	2.37	1.82
	1.73	2.81	2	2.28	1.43	2.44	1.89	1.95	2.04
	2.25	2.93	1.89	2.47	1.64	2.61	1.9	2.36	2.05
	2.08	2.83	2.02	2.76	2.16	2.37	1.86	2.22	2.3
	2.23	2.36	1.93	2.74	2.11	2.61	1.99	2.21	1.88
	2.24	2.72	2.12	2.63	1.62	2.61	1.98	1.98	2.02
	1.94	2.43	1.6	2.27	1.63	2.57	2.48	2.21	2.39
	2.18	2.58	1.69	2.14	1.6	2.54	1.97	2.27	2.31
	1.89	2.52	1.65	2.11	1.41	2.33	2.03	2.28	1.97
	1.8	2.93	1.51	2.87	1.69	2.52	2.03	2.56	2.03
	1.74	2.98	1.82	2.52	1.61	2.17	1.94	2.12	2.67
	2	2.4	1.77	2.45	1.75	2.79	2.01	2.37	2.22
	1.94	2.99	1.39	2.94	1.5	2.13	2.4	2.39	2.4
	1.77	2.43	1.67	2.93	1.33	2.43	2.42	2.39	2.31
	1.7	2.69	1.85	2.42	2.19	2.87	2.05	2.8	2.05
	2	2.66	1.92	2.99	1.36	2.91	2.01	2.78	2.07
	1.88	2.52	1.59	2.55	1.4	2.65	2.15	2.55	2.24
	2.33	2.27	1.57	2.71	1.44	2.73	2.19	2.53	2.24
	2.22	2.93	1.68	2.52	1.5	2.2	1.95	2.47	2.2
	2.1	2.6	1.72	2.32	1.57	2.28	1.95	2.86	2.19
	1.75	2.19	1.77	2.84	1.75	2.27	2.01	2.51	2.21
	2.06	2.67	1.84	2.64	1.82	2.19	2.02	2.45	2.24
	1.8	2.64	1.91	2.73	1.57	2.2	2.09	2.46	2.29
	2.27	2.41	1.74	2.37	1.5	2	2.02	2.55	2.11
	2.05	2.67	1.98	2.61	1.5	2.44	1.91	2.62	2
	1.75	3.03	1.53	3.38	1.48	2.63	2.06	2.59	2.25
	2.39	2.66	1.46	2.52	1.52	2.16	2.32	2.39	2.23
	2.01	2.44	1.74	2.74	1.96	2.19	2.2	2.61	2.2
	2.22	2.95	1.71	2.29	1.92	2.08	2.24	2.54	2.11
	1.91	2.6	1.65	2.09	1.8	2.69	1.71	2.21	2.41
	2.14	2.57	1.39	2.08	2.3	2.74	1.69	2.59	2.25
	1.87	2.74	1.54	2.32	2.15	2.58	1.92	2.98	2.04
	1.93	2.78	1.51	3.05	2	2.75	2.07	2.92	2.35
	2.16	2.71	1.61	2.54	2.22	2.23	1.86	2.73	2.49
	1.78	2.46	1.61	2.69	2.11	2.44	1.87	2.31	2.33
	2.34	2.63	1.62	2.82	2.12	2.35	2.41	2.64	2.03
	2.11	2.88	1.42	2.77	2.22	2.6	2.64	2.57	2.79
	1.97	2.81	1.41	2.58	2.15	2.42	2.68	2.43	2.29
	1.97	2.78	1.97	2.61	1.86	2.27	2.28	2.49	2.3
	2.07	2.83	1.96	2.59	1.99	2.26	2.12	2.42	2.38
	2.03	2.76	1.66	2.37	1.87	2.59	1.91	2.64	2.7
	2.04	2.81	1.63	2.5	1.76	2.15	2.06	2.88	2.8
	2	2.39	1.68	2.42	1.86	2.37	2.08	2.82	2.87
	1.67	2.76	1.79	2.34	2.27	2.45	2.52	2.4	2.42
	1.73	2.6	2.17	2.72	2.24	2.56	2.01	2.37	2.08
	1.67	2.62	1.48	2.97	1.77	2.79	1.94	2.78	2.17
	1.67	3.11	1.8	2.54	1.79	2.53	2.25	2.24	2.18
	2.14	2.89	1.92	2.3	1.52	2.22	2.12	2.38	2.46

Year	100W	100E	OW	OE	-100W	-100E	-200W	-300W	-400W
Ring No.	2978	2978	2878	2878	2778	2778	2678	2578	2478
3	3.06	2.52	2.9	2.47	2.77	2.27	2.66	2.68
2.5	3.02	2.61	3.11	2.63	2.84	1.99	2.72	1.83
2.66	3.01	2.59	2.64	2.71	3.09	2.63	2.67	2.64
2.41	3.53	2.69	2.57	2.7	2.63	2.23	2.7	2.35
2.45	3.52	2.68	2.85	2.29	2.63	2.15	2.58	2.06
2.22	2.73	2.63	2.94	2.49	2.45	2.37	2.67	2.38
2.21	2.67	2.79	2.87	2.71	2.59	2.24	2.58	2.68
2.72	2.8	2.9	3.04	2.89	2.65	1.88	2.72	2.79
2.72	2.57	2.96	2.66	2.89	2.42	1.74	2.89	2.59
2.44	2.84	2.74	2.64	2.34	2.98	1.86	2.55	2.32
2.47	3.57	2.8	2.68	2.38	2.39	1.79	2.86	2.59
2.32	2.77	2.58	2.67	2.22	2.5	2.33	2.43	2.54
2.68	2.82	2.57	2.47	2.33	2.52	1.8	2.27	2.6
2.41	3.04	2.22	2.65	2.09	2.88	1.98	2.14	2.61
2.56	2.9	2.6	2.71	2	2.58	1.85	2.34	2.73
2.48	2.7	2.77	2.65	2.5	2.84	1.52	2.6	2.69
2.37	2.8	2.45	2.91	2.46	2.5	2.22	2.48	2.31
2.64	3.07	2.39	2.77	2.3	2.65	2.58	2.37	2.82
2.45	2.93	2.38	2.68	2.2	2.66	2.12	2.61	2.25
2.68	3.03	2.05	2.7	2.32	2.55	2.28	2.05	2.5
2.63	3.35	2.14	2.55	2.49	2.57	2.32	2.18	2.98
2.38	2.75	2.66	2.66	2.48	2.72	2.55	2.5	2.94
2.42	2.71	2.61	2.78	2.44	2.71	2.31	2.46	2.61
2.2	2.97	3	2.68	2.05	2.64	2.14	2.65	2.7
2.6	3.33	2.65	2.9	2.7	2.56	1.93	2.52	2.92
2.03	3.01	2.3	2.6	2.41	2.57	2.11	2.57	1.87
2.34	3.28	2.52	2.6	2.4	3.07	1.86	2.7	2.38
2.03	3.31	2.65	2.59	2.43	2.59	1.71	2.65	2.28
2.08	3.31	2.49	2.83	2.66	2.88	2.16	2.91	2.16
2.33	2.83	2.7	2.88	2.67	3.07	2.07	2.24	2.61
2.12	3.04	2.82	2.89	2.52	2.75	1.96	2.5	2.47
2.24	2.47	2.82	2.84	2.46	3.07	2.22	2.07	2.42
2.61	2.65	2.57	2.76	2.46	2.62	2.54	2.1	2.19
2.01	3.08	2.57	2.86	2.45	2.99	2.15	2.13	1.99
2.13	2.49	2.86	2.89	2.39	2.72	2.03	2.06	2.26
2.2	3.05	2.53	3.03	2.15	2.63	2.03	2.81	2.58
2.21	2.71	2.64	2.78	2.64	2.73	2.65	2.71	2.53
2.77	2.53	2.61	2.75	2.68	2.83	2.51	2.91	2.52
2.54	2.8	3.04	2.52	2.58	2.65	2.35	2.11	2.71
2.24	2.53	2.72	2.91	2.48	2.84	2.07	2.21	1.96
2.9	2.59	2.63	2.66	2.62	2.7	2.85	2.18	1.98
2.83	2.72	2.63	2.78	2.64	2.96	2.71	2.4	2.36
2.33	3.33	2.64	2.74	2.65	2.75	2.78	2.05	2.22
2.63	3.15	2.65	2.9	2.73	2.72	2.74	2.08	2.97
2.1	3.06	2.75	2.55	2.15	2.95	2.35	1.92	2.99
2.46	2.53	2.14	2.57	2.44	2.7	2.63	2.26	2.25
2.54	3.16	2.6	2.42	2.34	2.86	2.1	2.21	2.28
2.32	2.86	2.56	2.56	2.41	2.73	2.32	2.31	2.93
2.94	2.76	2.26	2.93	2.31	3.07	2.4	2.24	2.7
2.21	2.82	2.64	2.39	2.61	3.26	2.19	2.28	2.6

116

Year	-400E	-500W	-500E	-600W	600E	-700W	-800W	800E	-900W
Ring No.	2478	2378	2378	2278	2278	2178	2078	2078	1978
	2.28	2.68	2.28	2.31	2.59	1.62	1.51	2.35	3.12
	2.64	2.47	2.31	2.8	2.17	1.46	1.47	1.97	3.12
	2.66	2.77	2.1	2.23	2.11	1.76	1.45	1.81	2.71
	2.64	2.77	2.35	2.11	2.24	2.06	1.53	1.98	3.06
	2.2	2.88	3.1	2.12	2.39	2.21	1.39	2.17	2.73
	2.21	2.93	2.41	2.41	3.22	1.96	1.49	2.08	2.88
	2.44	2.91	3.06	2.3	2.48	1.71	1.48	2.24	2.69
	2.42	2.88	3.09	2.67	3.18	2.17	1.34	2	2.96
	2.64	3.11	2.51	2.38	2.58	2.05	1.38	2.08	2.9
	1.97	2.62	3.09	2.68	2.39	2.01	1.72	2.23	2.94
	2.09	2.27	2.97	2.61	2.38	2	1.92	2.15	2.82
	2.5	2.42	3.06	2.62	2.51	2.24	1.85	2.15	2.65
	2.54	2.53	3.12	2.34	2.5	2.35	1.37	2.55	2.96
	2.79	2.78	3.03	2.76	2.75	2.14	1.73	1.84	3
	2.29	2.59	2.88	2.37	2.67	2.2	1.91	1.93	2.94
	2.19	2.77	2.71	2.37	2.45	2.13	1.69	1.88	3.36
	2.32	2.96	2.68	2.13	2.63	2.01	1.65	2	3.15
	2.55	3.16	2.85	2.42	2.64	2.08	2.04	2.24	3.18
	2.26	3.01	2.41	2.26	2.66	2.07	1.82	2.25	2.99
	2.51	2.7	2.84	2.52	2.63	2.02	1.91	2.18	2.83
	2.68	2.5	2.38	2.48	2.39	1.88	1.83	1.98	2.59
	2.53	2.81	2.35	2.33	2.82	1.83	1.87	2.12	2.5
	2.23	2.93	2.84	2.69	2.7	2.05	2.1	1.98	2.84
	2.11	2.82	2.36	2.27	2.39	1.85	1.71	1.91	2.66
	2.44	2.76	2.79	2.48	2.72	1.99	1.74	2.09	3
	2.62	2.89	2.77	2.18	2.53	1.95	1.78	2.03	2.65
	2.4	2.92	2.48	2.11	2.31	2.07	1.85	2.2	2.8
	1.84	2.55	2.58	2.11	2.63	2	1.72	2.13	2.93
	2.19	2.84	2.65	2.56	2.98	1.92	1.7	1.85	2.49
	2.18	2.85	2.65	2.25	2.71	2.04	2.32	2.14	2.62
	2.37	2.52	2.46	2.43	2.57	2.07	1.83	2.36	2.7
	3	3.13	2.37	2.46	2.65	2.07	1.93	2.3	2.67
	2.57	3.03	2.38	2.48	2.58	1.92	1.6	2.46	2.99
	2.47	3.12	2.84	2.18	2.95	1.72	1.7	2.49	2.67
	2.43	2.87	2.5	2.1	2.43	1.84	2.05	2.07	2.66
	2.28	3.03	2.3	2.14	2.17	2.05	1.88	2.38	2.41
	2.69	2.99	2.42	2.23	2.66	2.13	1.91	2.28	2.85
	2.69	2.91	2.82	2.31	2.86	2.08	1.78	1.98	3.05
	1.98	2.99	2.82	2.27	2.3	1.92	1.76	2.45	3.39
	2.38	2.66	2.35	2.14	2.29	1.91	1.83	2.46	2.08
	2.47	2.66	2.61	2.33	2.4	1.8	1.71	1.96	2.19
	2.41	2.97	2.86	2.35	2.65	2.06	1.53	2.05	2.65
	2.09	2.63	2.79	2.21	2.63	1.86	1.63	2.11	2.61
	1.77	2.72	2.91	2.37	2.63	1.9	1.83	1.96	2.26
	1.66	3.07	3.19	2.16	2.27	2.06	1.89	1.74	2.87
	2.46	3.19	2.06	2.73	2.8	2.29	1.95	1.98	2.33
	1.96	2.65	2.89	2.45	2.6	2.17	1.86	2.07	2.71
	1.98	2.83	2.34	2.29	2.78	2.01	1.9	2.17	3
	2.35	2.95	3	2.26	2.93	2.11	1.96	1.79	2.72
	2.55	3.03	2.45	1.98	2.51	2.12	1.8	2.17	2.65

117

Year	900E	-1000W	-1000E	-1100W	-1100E	-1200W	-1200E	-1300W	-1300E
Ring No.	1978	1878	1878	1778	1778	1678	1678	1578	1578
	2.21	3.02	3.16	2.86	3.53	2.63	2.65	3.08	3.03
	2.26	2.97	2.96	2.67	2.93	2.33	3.05	2.92	3.14
	2.62	2.78	3.27	2.53	2.78	2.7	2.69	2.96	3.22
	2.57	2.98	3.5	2.47	3.36	2.39	2.83	2.96	3
	2.72	3.1	3.41	2.72	2.62	2.79	2.99	2.49	3.08
	2.72	2.98	2.56	2.85	2.42	2.73	3.18	2.77	2.9
	2.12	2.94	2.98	2.54	3.27	2.94	2.86	2.46	3.23
	2.84	3.2	3.35	2.56	3.44	2.88	2.49	3.01	3.17
	2.86	2.92	2.68	2.68	3.53	2.73	3.13	2.98	3.11
	2.6	3.02	3.03	2.6	2.61	2.81	3.12	2.82	3.04
	3.01	3.36	2.95	2.65	3.23	2.72	2.86	2.85	2.98
	3.23	3.31	3.06	2.59	3.09	2.63	2.83	2.48	2.87
	3.1	3.16	3.29	2.81	2.79	2.5	3	2.48	2.69
	2.56	3.02	3.38	2.8	3.6	2.89	3.13	2.99	3.13
	2.87	3.18	2.9	2.54	2.84	2.75	3.01	2.46	2.78
	2.82	2.9	3.09	2.65	2.88	2.56	3.02	2.81	3.33
	2.87	2.9	2.81	2.52	2.8	3.14	3.33	2.69	3.08
	2.85	2.91	3.36	2.55	3.05	3.02	2.79	2.88	2.95
	2.68	3.34	3.42	2.44	2.44	2.68	2.42	2.77	2.9
	2.67	3.3	3.43	2.57	3.16	3.13	2.9	2.77	3.03
	2.52	3.44	2.92	2.55	3.2	2.63	2.77	2.88	2.77
	2.73	2.96	3.3	2.56	3.14	2.95	2.48	2.9	3.01
	3.15	2.75	3.13	2.56	3.44	3.11	2.61	2.8	2.95
	2.95	2.68	3.07	2.5	2.92	3.15	3.25	2.88	2.93
	2.57	3.12	3.26	2.67	3.07	2.95	2.65	2.98	2.87
	2.73	2.94	2.91	2.69	3.03	2.86	3.26	2.68	3.02
	2.73	2.94	2.82	3.27	3.37	3.16	3.34	2.75	3.36
	3.2	2.89	3.36	2.71	3.33	2.62	3.09	2.75	3.21
	2.99	2.92	3.04	2.65	2.73	2.74	2.87	3.06	3.11
	2.48	2.74	3.54	3.15	2.75	2.91	2.96	3.2	2.82
	2.96	3	3.24	2.84	3.17	2.88	2.49	2.77	3.32
	2.46	3.3	3.34	2.72	2.89	2.97	2.59	2.83	3.38
	3.14	3.21	3.3	2.61	3.35	2.39	2.86	2.69	2.75
	2.7	2.8	3.24	3.24	3.3	2.61	3.15	2.67	3.39
	3.11	3.08	3.49	2.62	4.12	2.59	3.19	2.59	3.04
	3.1	3.66	2.88	3.29	4.14	2.81	3.12	2.22	3.25
	3.02	3.08	3.17	2.88	3.31	2.53	3.12	2.48	2.94
	2.87	2.74	3.13	2.76	3.07	3.05	2.93	2.78	3
	2.87	2.95	4.16	2.78	3.22	2.62	3.04	2.68	2.84
	3.15	3.2	3.09	2.78	3.32	2.77	2.97	2.95	2.7
	2.72	2.99	3.43	2.95	3.09	2.86	3.21	2.89	3.11
	3.09	3.31	2.94	3.14	3.15	2.79	2.65	3.44	3.14
	2.9	2.94	3.46	3.17	3.35	2.52	3.1	3.18	2.94
	4.15	2.87	3.4	2.95	2.77	2.9	2.86	2.92	2.89
	3.72	3.12	3.04	3.14	2.92	2.95	3.01	2.37	2.97
	3.24	2.66	3.17	3.16	3.11	3.12	3.27	2.65	2.69
	3.43	2.86	3.26	3.04	2.88	2.62	3.24	3.12	2.75
	2.77	2.86	3.33	3.1	2.89	2.45	3.16	2.76	2.75
	3.13	3.14	3.15	3.05	3.1	3.16	2.9	3	3.01
	2.75	3.33	3.29	3.08	2.91	3.17	3.43	3.21	2.82

Year	-1400W	-1400E	-1500W	-1500E	-1600W	-1600E	-1700W	-1700E	-1800W
Ring No.	1478	1478	1378	1378	1278	1278	1178	1178	1078
	2.76	2.98	2.52	2.57	2.71	2.55	2.28	2.63	3.03
	2.3	3.21	3.12	2.54	2.75	3	2.19	2.36	3.12
	2.23	2.9	2.53	2.46	2.81	2.82	2.56	2.33	2.96
	3.7	2.9	2.95	2.57	2.75	2.41	2.57	2.99	2.79
	2.89	2.73	3.1	2.78	3.1	2.67	2.88	2.67	2.6
	3.01	2.83	2.9	2.76	2.9	3.17	2.59	2.72	2.55
	3.03	2.99	2.71	2.68	2.91	3.2	2.4	2.92	2.92
	2.71	2.87	2.74	2.59	2.55	2.63	2	2.99	2.83
	3.12	2.96	3.04	2.56	2.52	2.62	2.76	2.97	2.7
	3.43	3.2	2.59	3.01	2.49	2.65	2.37	2.86	3
	2.81	3.52	2.76	3.22	3.01	2.68	2.3	2.59	2.77
	2.96	3.17	2.58	3.05	2.72	2.69	2.16	2.63	2.58
	3.08	3.08	2.85	2.47	2.87	2.29	2.15	2.83	2.63
	3.02	3.13	2.87	2.39	2.79	3.16	2.1	2.53	2.77
	2.98	2.94	2.83	2.49	3.08	2.66	2.15	3.03	2.82
	2.77	3.28	3	3.14	2.74	2.58	2.37	3.01	3.64
	2.72	3.11	2.65	2.43	2.99	2.64	2.45	3.5	3.05
	2.72	2.87	2.88	2.72	3.11	2.99	2.42	3.14	2.96
	2.93	2.94	2.76	3.2	3.03	2.88	2.37	3.05	2.82
	2.76	3.42	3.05	2.9	2.64	2.66	2.4	2.9	2.74
	2.35	3.01	2.84	2.82	2.63	2.41	2.24	2.96	2.97
	2.91	3.31	2.75	2.67	2.58	2.55	3.02	3.1	3.08
	2.55	2.98	2.84	2.62	2.66	2.99	2.68	2.78	2.87
	2.42	3.16	2.86	3.02	3	2.57	3.29	3.28	3.05
	2.49	2.97	2.95	3.16	2.92	2.88	2.83	3.01	2.79
	2.47	2.67	2.74	2.64	2.6	2.87	2.78	2.76	2.84
	2.5	2.99	2.55	2.59	2.85	2.53	2.42	2.72	2.66
	3.44	2.91	2.97	2.79	3.13	2.83	2.67	2.71	2.45
	2.41	2.95	2.88	3.3	2.53	2.36	2.83	3.09	2.82
	2.92	3.57	3.74	2.81	3.17	2.7	2.69	2.92	2.59
	2.7	2.72	2.92	2.74	2.84	2.65	2.87	2.53	2.95
	3.01	2.71	2.92	2.88	2.81	3.01	3.29	2.52	2.99
	3.04	2.62	2.76	2.8	3.35	3.21	2.9	2.94	2.76
	3.1	3.42	2.63	2.97	3.3	3.12	2.74	2.9	2.81
	2.86	3.31	2.36	2.87	3.06	3.12	2.61	3.56	2.86
	2.3	3.23	2.9	2.96	3.3	2.89	2.73	2.63	3.18
	2.49	3.25	2.81	3.07	2.71	2.85	3.03	3.07	2.92
	2.52	3.28	2.64	2.62	2.59	3.08	2.98	2.8	2.89
	2.8	2.98	2.9	2.88	2.79	2.86	2.84	2.56	2.74
	3.11	2.72	2.77	3.39	2.89	3	2.56	2.94	2.6
	2.93	3.74	2.34	3.11	3.1	2.87	3.03	3.25	2.98
	2.91	2.78	2.79	3.01	2.91	2.83	2.34	2.92	2.78
	2.52	2.95	2.4	3.01	3.17	2.52	2.6	2.67	2.83
	2.69	2.98	2.59	2.66	3.37	2.9	2.81	2.66	2.76
	2.54	3.1	2.97	3.01	2.47	2.76	2.34	2.91	3
	2.9	3.47	2.44	2.75	2.92	3.27	2.59	2.76	2.81
	2.99	3.22	2.44	3.33	2.89	3.08	2.38	3.07	2.73
	2.9	2.75	2.53	2.6	2.52	2.81	2.37	2.93	3.02
	2.96	2.73	2.67	2.69	2.83	2.61	2.38	2.76	3.03
	2.61	2.81	3.04	2.84	2.61	2.61	2.55	3.09	2.76

Year	-1800E	-1900W	-1900E	-2000W	-2000E	-2100W	-2100E	-2200W	-2200E
Ring No.	1078	978	978	878	878	778	778	678	678
	2.72	2.36	2.3	2.76	2.52	2.71	2.07	2.45	2.08
	2.88	2.57	2.37	2.73	2.7	2.79	2.29	3.3	1.9
	2.93	2.82	2.02	2.78	2.71	2.77	2.66	2.77	2.13
	3.04	2.51	2.33	2.73	2.41	2.36	2.91	3.01	1.71
	3.06	2.2	2.84	3.01	2.57	2.47	2.82	2.9	1.76
	3.27	2.59	2.39	2.78	2.45	2.56	3.04	2.7	2.16
	2.79	3.07	2.66	2.89	2.52	2.55	2.84	2.54	1.81
	2.84	2.21	2.41	2.58	2.35	2.61	3.02	2.61	1.94
	2.7	2.42	2.38	3.19	2.77	2.34	2.74	2.63	1.98
	2.61	2.55	2.68	3.05	2.83	2.69	2.78	3.2	1.91
	3.1	2.71	2.71	3.47	2.27	2.11	2.56	2.79	2.13
	2.83	2.91	2.93	2.5	2.5	2.24	2.77	2.75	1.9
	2.83	2.88	2.71	3.13	2.21	2.31	2.54	2.84	2.29
	2.91	2.74	2.69	2.72	2.46	2.44	2.66	2.67	2.35
	2.98	2.68	2.56	2.77	2.54	2.49	2.65	2.8	1.81
	2.87	2.87	3.15	2.79	2.44	3.16	2.53	2.85	2.29
	2.98	2.93	2.76	2.77	2.95	2.48	2.82	3.6	2.05
	2.95	2.93	2.63	2.78	2.29	2.32	2.48	3.34	2.24
	3.47	3.06	2.76	2.76	2.64	2.28	2.49	2.84	2.2
	2.87	2.76	2.87	2.92	2.46	2.38	2.62	2.79	2.57
	2.73	2.64	2.15	2.71	2.65	2.7	2.96	2.76	1.87
	3.3	3.03	2.46	3.02	2.49	2.32	2.56	3	2.29
	2.88	2.76	2.4	2.73	2.7	2.57	2.46	3.27	2.1
	2.89	2.66	2.46	2.54	2.42	2.67	2.87	3.31	1.68
	3.03	2.88	2.44	2.53	2.83	2.57	2.58	3.34	1.7
	3.06	2.68	2.26	2.38	2.42	2.51	3.03	3.32	1.9
	2.95	2.77	2.76	2.5	2.49	2.38	2.37	3.18	2.17
	2.91	3.03	2.95	2.36	2.69	2.24	2.19	2.8	1.99
	2.92	2.52	2.45	2.46	2.73	2.25	2.96	2.72	1.94
	3	2.54	3.23	2.3	2.67	1.9	3.03	2.81	2.21
	3.08	2.12	3.2	2.91	2.46	2.82	2.69	2.64	2.16
	3.16	2.27	2.79	2.72	2.43	2.22	2.91	2.42	2.4
	3.15	2.32	3.07	2.63	2.39	2.52	2.52	2.58	2.35
	2.62	2.78	2.56	2.49	2.25	2.06	2.83	2.86	2.32
	3.03	2.66	2.64	2.21	2.25	2.46	3.15	2.68	2.27
	3.04	2.37	2.89	2.99	2.49	2.51	2.95	2.73	2.01
	2.98	2.87	3.14	2.63	2.33	2.13	2.87	2.74	2.14
	3.09	2.92	2.97	2.61	2.64	2.36	2.76	2.71	2.37
	3.01	2.92	2.41	2.67	2.5	2.08	2.61	2.47	2.64
	3.02	2.58	2.81	2.69	2.3	2.28	2.59	2.94	1.94
	2.73	2.87	2.54	2.36	2.33	2.59	2.33	2.95	2.19
	2.93	3.03	3.02	2.13	2.24	2.73	2.84	2.45	2.14
	3.15	2.58	2.63	2.54	2.25	2.29	3.15	2.78	2.14
	2.97	2.7	2.27	2.73	2.54	2.54	2.55	2.77	2.3
	3.11	2.71	2.34	2.81	2.71	3.01	2.41	3.02	2.14
	3.05	2.77	3.03	2.81	2.56	2.54	2.51	3.02	2.21
	2.93	2.3	2.78	2.41	2.45	2.42	2.4	2.68	1.97
	3.09	2.73	2.69	2.89	2.69	2.38	2.75	2.91	2.07
	2.91	2.77	3.06	2.79	2.68	2.56	3	2.42	2.2
	3.14	2.61	2.83	2.74	2.39	2.74	2.71	2.67	1.98

Year Ring No.	-2300W 578	-2300E 578	-2400W 478	-2400E 478	-2500W 378	-2500E 378	-2600E 278	-2700W 178	-2700E 178
	2.93	2.12	2.96	2.33	2.48	3.02	2.69	2.67	2.26
	2.96	2.3	2.66	2.62	3.13	2.65	2.5	2.65	2.68
	2.97	2.9	2.85	2.5	3.02	3.09	2.67	2.87	2.46
	2.94	2.4	2.72	2.68	3.03	2.87	2.75	2.75	2.7
	2.93	2	2.95	2.68	2.61	2.79	2.22	2.68	2.44
	3.07	2.19	2.83	2.53	2.85	2.52	2.43	2.48	2.52
	2.9	2.34	3.1	2.22	2.82	2.76	2.58	2.47	2.52
	2.81	2.8	3.13	2.51	3.01	2.55	2.53	3.05	2.55
	2.91	2.14	3.05	2.37	2.85	2.79	2.67	3.09	2.47
	3.25	2.24	2.65	2.37	2.69	3.27	2.24	2.85	2.24
	2.89	2.85	2.52	2.09	2.78	2.89	2.27	2.46	2.69
	2.8	2.38	2.61	2.27	2.95	2.84	2.46	2.85	2.74
	2.85	2.08	2.55	2.66	3.13	2.9	2.56	2.66	2.47
	3.04	2.43	3.28	2.2	3.19	2.86	2.57	2.62	2.38
	3.1	2.63	3.06	2.54	2.65	3.96	2.34	3.11	2.11
	2.71	3.06	3.09	2.27	2.83	3.31	2.56	3.07	2.62
	3.26	2.56	3.1	2.25	3.11	2.98	2.54	2.66	2.53
	3.33	2.89	3.12	2.78	2.78	2.96	2.2	2.63	2.65
	3.09	2.81	3.12	2.75	2.78	2.72	2.4	2.42	2.78
	3.01	2.63	2.83	2.83	3.03	2.56	2.21	2.84	2.54
	2.91	2.69	2.59	2.34	2.95	2.65	2.56	2.71	2.97
	2.77	2.86	2.54	2.53	2.67	2.74	2.63	3.21	2.34
	2.72	2.85	2.57	2.42	2.75	2.83	2.36	2.58	2.42
	3.32	2.85	2.48	2.2	3.01	2.77	2.54	3.02	2.65
	3.38	2.58	3	2.1	3.27	3.04	2.23	2.9	2.55
	3.21	2.64	2.89	2.1	3.44	2.68	2.7	2.77	2.53
	2.94	2.99	3.22	2.08	3.05	2.91	2.52	2.74	2.51
	3.1	2.66	2.9	2.41	3.41	2.79	2.34	2.92	2.64
	3.1	3.08	2.91	2.45	2.95	2.8	2.33	2.73	2.63
	3.06	2.99	2.93	2.68	2.77	2.56	2.53	2.69	2.48
	3.1	2.47	2.92	2.47	2.63	2.9	2.37	3.05	2.69
	3.12	2.97	2.91	2.51	2.8	2.84	2.24	3.02	2.53
	2.78	2.78	3.25	2.65	3.16	2.91	2.21	2.77	2.59
	3.13	2.41	2.52	2.57	2.75	3.24	2.17	2.62	2.41
	2.97	2.8	2.91	2.38	2.8	3.2	2.42	2.62	2.77
	2.94	2.9	3.17	2.85	2.91	3.19	2.07	2.78	2.61
	2.82	2.96	2.71	2.35	2.9	2.86	2.01	2.78	2.57
	2.66	2.84	2.81	2.37	2.83	3.04	2	2.5	2.68
	2.82	2.69	2.81	2.53	2.75	3.18	2.27	2.46	2.45
	2.66	2.69	2.55	2.57	2.62	3.16	2.3	2.34	2.33
	2.89	2.7	2.6	2.29	2.87	2.97	2.2	2.67	2.48
	2.74	2.69	2.86	2.58	2.8	2.81	2.55	2.51	2.7
	2.8	2.35	2.57	2.56	2.51	2.75	2.27	2.93	2.69
	3.02	2.14	2.65	2.72	2.96	2.74	2.4	2.85	2.52
	2.75	2.74	3.31	2.38	2.94	3	2.17	2.62	2.84
	2.93	2.46	2.67	2.47	3.08	3.15	2.09	2.44	2.48
	2.69	2.45	2.74	2.66	2.72	2.79	2.65	2.82	2.48
	2.91	2.96	2.52	2.63	2.97	2.93	2.21	3.19	2.63
	3.34	2.23	2.49	2.26	2.68	2.89	2.56	2.67	2.15
	2.79	2.44	2.43	2.41	2.81	2.96	2.29	2.64	2.46

121

Year	-2800W	-2800E	-2834W	-2834E
Ring No.	78	78	44	44
	1.92	2.52	1.93	2.52
	2.11	2.13	1.83	2.21
	2.38	2.07	1.79	2.24
	2.24	1.98	2.09	2.26
	2.32	1.78	2.17	2.22
	2.51	1.94	2.49	1.96
	2.33	1.98	1.99	2.16
	2.32	2.02	2.13	2.09
	2.09	1.64	2.39	2.1
	2.06	1.57	2.19	2.16
	2.24	1.88	2.18	1.74
	2.46	1.57	2.32	2.04
	2.02	2.24	2.32	2.18
	2.34	1.95	2.18	2.08
	2.55	2.26	2.24	2.41
	2.32	1.79	1.72	2.24
	2.17	1.89	1.94	2.27
	2.02	2.05	2.2	2.47
	2.47	1.72	2.02	2.26
	2.04	1.9	2.18	2.21
	2.52	1.91	1.92	2.26
	2.3	1.92	1.86	2.29
	2.31	1.76	1.95	2.2
	2.09	1.73	2.1	2.27
	1.93	1.81	2.11	2.48
	2.12	1.64	1.79	2.66
	2.02	1.68	2	2.17
	2.25	1.84	2.11	2.3
	2.21	2.1	2.12	2.16
	2.16	1.88	2.13	2.12
	1.93	1.98	2.13	2.12
	2.19	1.95	2.25	2.23
	2.21	1.87	2.26	1.81
	2.47	1.83	2.03	2.25
	2.74	2.02	2.11	2.05
	2.38	1.8	1.89	2.18
	2.33	1.69	2.11	2.18
	2.22	1.61	2.23	2.14
	2.56	2.32	2.08	2.2
	2.39	2.16	1.94	2.1
	2.55	1.75	2.26	2.36
	2.13	2.13	2.05	2.48
	2.14	2.15	2.17	2.35
	2.33	1.99	2.08	2.27
	2.37	2.11	2.1	2.06
	2.31	1.82	2.41	2.15
	2.54	1.88	2.13	2.47
	2.46	1.71	2.23	1.92
	2.47	1.85	2.39	2.04
	2.28	1.8	1.93	2.25

APPENDIX C

SEPARATED TRACHEIDS ON MICROSCOPE SLIDES
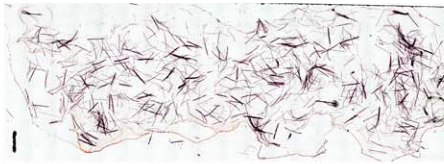
0E_1

0E_2

0W_1

0W_2
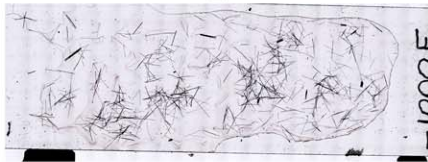
1000EBC_1

1000EBC_2

1000W_1
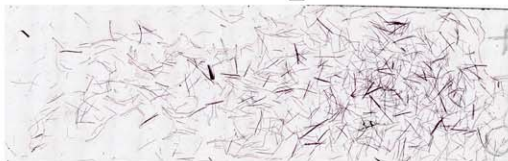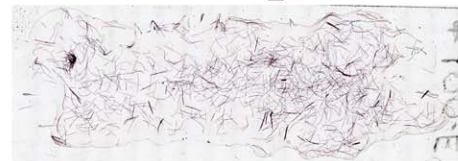
1000W_2

1000WBC_1

1000WBC_2

100E_1

100E_2

100EBC_1

100EBC_2

124

100W_1

100W_2

100WBC_1

100WBC_2

1100EBC_1

1100EBC_2

1100W_1

1100W_2

1100WBC_1

1100WBC_2

1200EBC_1

1200EBC_2

1200W_1

1200W_2

1200WBC_1

1200WBC_2

1300E_1

1300E_2

1300E2_1

1300E2_2

1300EBC_1

1300EBC_2

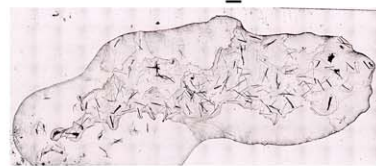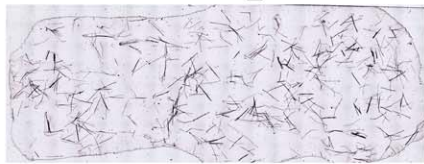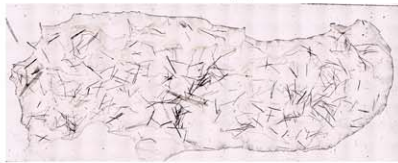1300WBC_1

1300WBC_2

1400E_1

1400E_2

1400EBC_1

1400EBC_2

1400W_1

1400W_2

1400WBC_1

1400WBC_2

1500E_1

1500E_2

1500EBC_1
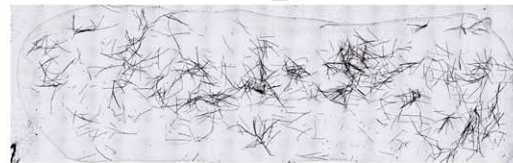
1500EBC_2

1500WBC_1

1500WBC_2

1600E_1

1600E_2

1600EBC_1

1600EBC_2

1600W_1

1600W_2

1600WBC_1

1600WBC_2

1700EBC_1

1700EBC_2

1700W_1

1700W_2

1700WBC_1

1700WBC_2

1800EBC_1
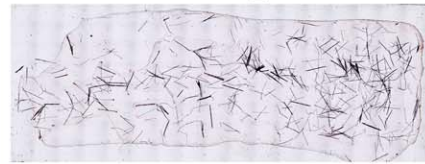
1800EBC_2

1800W_1

1800W_2

1800WBC_1

1800WBC_2

1900EBC_1

1900EBC_2

1900W_1

1900W_2

1900WBC_1

1900WBC_2

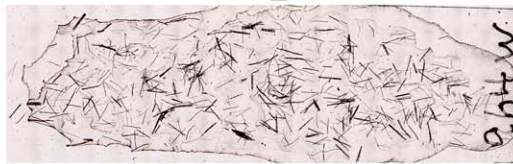1964E_1

1964E_2

1964W_1

1964W_2

1964W2_1

1964W2_2

2000EBC_1

2000EBC_2

2000WBC_1

2000WBC_2
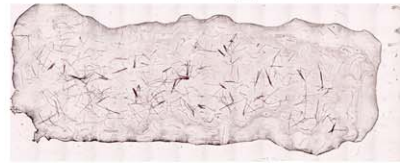
2100EBC_1

2100EBC_2

2100WBC_1

2100WBC_2
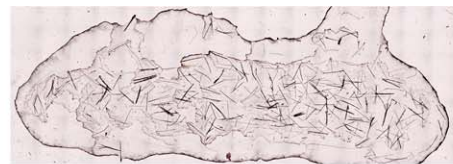
2200EBC_1

2200EBC_2

2200WBC_1

2200WBC_2

2300EBC_1

2300EBC_2

130

2300WBC_1

2300WBC_2

2400EBC_1

2400EBC_2

2400WBC_1

2400WBC_2

2500EBC_1

2500EBC_2

2500WBC_1

2500WBC_2

2600EBC_1

2600EBC_2

2700EBC_1

2700EBC_2
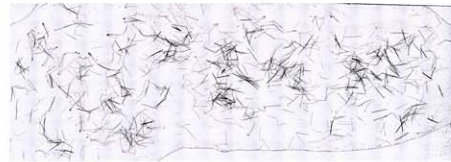
131

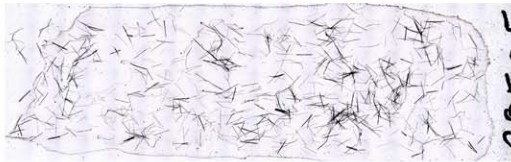2700WBC_1

2700WBC_2

2800EBC_1

2800WBC_1

2800WBC_2

2850BC_1

2850BC_2

2850EBC_1

2850EBC_2

REFERENCES

Anderson EA. 1951. Tracheid length variation in conifers as related to distance from pith. Journal of Forestry 49(1):38-42.

Arnold JR, Libby WF. 1949. Age determinations by radiocarbon content: checks with samples of known age. Science. 110:678-680.

Arnott HJ. 2008. Personal communication.

Baas P, Schmid R, van Heuven BJ. 1986. Wood anatomy of *Pinus longaeva* (Bristlecone pine) and the sustained length-on-age increase of its tracheids. IAWA Bulletin. 7(3):221-227.

Bailey DK. 1970. Phytogeography and taxonomy of *Pinu*s Subsection *Balfourianae.* Annals of the Missouri Botanical Garden. 57(2):210-249.

Bailey IW. 1920. The cambium and its derivative tissues. II. Size variations of cambial initials in gymnosperms and angiosperms. American Journal of Botany. 7(9):355-367.

Bailey IW. 1923. The cambium and its derivative tissues. IV. The increase in girth of the cambium. American Journal of Botany. 10(9):499-509.

Bailey IW and Shepard HB. 1915. Sanio's laws for the variation in size of coniferous tracheids. Botanical Gazette. 60(1):66-71.

Bannan MW. 1957. The relative frequency of the different types of anticlinal divisions in conifer cambium. Canadian Journal of Botany. 35:875-884.

Bannan MW. 1960. Cambial behavior with reference to cell length and ring width in *Thuja occidentalis* L. Canadian Journal of Botany. 38:177-183.

Bannan MW. 1967. Anticlinal division and cell length in conifer cambium. Forest Products Journal. 17(6):63-69.

Bannan MW, Bayly IL. 1956. Cell size and survival in conifer cambium. Canadian Journal of Botany. 34:769-776.

Bannan MW, Bindra M. 1970. The influence of wind on ring width and cell length in conifer stems. Canadian Journal of Botany. 48:255-259.

Beasley RS, Klemmedson JO. 1980. Ecological relationships of bristlecone pine. The American Midland Naturalist. 104(2): 242-252.

Bendtsen BA, Senft J. 1986. Mechanical and anatomical properties in individual growth rings of plantation-grown eastern cottonwood and loblolly pine. Wood and Fiber Science. 18(1):23-28.

Bisset IJW, Dadswell HE. 1950 The variation in cell length with one growth ring of certain angiosperms and gymnosperms. Australian Forestry. 14: 17–25

Bisset IJW, Dadswell HE, Wardrop AB. 1951. Factors influencing tracheid length in conifer stems. Australian Forestry Journal. 15:17-30.

Bollschweiler MB, Stoffel M, Schneuwly DM, Bourqui D. 2008. Traumatic resin ducts in *Larix deciduas* stems impacted by debris flows. Tree Physiology. 28(2):255-263.

Bond G, Showers W, Cheseby M, Lotti R, Almasi P, deMenocal P, Priore P, Cullen H, Hajdas I, Bonani G. 1997. A pervasive millennial-scale cycle in North Atlantic Holocene and glacial climates. Science. 278:1257-1266.

Bormann FH. 1965. Changes in the growth pattern of white pine trees undergoing suppression. Ecology. 46(3):269-77.

Chalk, L. 1930. Tracheid length, with special reference to Sitka spruce (*Picea sitchensis* Carr.). Forestry. 4(1):7-14.

Cohen, M.P. 1998. A garden of bristlecones: Tales of change in the Great Basin. Reno, Nevada:University of Nevada Press. 308 p.

Conifer Specialist Group. 1998. *Pinus longaeva*. In: IUCN 2006. 2006 IUCN Red List of Threatened Species. <www.iucnredlist.org>. Downloaded on 24 August 2007.

Connor KF, Lanner RM. 1990. Effects of tree age on secondary xylem and phloem anatomy in stems of Great Basin Bristlecone pine (*Pinus longaeva*). American Journal of Botany. 77(8):1070-1077.

Crowley TJ, Lowery TS. 2000. How warm was the Medieval Warm Period? Ambio. 29(1):51-56.

Currey DR. 1965. An ancient bristlecone pine stand in eastern Nevada. Ecology. 46(4):564-566.

Currie LA. 2004. The remarkable metrological history of Radiocarbon Dating (II). Journal of Research of the National Institute of Standards and Technology. 109(2):185-217.

Dadswell HF, Fielding JM, Nichols JWP, and Brown AG. 1961. Tree to tree variations and the gross heritability of wood characteristics of *Pinus radiata*. Tappi. 44:174-179.

Daubenmire R. 1954. Alpine timberlines in the Americans and their interpretation. Butler University Botanical Studies. 11:119–136.

Dinwoodie JM. 1963. Variation in tracheid length in *Picea sitchensis*. Forest Products Research Report. No. 16.

du Monceau D. 1755. Traité des arbres et arbustes qui se cultivent en France en pleine terre. H.L. Guérin et L.F. Delatour:Paris. 387 p.

Echols RM. 1955. Linear relationship of fibrillar angle to tracheid length, and the genetic control of tracheid length in slash pine. Tropical Woods. 102:11-22.

Eckstein D, Wazny T, Bauch J, Klein P. 1986. New evidence for the dendrochronological dating of Netherlandish paintings. Nature. 320:465- 466.

Engelmann G. 1863. On *Pinus aristata*, a new species of pine, discovered by Dr C. C. Parry in the alpine regions of Colorado Territory, and on some other pines of the Rocky Mountains. Transactions of the Academy of Science of Saint Louis. 2: 205-214.

Engelmann G. 1880. Revision of the Genus *Pinus* and the description of *Pinus elliottii*. Transactions of the Academy of Science of Saint Louis. 4:161-189.

Erickson HD, Harrison AT. 1974. Douglas-fir wood quality studies Part I: Effects of age and stimulated growth on wood density and anatomy. Wood Science and Technology. 8:207-226.

Esau K. 1965. Plant anatomy. 2nd ed. New York:John Wiley & Sons, Inc. 767 p.

Esau K. 1977. Anatomy of seed plants. 2nd ed. New York:John Wiley & Sons, Inc. 550 p.

Ewers FW. 1982. Secondary growth in needle leaves of *Pinus longaeva* (Bristlecone Pine) and other conifers: Quantitative data. American Journal of Botany. 69(10):1552-1559.

Ewers FW, Schmid R. 1981. Longevity of needles fascicles of *Pinus longaeva* (Bristlecone pine) and other North America pines. Oecologia. 51(1):107-115.

Fahn A. 1969. Plant anatomy. London:Pergamon. 534 p.

Farjon A. 2005. Pines: Drawings and descriptions of the Genus *Pinus*. Leiden, The Netherlands:Brill Academic Publishers. 236 p.

Franklin GL. 1945. Preparation of thin sections of synthetic resins and wood-resin composites, and a new macerating method for wood. Nature. 155(3924):51.

Fritts HC. 1976. Tree Rings and Climate. New Jersey:Blackburn Press. 567 p.

Fujiwara S, Yang KC. 2000. The relationship between cell length and ring width and circumferential growth rate in five Canadian species. IAWA Journal. 21(3):335-345.

Gernandt DS, López GG, Ortiz-Garcia S, Liston A. 2005. Phylogeny and classification of Pinus. Taxon. 54(1):29-42.

Gerry E. 1916. The Botanical Society of America. Fiber measurement studies: A comparison of tracheid dimensions in longleaf pine and Douglas fir, with data on the strength and length, mean diameter and thickness of wall of the tracheids. Science. 43(1106):360.

Google Maps. 2008. <http://maps.google.com/>

Grace J. 1977. Plant response to wind. New York:Academic Press. 216 p.

Great Basin National Park. 2008. <http://www.nps.gov/grba/>

Harris JM 1952: Discontinuous growth layers in *Pinus radiata*. New Zealand Forest Service, Forest Products Research Notes. I(4):1-10.

Hauksson JB, Bergqvist G, Bergsten U, Sjöström M, Edlund U. 2001. Prediction of basic wood properties for Norway spruce. Interpretation of Near Infrared Spectroscopy data using partial least squares regression. Wood Science and Technology. 35:475-485.

Hiebert RD, Hamrick JL. 1983. Patterns and levels of genetic variation in Great Basin Bristlecone Pine, *Pinus longaeva*. Evolution. 37(2):302-310.

Hiebert RD, Hamrick JL. 1984. An ecological study of bristlecone pine *(Pinus longaeva)* in Utah and eastern Nevada. The Great Basin Naturalist. 44:487-494.

Hoadley RB. 1980. Understanding wood: A craftsman's guide to wood technology. Newtown, Connecticut:Taunton. 272 p.

ITIS. 2008. Integrated Taxonomic Information System. http://www.itis.gov/

Jagels R, Telewski FW. 1990. Computer-aided image analysis of tree rings. In: Methods of dendrochronology: Applications in the environmental sciences. Eds:Cook E, Kairūkštis L. New Jersey:Springer. 394 p.

Jones PD, Briffa KR, Barnett TP, Tett SFB. 1998. High-resolution paleoclimatic records for the last millennium: Interpretation, integration and comparison with General Circulation Model control-run temperatures. The Holocene. 8(4):455-471.

Kienholz R. 1931. Effect of environmental factors on the wood structure of Lodgepole pine, *Pinus contorta* Loudon. Ecology. 12(2):354-379.

Körner C. 1998. A re-assessment of high elevation treeline positions and their explanation. Oecologia. 115(4):445-459.

Kral R. 1993. Pinus. Flora of North America: North of Mexico Volume 2: Pteridophytes and Gymnosperms. Eds:Flora of North America Editorial Committee. New York:Oxford University Press. 496 p.

Kramer PR. 1957. Tracheid length variation in Loblolly pine. Technical Report – Texas Forest Service. 10:1-22.

Kullman L. 1988. Holocene history of the forest-alpine tundra ecotone in the Scandes Mountains (central Sweden). New Phytologist. 108:101-110.

Kuniholm PI. 2001. Dendrochronology and other applications of tree-ring studies in archaeology. Eds:Brothwell DR, Pollard AM. London:John Wiley & Sons, Ltd. 782 p.

Kuroda K. 1986. Wound effects on cytodifferentiation in the secondary xylem of woody plants. Wood Research. 72:67-118.

Ladell JL. 1959. A new method of measuring tracheid length. Forestry. 32(2):124-125.

LaMarche Jr VC. 1969. Environment in relation to age of bristlecone pines. Ecology. 50(1):53-59.

LaMarche Jr VC. 1974. Paleoclimatic inferences from long tree-ring records. Science. 183:1043-1048.

Lanner RM, Hutchins HE, Lanner HA. 1984. Bristlecone pine and Clark's nutcracker: probable interaction in the White Mountains, California. Great Basin Naturalist. 44(2):357-360.

Larson PR. 1956. Discontinuous growth rings in suppressed slash pine. Tropical Woods. 104:80-99.

Lee S-W, Ledig FT, and Johnson DR. 2002. Genetic variation at allozyme and RAPD markers in *Pinus longaeva* (Pinaceae) of the White Mountains, California. American Journal of Botany. 89(4):566-577.

Lev-Yadun S. 2002. The distance to which wound effects influence the structure of secondary xylem of decapitated *Pinus pinea*. Journal of Plant Growth Regulation. 21:191-196.

Libby WF. 1952. Radiocarbon dating. Chicago:University of Chicago Press.124 p.

Liese W, Dadswell HE. 1959. Uber den Einfluss der Himmelsrichtung auf die Lange von Holzfasern und Tracheiden. Holz als Roh-u. Werkstoff. 17:421-427.

Lindstrom H. 1997. Fiber length, tracheid diameter, and latewood percentage in Norway spruce: Development from pith outward. Wood and Fiber Science. 29(1):21-34.

Linnaeus C. 1753. Species Plantarum. 1st ed. Vol. 2. Stockholm:Impensis Laurentii Salvii. 1200 p.

Little Jr EL, Critchfield WB. 1969. Subdivisions of the Genus Pinus. USDA Forest Service Miscellaneous Publication 1144.

LTRR. 2008. Laboratory of tree ring research. Skeleton plotting. <http://www.ltrr.arizona.edu/~sheppard/SkeletonPlot/plotting.htm>

MacMillan WB. 1925. A study of comparative lengths of tracheids of Red spruce, grown under free and suppressed conditions. Journal of Forestry. 23:34-42.

Mann ME, Bradley RS, Hughes MK. 1998. Global-scale temperature patterns and climate forcing over the past six centuries. Nature. 392:779-787.

National Park Service. 2008. http://www.nps.gov/

Panshin AJ, de Zeeuw C. 1980. Textbook of wood technology. New York:McGraw-Hill Publishing Company. 722 p.

Pendley KA. 2008. Changes in tracheid length in Prometheus: A bristlecone pine of the species *Pinus longaeva*. Thesis in fulfillment of an Honors Bachelor of Science in Medical Technology. 42 p.

Philipson WR, Butterfield BG. 1967. A theory on the causes of size variation in wood elements. Phytomorphology. 17:155-159.

Raczkowski J, Helińska-Raczkowska, Moliński, W. 2004. Relationship between lengthwise ultrasound transmission and tracheid length in wood of selected softwood species. Folia Forestalia Polonica, Seria B. 35:3-12.

Renfro M. 2008. Personal communication.

Richardson S.D. 1964. The external environment and tracheid size in conifers. In: The formation of wood in forest trees. Ed.: Zimmerman MH. New York:Academic Press. 562 p.

Richardson DM. 1998. Ecology and biogeography of Pinus. New York:Cambridge University Press. 525 p.

Salzer MW, Kipfmueller KF. 2005. Reconstructed temperature and precipitation on a millennial timescale from tree-rings in the Southern Colorado Plateau, U.S.A. Climatic Change. 70:465-487.

Sanio K. 1872. Über die Grösse der Holzzellen bei der gemeinen Kiefer (Pinus silvestris). Jahrbuch für Wissenschaftliche Botanik. 8:401-420.

Schmid R. 1982. Sonification and other improvements on Jeffrey's technique for macerating wood. Biotechnic and Histochemistry. 57(5):293-299.

Schimleck LR, Jones PD, Peter GF, Daniels RF, Clark III A. 2004. Nondestructive estimation of tracheid length from sections of radial wood strips by near infrared spectroscopy. Holzforschung. 58:375-381.

Shupe TF, Hse CY, Choong ET, Groom LH. 1997. Differences in some chemical properties of innerwood and outerwood from five silviculturally different loblolly pine stands. Wood and Fiber Science. 29(1):91-97.

Stine S. 1994. Extreme and persistent drought in California and Patagonia during mediaeval time. Nature. 369:546-549.

Stoffel M, Hitz OM. 2008. Rockfall and snow avalanche impacts leave different anatomical signatures in tree rings of juvenile *Larix deciduas*. Tree Physiology. 28:1713-1720.

Strickland RK, Goddard RE. 1966. Correlation studies of slash pine tracheid length. Forest Science. 12(1):54-62.

Taylor FW, Wang EIC, Yanchuk A, Micko MM. 1982. Specific gravity and tracheid length variation of white spruce in Alberta. Canadian Journal of Forest Research. 12(3):561-566

Telewski FW, Jaffe MJ. 1986. Thigmomorphogenesis: Anatomical, morphological and mechanical analysis of genetically different sibs of *Pinus taeda* in response to mechanical perturbation. Physiologia Plantarum. 66(2):219-226.

Via BK, Shupe TF, Stine M, So CL, Groom LH. 2005. Tracheid length prediction in *Pinus palustris* by means of near infrared spectroscopy: the influence of age. Holz als Roh- und Werkstoff. 63(3):231-236.

Wardle P. 1965. A comparison of alpine timber lines in New Zealand and North America. New Zealand Journal of Botany. 3:113-135.

Wareing PF. 1958. The physiology of cambial activity. Journal of the Institute of Wood Science. 1:34-42.

World Data Center for Paleoclimatology. 2008. International Tree Ring Data Bank. <http://www.ncdc.noaa.gov/paleo/treering.html>

Wilcox H. 1962. Cambial growth characteristics. In: Tree growth. Ed:Kozlowski TTT. New York:Ronald Press Company. 442 p.

BIOGRAPHICAL INFORMATION

Tina Halupnik started her academic career in 1974 at Miami University of Ohio and finished her B.S. in Biology in 2001 at the University of Texas at Arlington. Along the way, she married and raised two children. As part of her philosophy to never do a project halfway, she became actively involved in her children's schools, elected as a P.T.A. Life Member twice. When her youngest child entered junior high school in 1998, she decided to go back to college and, true to form, she threw herself into the study of Biology. Finishing her B.S. in 2001, she stayed to study for a M.S. in Biology (2003). Deciding that botany was the most exciting discipline in Biology, she was thrilled to work under Dr. Howard Arnott for a PhD degree in Quantitative Biology. From 2003 on, she discovered a love of teaching that will continue for the rest of her life. As a Graduate Teaching Assistant in freshman Biology labs, it only took one semester before she was leading other GTAs in the labs. Her future plans include travel (seeing live bristlecone pine trees), to continue her education in dendrochronology, and to explore new teaching methods in Biology.